

RETROFITTING GTL NATURAL GAS REFORMING USING CARGEN™  
TECHNOLOGY TO TARGET NATURAL GAS, OXYGEN AND WATER  
UTILIZATION AND CARBON DIOXIDE EMISSIONS

A Thesis

by

ZEINAB ATAYA

Submitted to the Graduate and Professional School of  
Texas A&M University  
in partial fulfillment of the requirements for the degree of

MASTER OF SCIENCE

Chair of Committee,	Nimir Elbashir
Committee Members,	Dhabia M. Al-Mohannadi
	Nayef M. Alyafei
Head of Department,	Arul Jayaram

August 2021

Major Subject: Chemical Engineering

Copyright 2021 Zeinab Ataya

## ABSTRACT

Reforming natural gas is an essential first step in the gas to liquid (GTL) conversion to produce synthetic fuels. Among the various available options in natural gas reforming, dry reforming of methane (DRM), a catalytic reaction in which  $\text{CO}_2$  and natural gas are converted into syngas, is seen as a method to convert  $\text{CO}_2$  to valuable products. DRM however suffers from thermodynamic limitations and coke formation that hinder its commercialization. CARGEN<sup>TM</sup> is the latest advancement in natural gas reforming that addresses the shortcomings of DRM and enables its commercial implementation. CARGEN<sup>TM</sup> technology comprises of two integrated reactors in which the first reactor converts greenhouse gases to solid multi-walled carbon nanotubes (MWCNT) while the second reactor produces syngas that meets downstream process requirements. CARGEN<sup>TM</sup> reduces the DRM process net energy requirement by 50% and could enable more than 80%  $\text{CO}_2$  conversion. The co-production of MWCNT presents significant economic incentives unmatched by the benchmark reforming processes in addition to the sustainability benefit of converting  $\text{CO}_2$ . This work retrofits an existing GTL processing plant that produces 50,000 bbl/day equivalent GTL fuels using the novel CARGEN<sup>TM</sup> technology. Highlighted in this work are the various advantages of replacing the commercial autothermal reforming (ATR) of methane reactor with the novel CARGEN<sup>TM</sup> technology. The comparative study is built on a systematic approach started with a base

case simulation of an ATR-based GTL plant. The model has been validated with experimental data at the industry scale and compared to the retrofit the base case model of the CARGEN<sup>TM</sup> technology represented by the two-reactor setup. The simulation results demonstrate the capability of the CARGEN<sup>TM</sup> to reduce the overall carbon footprint by 1,167 lb CO<sub>2</sub>/bbl GTL (73% reduction). Furthermore, the CARGEN<sup>TM</sup> reformer unit improves the net water generation by 531 lb H<sub>2</sub>O/bbl GTL (141% increase). The novel technology further improves the GTL process as it reduces the oxygen requirement by 481 lb oxygen/bbl GTL (79% less). While the CARGEN<sup>TM</sup>-based process requires an additional 5,455 SCF of natural gas/bbl GTL (61% more), it produces 536 lb of MWCNT for each barrel of GTL.

*To my parents and my sisters, with love and appreciation.*

## ACKNOWLEDGEMENTS

I would like to thank everyone that was part of my master's journey. First, I would like to express the deepest appreciation to my committee chair, Professor Nimir Elbashir, for his guidance and support. He has deeply contributed to my personal and professional growth since my undergraduate studies, and I couldn't have chosen anyone better as my graduate advisor.

I would like to extend my sincerest gratitude to Dr. Mohamed Sufiyan Challiwala for his patience, constant assistance, and encouragement. He was always available to answer all my questions and help out with any doubts I had throughout my work. This work couldn't have been a reality without his support.

I would also like to thank my committee members Dr. Dhabia Al-Mohannadi and Dr. Nayef Alyafei, for their valuable advice and guidance.

Special thanks also go to my friends and colleagues who made my master's experience truly enjoyable and unforgettable.

Finally, I am most grateful to my family for their unconditional love and patience. They always encouraged me to aspire to the highest and bring out the best in me.

## CONTRIBUTORS AND FUNDING SOURCES

### **Contributors**

This work was supervised by a thesis committee consisting of the advisor Professor Nimir Elbashir and the committee members Professor Dhabia Al-Mohannadi of the Department of Chemical Engineering and Professor Nayef Alyafei of the Department of Petroleum Engineering.

All work conducted for the thesis was completed by the student independently.

### **Funding Sources**

Graduate study was supported by a fellowship from Texas A&M University.

This work was also made possible in part by the Qatar National Research Fund (QNRF), a member of Qatar Foundation, under Grant Number NPRP X-100- 2-024. Its contents are solely the responsibility of the authors.

## NOMENCLATURE

ACFM	Actual cubic feet per minute
ASF	Anderson-Schulz-Flory
ASPEN	Advanced system for process engineering
ASU	Air separation unit
ATR	Autothermal reforming of methane
Bbl	Barrel
MBtu/hr	Thousand British thermal unit
C	Cooler
CC	Composite curve
CO <sub>FT</sub>	Flowrate of CO in the stream taken to the FT reactor
CRM	Combined reforming of methane
C <sub>p</sub>	Heat capacity
C <sub>1-DRY</sub>	Flowrate of methane in the dry natural gas stream
C <sub>1</sub>	Flowrate of methane in the combined stream of the ATR-based plant
C' <sub>1</sub>	Flowrate of methane in the combined stream of the CARGEN <sup>TM</sup> -based plant
C <sub>1-SAT</sub>	Methane flowrate in the saturated natural gas stream
C <sub>2</sub>	Flowrate of ethane in the combined stream

$C'_2$	Flowrate of ethane in the combined stream of the CARGEN™-based plant
$C_{2-SAT}$	Ethane flowrate in the saturated natural gas stream
$C_{3-SAT}$	Propane flowrate in the saturated natural gas stream
$C_9$	Flowrate of nonane in the combined stream of the ATR-based plant
$C'_9$	Flowrate of nonane in the combined stream of the CARGEN™-based plant
$C_{10}$	Flowrate of decane in the combined stream of the ATR-based plant
$C'_{10}$	Flowrate of decane in the combined stream of the CARGEN™-based plant
$CO'_{2-Fresh}$	Flowrate of the additional fresh CO <sub>2</sub> to be fed to the reactor
$CO'_{2-i}$	Flowrate of the recycled CO <sub>2</sub> coming from the amine unit
DEA	Diethanolamine
DRM	Dry reforming of methane
FT	Fischer-Tropsch
GCC	Grand composite curve
GHG	Greenhouse gases
GJ	Gigajoule
GTL	Gas-to-liquid
H	Heater



HC	Hydrocarbons
HE	Heat exchanger
HPSTEAM <sub>1</sub>	Steam flowrate to be fed to the pre-reformer
Hr	Hour
HTFT	High-temperature Fischer-Tropsch
H <sub>2</sub> -PSA	Flowrate of H <sub>2</sub> in the stream taken to the PSA
M	Thousand
MW	Megawatt
MWH	Megawatt hour
Lb	Pound
Lbmol	Pound mole
LCA	Life cycle assessment
LTFT	Low-temperature Fischer-Tropsch
Mton	Metric ton
MWCNT	Multi-walled carbon nanotubes
NO <sub>x</sub>	Nitrogen Oxides
O <sub>2</sub> -FRESH	Flowrate of additional fresh oxygen to be fed
O <sub>2</sub> -i	Flowrate of the oxygen initially present in the combined stream
POX	Partial oxidative reforming
PSA	Pressure swing absorption
PSE	Process safety engineering

Psia	Pounds per square
RWGSR	Reverse water gas shift reaction
R&D	Research and development
SCFM	Standard cubic feet per minute
SCF	Standard cubic feet
Syngas	Synthesis Gas
Syncrude	Synthetic crude oil
SRM	Stream reforming of methane
TRM	Tri-reforming of methane
USD	United States dollar
WGSR	Water gas shift reaction
WGSR	Water gas shift reaction
$W_{1-i}$	Flowrate of the water already present in the saturated natural gas stream
$^{\circ}\text{F}$	Degree Fahrenheit

## TABLE OF CONTENTS

	Page
ABSTRACT .....	ii
DEDICATION .....	iv
ACKNOWLEDGEMENTS .....	v
CONTRIBUTORS AND FUNDING SOURCES.....	vi
NOMENCLATURE.....	vii
TABLE OF CONTENTS .....	xi
LIST OF FIGURES.....	xiii
LIST OF TABLES .....	xv
1. INTRODUCTION.....	1
2. LITERATURE REVIEW .....	8
3. BACKGROUND DESCRIPTION.....	12
3.1. Natural Gas Reforming .....	12
3.1.1. Steam Reforming of Methane (SRM) .....	12
3.1.2. Partial Oxidative Reforming of Methane (POX) .....	13
3.1.3. Autothermal Reforming of Methane (ATR) .....	13
3.1.4. Dry Reforming of Methane (DRM) .....	14
3.1.5. CARGEN™ Technology.....	15
3.1.6. Thermodynamic Assessment of the CARGEN™ Technology .....	17
3.2. Fischer-Tropsch (FT) Reaction .....	20
3.3. Syncrude Refining.....	21
4. RESEARCH OBJECTIVES .....	23
5. DEVELOPMENT OF THE ASPEN PLUS® FLOWSHEET OF THE GTL MODEL .....	25

5.1. ATR.....	25
5.1.1. Saturation.....	26
5.1.2. Pre-Reforming.....	28
5.1.3. Reforming.....	29
5.1.4. Syngas Conditioning .....	31
5.1.5. Fischer-Tropsch Synthesis .....	33
5.1.6. Refinery .....	35
5.1.7. Water Pre-Treatment Unit.....	40
5.1.8. Fuel Gas Header and Flaring.....	41
5.2. CARGEN™ .....	42
5.2.1. Reforming.....	42
5.2.2. Syngas Conditioning .....	45
6. RESULTS AND DISCUSSION .....	49
6.1. Validation of Model Convergence .....	49
6.2. ATR-based Model Validation .....	54
6.3. Comparison of ATR and CARGEN™ KPI Results.....	56
6.4. Power Utilization.....	60
6.5. Heat Integration and Energy Targeting .....	62
6.6. Overall CO <sub>2</sub> Emissions.....	85
6.7. Summary of Results .....	86
7. CONCLUSIONS AND RECOMMENDATIONS FOR FUTURE WORK.....	88
8. RECOMMENDATIONS FOR FUTURE WORK.....	91
REFERENCES.....	92

## LIST OF FIGURES

	Page
<b>Figure 1</b> World energy supply by source in 2018 and projected supply in 2050 (Recreated from IEA <sup>1</sup> ).....	1
<b>Figure 2</b> Schematic of the gas-to-liquid (GTL) processing from the well to the wheel....	3
<b>Figure 3</b> CO <sub>2</sub> sources and conversion to valuable products.....	4
<b>Figure 4</b> A systematic two-reactor CARGEN <sup>TM</sup> technology for the co-production of MWCNT's and syngas .....	6
<b>Figure 5</b> CARGEN <sup>TM</sup> process two-reactor setup .....	16
<b>Figure 6</b> Carbon formation comparison between SRM, POX, and DRM at stoichiometric feed conditions and a pressure of 14.5 psia. ....	18
<b>Figure 7</b> Operational window of the CARGEN <sup>TM</sup> process reactors .....	19
<b>Figure 8</b> Saturation and pre-reforming of natural gas .....	27
<b>Figure 9</b> Reforming unit, heat recovery, and water separation unit of an ATR-based GTL plant.....	31
<b>Figure 10</b> ATR syngas conditioning unit .....	31
<b>Figure 11</b> FT synthesis and product recovery .....	35
<b>Figure 12</b> Hydrocracking unit of the GTL plant .....	38
<b>Figure 13</b> Hydrocracking product recovery and fractionation .....	39
<b>Figure 14</b> Water pre-treatment unit .....	40
<b>Figure 15</b> Fuel gas combustion unit .....	41
<b>Figure 16</b> Reforming unit of a CARGEN <sup>TM</sup> -based GTL plant .....	44
<b>Figure 17</b> CARGEN <sup>TM</sup> syngas conditioning .....	45
<b>Figure 18</b> ATR-based GTL plant flowsheet.....	47

<b>Figure 19</b> CARGEN™-based GTL plant flowsheet .....	48
<b>Figure 20</b> Comparison of the literature and reproduced ATR model KPI results.....	56
<b>Figure 21</b> Comparison of the ATR-based and CARGEN™-based model natural gas and syngas conversion .....	57
<b>Figure 22</b> Comparison of the ATR-based and CARGEN™-based water generation, oxygen consumption, carbon nanotubes production, and direct CO <sub>2</sub> emissions.....	58
<b>Figure 23</b> ATR-based model composite curve.....	66
<b>Figure 24</b> CARGEN™-based process composite curve .....	66
<b>Figure 25</b> Heat exchanger network of the ATR-based model – above the pinch .....	68
<b>Figure 26</b> Heat exchanger network of the ATR-based model – below the pinch .....	69
<b>Figure 27</b> Heat exchanger network of the CARGEN™-based model – above the pinch .....	70
<b>Figure 28</b> Heat exchanger network of the CARGEN™-based model –below the pinch .....	71
<b>Figure 29</b> Cascade diagram of the ATR-based GTL plant.....	78
<b>Figure 30</b> Cascade diagram of the CARGEN™-based GTL plant .....	79
<b>Figure 31</b> Grand composite curve of the ATR-based GTL plant before integration .....	80
<b>Figure 32</b> Grand composite curve of the CARGEN™-based GTL plant before integration .....	81
<b>Figure 33</b> Grand composite curve of the ATR-based GTL plant after integration .....	83
<b>Figure 34</b> Grand composite curve of the ATR-based GTL plant after integration .....	83
<b>Figure 35</b> Comparison of the ATR-based and CARGEN™-based direct and indirect CO <sub>2</sub> emissions .....	86
<b>Figure 36</b> Conversion of greenhouse gases to fuels and MWCNT .....	89

## LIST OF TABLES

	Page
<b>Table 1</b> Syncrude fractions .....	22
<b>Table 2</b> Natural gas feedstock properties .....	26
<b>Table 3</b> Feedstock properties .....	26
<b>Table 4</b> Stoichiometric coefficients of the FT reaction .....	34
<b>Table 5</b> Stoichiometric coefficients for the hydrocracking reactions .....	37
<b>Table 6</b> Flare gas properties.....	43
<b>Table 7</b> ATR-based model flowsheet balance .....	50
<b>Table 8</b> CARGEN <sup>TM</sup> -based model flowsheet balance .....	52
<b>Table 9</b> Comparison of the literature and reproduced model mass balance results .....	55
<b>Table 10</b> Comparison of the power requirement in the developed GTL models .....	61
<b>Table 11</b> Stream data for ATR-based GTL process .....	64
<b>Table 12</b> Stream data for CARGEN <sup>TM</sup> -based GTL process.....	64
<b>Table 13</b> Summary of ATR-based GTL model heat exchanger network specifications.	72
<b>Table 14</b> Summary of CARGEN <sup>TM</sup> -based GTL model heat exchanger network specifications .....	73
<b>Table 15</b> Summary of external cooling duties and specifications for each model .....	75
<b>Table 16</b> Summary of external heating duties and specifications for each model .....	75
<b>Table 17</b> Process unit heat duties of each model before integration .....	76
<b>Table 18</b> Total energy requirement and CO <sub>2</sub> emissions before and after integration .....	84
<b>Table 19</b> KPI results summary .....	87

<b>Table 22</b> ATR-based GTL model mass balance.....	125
<b>Table 23</b> CARGEN <sup>TM</sup> -based GTL model mass balance .....	131



## 1. INTRODUCTION

Energy and water are the pillars for the survival and development of humanity. With the increase in global population and continuous industrial expansions, the demand for natural resources is rising, but challenges with their rapid depletion and the major environmental concerns. Therefore, it is necessary to find alternative and environmentally attractive methods for the conservation of the resources. This challenge, along with the enforcement of more strict regulations, has led to a global shift from the focus on fossil fuels to renewable resources as well as natural gas as it is more abundant and cleaner than crude oil and coal.

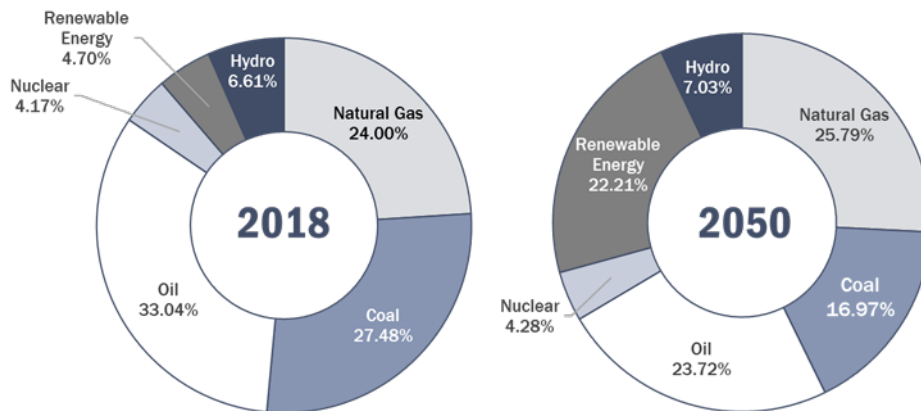


**Figure 1** World energy supply by source in 2018 and projected supply in 2050 (Recreated from IEA<sup>1</sup>)

Natural gas is one of the cheapest sources of energy<sup>2</sup>. It has a market price of around 4.4 USD/GJ<sup>3</sup>. It can be used for the production of heat and electricity as well as a precursor

for a variety of value-added products. Natural gas has been successfully monetized at large scales either as Liquefied Natural Gas (LNG) or chemically converted into valuable products through GTL technologies<sup>4</sup>. Recently, conversion technologies such as the Fischer-Tropsch (FT) that represents the heart of the GTL technologies became the focus of the production of ultra-clean fuels and value-added chemicals from natural gas<sup>5-8</sup>. GTL fuels are environmentally attractive because they lack sulfur and aromatics and generated less CO<sub>2</sub>, NO<sub>x</sub> (nitrogen oxides), and particulate matter upon combustion. In addition, the GTL diesel has a high cetane number of 70 to 80 and therefore can be used as premium fuels blended with crude oil diesel to enhance the performance of combustion engines<sup>9,10</sup>. Moreover, GTL technologies provide vast opportunities for the natural gas producing countries to expand their export market and gain from the value-addition to premium products<sup>11</sup>.

In a typical GTL process plant, the pre-treated natural gas from the midstream processing facility is first converted to synthesis gas (H<sub>2</sub> and CO) through methane reforming<sup>12</sup>. The produced synthesis gas (or syngas) will then be converted to long-chain HC in the FT process, followed by product upgrading where the long-chain HC are cracked to lower carbon number products (e.g. fuels) that are later separated in the refinery unit into fractions of desired valuable products<sup>13-16</sup>. This illustrated is presented in *Figure 2*.

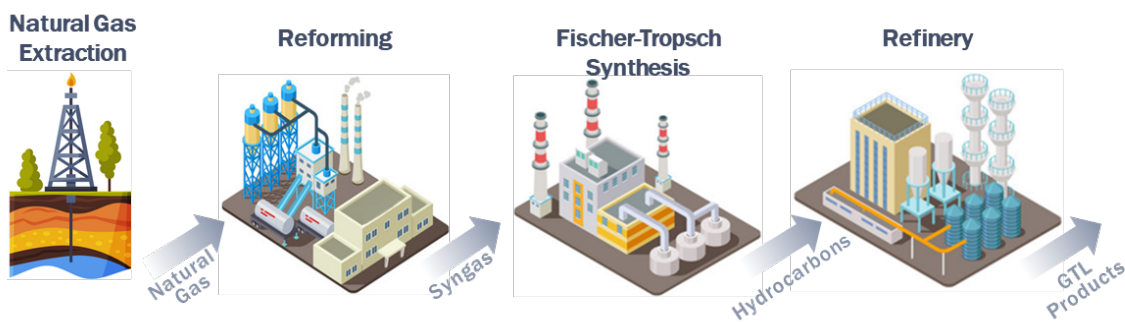


**Figure 2** Schematic of the gas-to-liquid (GTL) processing from the well to the wheel

Different reforming processes have been developed and used industrially; steam methane reforming (SRM), partial oxidation (POX), and autothermal reforming (ATR)<sup>17</sup>. These processes differ in terms of the quality of the syngas obtained, oxidant used, emissions released, and the steam utilization/generation<sup>18</sup>.

Although the GTL industry has been successfully established through century-long research and development (R&D) activities in the areas of natural gas reforming and Fischer Tropsch<sup>19</sup>, there is a significant number of research avenues that would improve its economics and sustainability. One such avenue to enhance the reforming technology, which is the most expensive and energy intensive part of the GTL plant. Dry reforming of methane (DRM) is another option for the improvement of the carbon footprint of the GTL plant via utilization of CO<sub>2</sub> as soft oxidant in methane reforming.

*Figure 3* shows some pathways for the industrial utilization of CO<sub>2</sub>. As the world slowly shifts towards environmentally friendly processes, these routes offer a great opportunity to utilize CO<sub>2</sub> in industrial processes and form products that use CO<sub>2</sub> as a reactant.

Therefore, DRM has attracted significant attention recently due to the envisioned possibility of re-inserting CO<sub>2</sub> into the synthetic fuels cycle<sup>19</sup>.

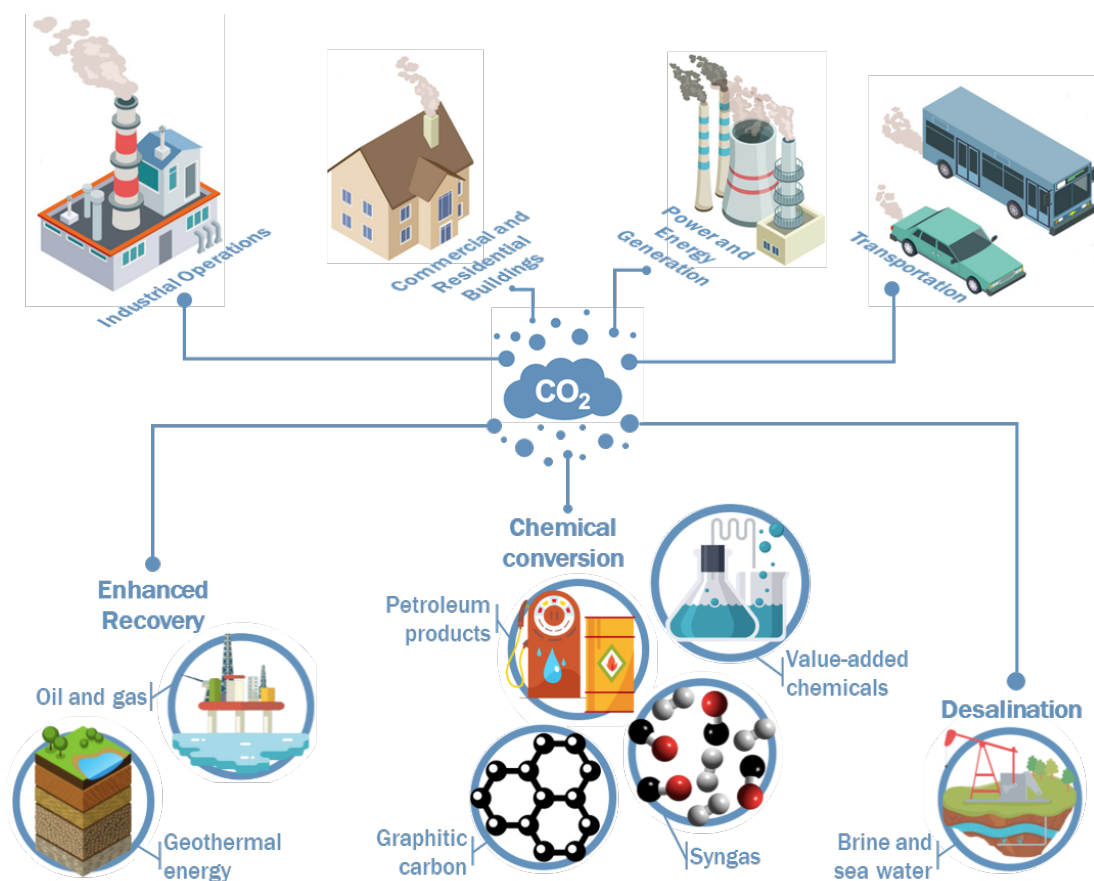


*Figure 3 CO<sub>2</sub> sources and conversion to valuable products*

However, DRM could not yet be implemented industrially due to inherent and prohibitive technical challenges:

- The high CO<sub>2</sub> activation energy makes this reaction highly endothermic and increases the tendency of the side reactions that form coke, which rapidly deactivates the catalyst<sup>20</sup>

- DRM produces much less hydrogen in syngas compared to SRM for example ( $H_2:CO$  ratio of 1 for DRM, while 2:1 and 3:1 for POX and SRM respectively) than the 2:1 ratio for commercial cobalt-based FT process
- DRM requires a clean and steady source of  $CO_2$  which is not easy to access in gas processing units.

These specific process constraints make a stand-alone DRM process infeasible, both technically as well as economically. Therefore, significant R&D activities are needed to make the commercial implementation of DRM a reality<sup>12,21–27</sup>.

A novel technological solution that simultaneously addressed DRM challenges, known as CARGENT<sup>TM</sup> (or CARbon GENerator), was developed in our group and reported in Challiwala et al.<sup>19,20,28,29</sup>. This technology utilizes an integrated two-reactor setup in which high-quality Multi-Walled Carbon Nanotubes (MWCNTs) are produced in the first reactor while downstream compatible syngas is produced in the second reactor<sup>19,28,29</sup>. CARGENT<sup>TM</sup> was conceptualized on the grounds of thermodynamics equilibrium modeling and proven experimentally in our previous work<sup>19,40</sup>. This process reduces the net energy requirements of a typical DRM process by 50% while converting at least 65%  $CO_2$  per pass. Moreover, from an LCA study, it was demonstrated that CARGENT<sup>TM</sup> enables a 40% reduction in the net operating costs and  $CO_2$  footprints<sup>19</sup>.

The concept was developed within a framework of process systems engineering (PSE). It takes advantage of the low operating temperature (752 to 1292 °F) and high C:H ratio in

the feed to selectively produce MWCNTs from the greenhouse gases (GHGs) in the first reactor. The second reactor is a tri-reformer that takes advantage of the high temperature (>1382 °F) and low C:H ratio to produce syngas of the desired ratio at minimal carbon formation<sup>19</sup>. A systematic two-reactor CARGEN<sup>TM</sup> technology is shown in *Figure 4*.

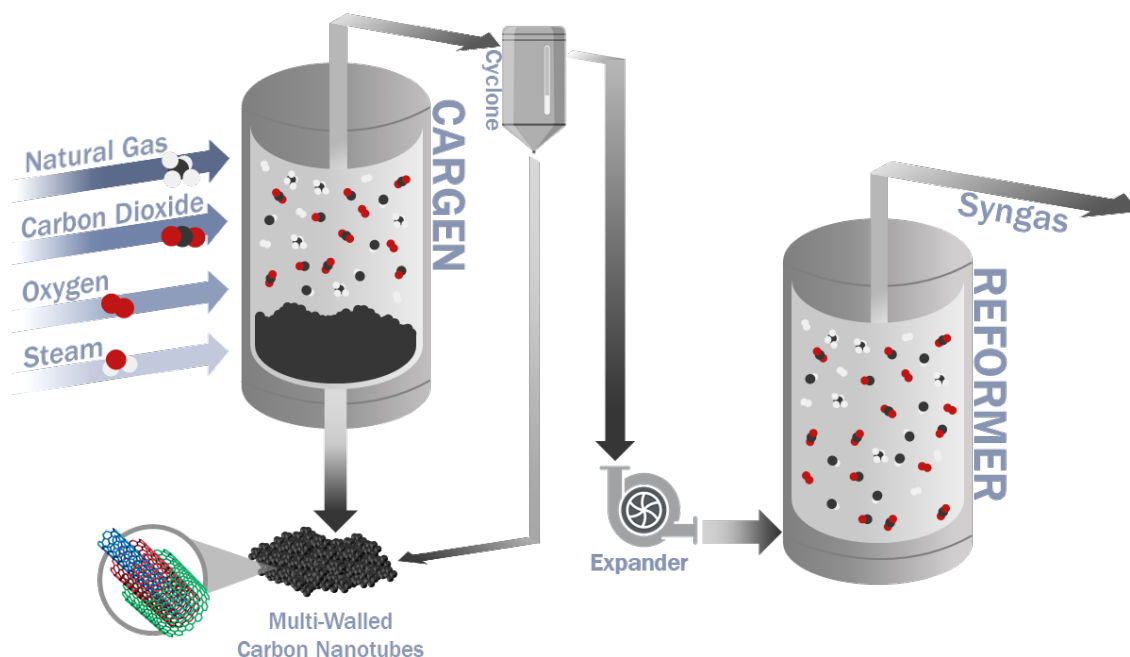


**Figure 4** A systematic two-reactor CARGEN<sup>TM</sup> technology for the co-production of MWCNT's and syngas

The CARGEN<sup>TM</sup> process offers various advantages as it utilizes CO<sub>2</sub> to produce syngas of the required ratio while also forming high-quality MWCNTs, which significantly improves the plant's economy. It can also use a relatively inexpensive catalyst in the first reactor that is highly selective for carbon formation. Furthermore, this reduces the coking tendency in the second reactor that employs a conventional reforming catalyst<sup>20</sup>.

It is evident that the GTL process has undergone exhaustive R&D over the past many decades starting from the beginning of the 20<sup>th</sup> century<sup>19</sup>. In order to improve the overall GTL plant performance in the industry, integration is done between the FT and reforming unit through internal and external recycles. The external recycling is done by rerouting some of the FT reactor products back to the reformer. Meanwhile, internal recycle is done by recycling some of the high-temperature FT products with the low-temperature section within the FT. Currently, the world's largest GTL plant is the Pearl GTL commissioned by Shell in Qatar<sup>32</sup>. This plant can produce 140,000 barrels of GTL product per day while also producing 120,000 barrels of natural gas liquids and ethane daily<sup>32</sup>. The Pearl GTL utilizes the POX technology; meanwhile, its competitor, ORYX GTL, uses the ATR technology. The latter is a SASOL-Qatar Petroleum joint venture located as well in Qatar<sup>33</sup>. This plant produces 34,000 barrels of petroleum products per day. Each of these plants also utilizes a different FT technology, where the Pearl project utilizes a multi-tubular fixed-bed reactor while Oryx uses a slurry phase distillate process. These processes have been heavily used in industrial applications, which significantly raises the expectations for new and emerging technologies.

The objective of this work is to study the effect of replacing the ATR unit of a pre-existing GTL plant with the CARGEN<sup>TM</sup> technology. More specifically, the retrofitted CARGEN<sup>TM</sup>-based GTL process will be compared with the ATR-based in terms of the natural gas conversion, water and oxygen consumption, power and energy utilization, and CO<sub>2</sub> emissions.

## 2. LITERATURE REVIEW

The different reforming technologies, SRM, POX, and ATR, have been used widely in the industry over the past decades. However, limited information is available in open literature on the heuristics in utilizing these processes or the water-energy implications of the reforming on the remaining units of the GTL plant<sup>34</sup>.

Hence, many researchers have been studying these processes in order to set benchmarks for each process and compare them in terms of overall energy and water requirements, as seen in a study by Martinez et al.<sup>35</sup>. Another study by Gabriel et al.<sup>36</sup> evaluated a number of GTL processes using different reforming technologies and compared their heat, mass, power, and greenhouse gas emissions. In addition, their study identified key performance indicators for each GTL process utilizing a well-structured ASPEN Plus<sup>®</sup> model<sup>36</sup>. The methodology to retrofit a full scheme of a GTL plan while providing a techno-economic assessment has previously been reported by our group (Bao et al.)<sup>37</sup>. This paper as well identified several novel opportunities for performance improvements and integration in existing GTL plants. Following the flowsheet synthesis, heat integration is performed through pinch analysis to determine the minimum heating and cooling requirements to conserve energy, Mass integration is then performed to minimize wastage of material while maximizing recycling. Finally, a cost evaluation was done for a comprehensive techno-economic assessment<sup>37</sup>.



In attempts to shift towards cleaner and more environmentally friendly processes, the DRM process has also been heavily investigated in order to address its aforementioned thermodynamic limitations and improve its syngas ratio. Among several studies in the literature targeted to address the DRM challenges<sup>38-41</sup>, Afzal et al.<sup>42</sup> investigated the approach of integrating the DRM with an absorption column, COSORB. This process produces syngas along with an additional carbon monoxide stream while also reducing the overall carbon footprint by over 65% and more than a 20% reduction in the operating cost. This process is unique as it utilizes an absorption column to improve the H<sub>2</sub>:CO ratio and produces a CO stream that can be used as feedstock to produce other petrochemicals. Moreover, it doesn't require steam or oxygen production, hence reducing the overall capital cost.

Numerous research studies have suggested the use of combined reforming process (CRM) wherein DRM is combined with the conventional technologies, SRM and POX<sup>26,43-50</sup> to address the DRM challenges. A previous study in our team reported in-depth research on the CRM processes and their comparison with the DRM regarding the quality of syngas produced, operating conditions, carbon formation, and energy requirement<sup>26</sup>. In another study earlier in our group, we also reported an estimation of the amount of CO<sub>2</sub> fixation using the CRM processes<sup>43</sup>. Similar work was done by Jonas *et al.*<sup>51</sup>, who studied combinations of SRM, DRM, ATR, and reverse water gas shift reaction (RWGSR). The Jonas *et al.*<sup>51</sup> study also focused on the effect of the cost of natural gas, oxygen, and carbon tax on the reforming process, as they are the main drivers for the final cost of the

GTL synthetic fuels. Luyben *et al.*<sup>52</sup> explored the design trade-offs of the DRM conditions on the downstream processes while conducting a sensitivity analysis on the methane conversion, carbon dioxide consumption, and energy consumption in various processes within a GTL plant. Experimental and computational studies done by Song *et al.*<sup>53</sup> prove that the tri-reforming (TRM, a combination of SRM, POX, and DRM) process has the potential of producing syngas ratio of 1.5 to 2, while also eliminating the formation of soot (solid carbon) in the reactor. Similar results were seen by Kang *et al.*<sup>50</sup>, where the TRM proved to be more favorable for the production of Syngas than DRM on its own.

Lee *et al.*<sup>47</sup> also evaluated the catalytic performance of the TRM process over a Ni/ZrO<sub>2</sub> catalyst, which showed a dramatic decrease in the coke formation on the reactor walls and the catalyst surface. Their work also shows that the optimization of the feed ratios is crucial for producing high-quality syngas. Similar work was also done in our group by Chatla *et al.*<sup>54</sup>, who performed a combined experimental, density function theory (DFT) and mathematical deconvolution study to determine the carbon resistance effect of the Cu doped Ni bimetallic catalysts on the DRM reaction. Their work demonstrated the superiority of the bimetallic Ni/Cu catalyst over mono-metallic catalysts. This was also proven by Omran *et al.*<sup>55</sup>, who also performed DFT calculations to evaluate the DRM reaction mechanism over bimetallic Ni/Cu catalyst and investigated the effect of temperature on carbon deposition and catalysts stability.

Therefore, the novelty of the CARGEN™ technology is that it takes advantage of the high carbon deposition in the dry reforming reactor to selectively produce MWCNT's. And using the two-reactor setup, this technology produces MWCNT's while also producing syngas with a ratio that meets the downstream requirements.

### 3. BACKGROUND DESCRIPTION

This section presents the details and operating parameters of the GTL process. The GTL plant is comprised of three main blocks:

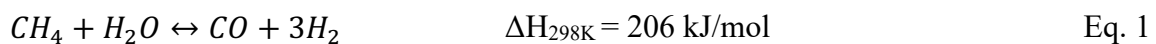
- a. Reforming unit for the production of syngas
- b. FT unit for the conversion of syngas to long-chain HC
- c. Refinery for the cracking and fractionation of HC

#### 3.1. Natural Gas Reforming

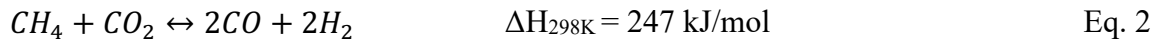
Reforming natural gas is the first step in GTL processing. The oxidant used in reforming determines its type<sup>20</sup>. As indicated earlier, the three benchmark reforming processes are SRM, POX, and ATR, while DRM is an area undergoing significant R&D. Presented below is a brief description of these reforming processes within the context of the GTL industry.

##### 3.1.1. Steam Reforming of Methane (SRM)

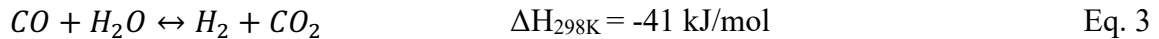
SRM is a large-scale commercialized catalytic process for converting natural gas to syngas through a reaction with steam. This reaction is favored at a pressure of 300 psia and temperatures higher than 1300 °F<sup>56</sup>. SRM is endothermic, and its reaction is limited by equilibrium. This reaction produces syngas with an H<sub>2</sub>:CO ratio higher than 3:1<sup>57</sup>.



In the presence of CO<sub>2</sub>, the following reaction takes place as well<sup>58</sup>.



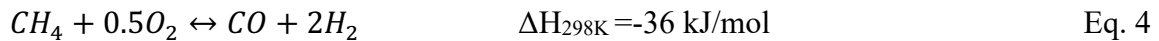
Additionally, a water gas shift reaction (WGSR) takes place as the product approaches equilibrium.



### 3.1.2. Partial Oxidative Reforming of Methane (POX)

POX is the reaction of methane with oxygen to produce syngas. It is an exothermic reaction that takes place through the partial combustion of natural gas<sup>59</sup>. The reformer is operated adiabatically with an outlet temperature of 3272 °F and pressure of 435 psia.

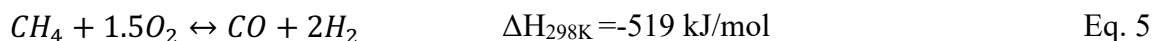
POX produces syngas of 1.6 to 1.9 ratio<sup>58</sup>.



To avoid carbon formation, steam is added near the entrance and exit of the reformer, which are the regions of high coke formation<sup>19</sup>.

### 3.1.3. Autothermal Reforming of Methane (ATR)

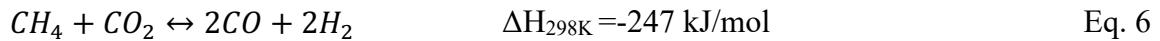
It is a combination of SRM and POX. In this process, the partial combustion of the HC feeds the endothermic requirement of the SRM. The ATR is operated adiabatically with an outlet temperature of 1949 °F at 435 psia<sup>35</sup>.



ATR is a catalytic process that combines the advantages of both reactions. Similar to the SRM, the WGSR also co-exists as a side reaction<sup>60</sup>. ATR generally produces syngas of ratio ranging between 1.9 and 3.5. This ratio can be controlled to the desired value by varying the amount of steam or oxygen fed to the reactor<sup>58</sup>.

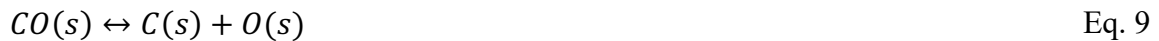
### 3.1.4. Dry Reforming of Methane (DRM)

DRM is the catalytic conversion of natural gas to syngas using CO<sub>2</sub> as an oxidant. It has the potential to produce syngas in an environmentally friendly approach while also offering an added benefit of reducing the utilization of steam and oxygen resources<sup>20</sup>.



As highlighted earlier, this process is not commercialized due to shortcomings that include (a) the catalyst deactivation by carbon formation, (b) the high endothermic nature of the reaction, and (c) the low quality of the syngas produced (syngas ratio less than 1). Therefore, it requires a high energy demand in addition to the presence of a steady and pure CO<sub>2</sub> supply, which increases the cost of the process<sup>20</sup>.

During the DRM process, carbon is formed via the following side reactions<sup>19</sup>.



Therefore, valuable hydrogen product is consumed to produce water. In the SRM and ATR processes, the WGSR promotes the production of more H<sub>2</sub>. However, in DRM, the increase in pressure leads to a shift in the equilibrium of the reaction towards the reverse WGSR (RWGSR), and it starts to dominate the DRM reaction at high temperatures (>1112 °F)<sup>16,27</sup>.

### 3.1.5. CARGEN™ Technology

CARGEN™ (CARbon GENerator) is an innovative approach for producing syngas and carbon from CO<sub>2</sub> developed by our research team<sup>19,20</sup>. This process addresses the DRM challenges by a unique reaction design that segregates the competing side reactions within DRM, which are carbon formation reactions and syngas production. CARGEN™ comprises an integrated two-reactor setup in which solid carbon is produced from the reaction of natural gas with CO<sub>2</sub> in the first reactor while syngas is formed in the second reactor. The CARGEN™ technology two-reactor setup is provided in *Figure 5*.

The first reactor promotes methane decomposition (Eq. 7) and Boudouard reaction (Eq. 12), which are highly active at low-temperature conditions (752 to 1112 °F), to selectively produce solid carbon in the first reactor.



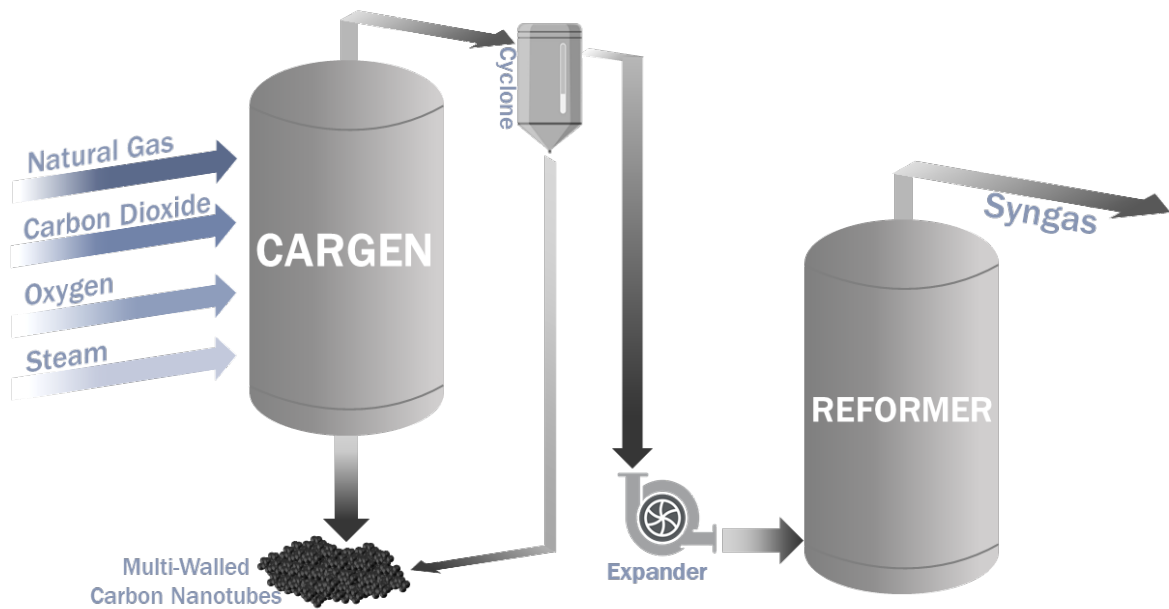


*Figure 5 CARGEN™ process two-reactor setup*

From the CO<sub>2</sub> life cycle assessment (LCA) perspective, the first reactor presents an excellent opportunity for long-term sequestration of GHGs into solid carbon, an environmentally stable material<sup>19,20</sup>. Also, it must be noted that the carbon product obtained from this process is industrially valuable as it can be used in the production of value-added chemicals and materials and in niche applications like batteries, fuel cells, and photovoltaics in addition to bulk applications like asphaltene and cement, as well as graphite, carbon black, and activated carbon. It can also be added to structural materials such as tar or cement. Moreover, it has been recently demonstrated in our experimental work that the carbon material produced from CARGEN™ is MWCNTs quality and therefore brings a significant scope of economic value-addition<sup>28</sup>.



The reaction in the first reactor is carried out in an oxygen-limited atmosphere at low temperatures to produce solid carbon. The operating conditions of CARGEN™ maximize the CO<sub>2</sub> fixation in the first reactor, increasing the carbon production while the partial presence of oxygen drives the reaction auto-thermally. The product gases from the first reactor are sent to the second reactor, which is in series to the first.

The second reactor in CARGEN™ is a tri-reformer, which uses a combination of SRM, DRM, and/or POX to produce a flexible syngas ratio at high temperatures that meets downstream applications like FT and methanol synthesis. Removing carbon from the first reactor allows for the operation of the second reactor at a temperature lower than conventional reforming processes (around 1,472 °F). Moreover, the reaction is driven by a lower energy requirement of approximately 114 Btu, making the system more energy efficient.

### **3.1.6. Thermodynamic Assessment of the CARGEN™ Technology**

The optimal operational conditions for each reactor are determined through thermodynamic analysis, which is a method to rapidly determine the conversions of reforming reactions at known industrial operating conditions and real thermodynamic equilibrium. These calculations show that low operational temperatures (less than 932 °F) favor the conversion of CO<sub>2</sub> to carbon, and the extent of the methane decomposition reaction is very high at these conditions. *Figure 6* compares the three different reforming technologies' carbon formation tendency at a pressure of 14.5 psia.

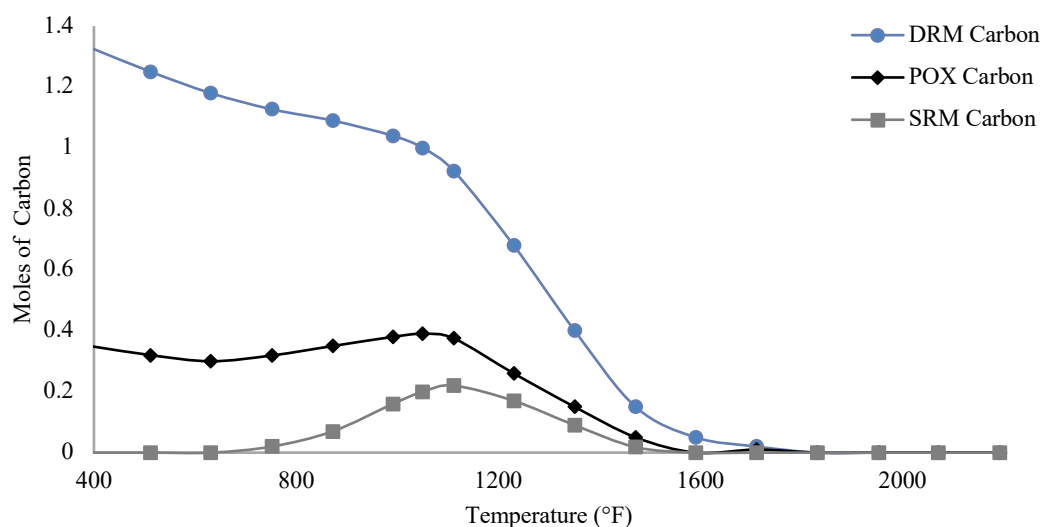


**Figure 6** Carbon formation comparison between SRM, POX, and DRM at stoichiometric feed conditions and a pressure of 14.5 psia.

This figure shows that the DRM process has a much higher carbon formation potential at lower temperatures due to the high feed C:H ratio. SRM has the least tendency to form carbon as it contains the largest amount of H<sub>2</sub> in the feed. Further details on this context are provided in our published work<sup>19</sup>. Therefore, to reduce the coke formation, the C:H ratio must be reduced by either removing the excessive carbon or increasing the H<sub>2</sub> concentration. This can be done by segregating the carbon formation reaction from the syngas formation reaction, as seen in *Figure 7*.

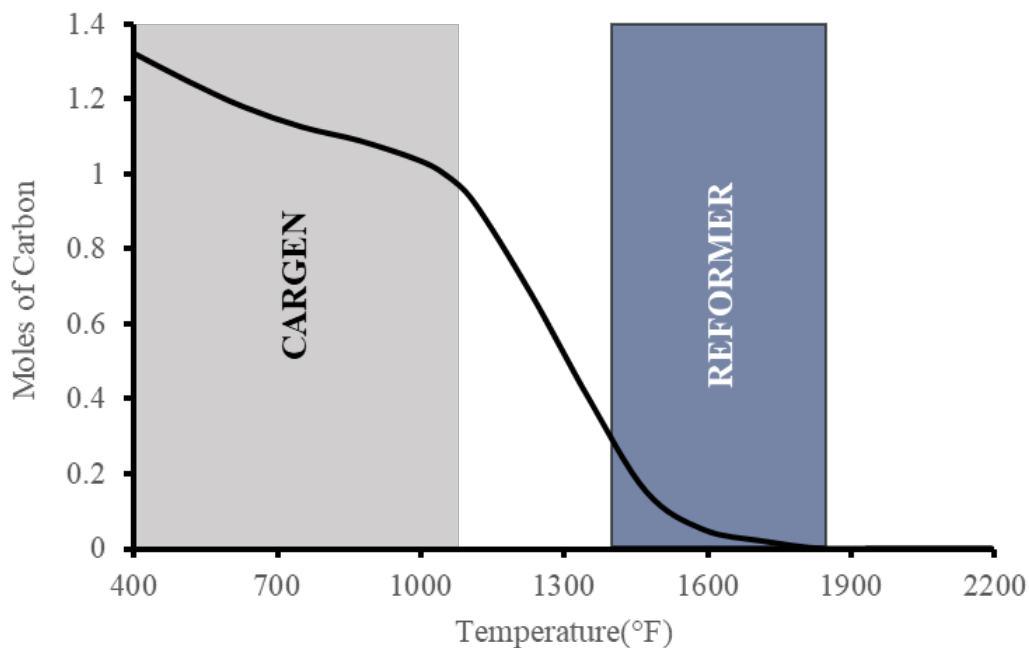


**Figure 7** Operational window of the CARGEN™ process reactors

This provides a clear insight into the operational window of each reactor. The grey zone represents the most favorable conditions for the production of carbon in the CARGEN™ reactor. While carbon is the main product from this reactor, syngas is also produced as a byproduct. However, this syngas has a relatively high ratio with a low yield due to the low selectivity towards forming syngas at low temperatures. Furthermore, the operational conditions of the CARGEN™ reactor do not favor a 100% conversion. While this leads to a lot of unreacted feed components, those reacted will mostly form solid carbon only. This serves in reducing the C:H ratio in the second reactor. The blue zone represents the conditions at which syngas is produced from the reformer with relatively low solid carbon formation due to the favored selectivity towards producing syngas at high temperatures.

This segregation of the product generation leads to a symbiotic relationship between the two reactors, which resulted in the development of the CARGEN™ technology.

### 3.2. Fischer-Tropsch (FT) Reaction

The FT process is a catalytic reaction that converts the syngas to synthetic crude oil (syncrude) that contains a range of HC ranging from C<sub>1</sub> to C<sub>100</sub>. This reaction is modeled by assuming the following stoichiometric reaction<sup>58</sup>.



The composition of the FT products depends on the catalyst used and the operating conditions. The product distribution is determined by the chain growth probability factor, or the Anderson Schulz Flory (ASF) distribution model known as the  $\alpha$ -value of the catalyst in addition to the carbon number  $n$ . They are related to the weight fraction of each carbon number in the product  $x_n$  through the Schulz-Flory Equation<sup>58</sup>.

$$x_n = (1-\alpha) \alpha^{(n-1)} \quad \text{Eq. 14}$$

The alpha value is dependent on the catalyst type and the reactor operating conditions. Much research has been done on studying the effect of different catalysts on the FT process performance<sup>61-63</sup>. Iron and cobalt-based catalysts are the most commonly used in the industry. These two catalysts have different hydrogenation activities where the iron-based catalyst produces more olefinic products and containing oxygenates, unlike cobalt-based catalysts, which form more paraffinic products<sup>58</sup>. The choice of the catalyst depends on the desired end products in addition to the operational experience and license availability.

The operating temperature and pressure are additional and critical parameters that offer flexibility in the product selectivity and conversion of syngas. The FT reaction can be deployed in a fixed-bed, slurry bed, or fluidized bed reactor. The process can be classified as a high-temperature FT process (HTFT) or low-temperature FT process (LTFT). The HTFT process occurs at a temperature range of 572 to 662 °F, while the LTFT occurs at a range of 392 and 428 °F.

Moreover, the H<sub>2</sub>:CO ratio required in the FT reactor depends on the type of catalyst used. When using a cobalt-based catalyst, the required H<sub>2</sub>:CO ratio is 1.8 to 2.1, while that for the iron-based catalyst is less than 1, which favors the WGS<sup>64</sup>. Therefore, iron-based catalysts are more widely used for coal-derived syngas, while cobalt-based are used for natural gas-based GTL plants.

### 3.3. Syncrude Refining

The design of the refinery unit in a GTL plant depends on the desired end product. In this work, the SASOL ORYX GTL plant design is followed in which only intermediate products and LPG are produced. The syncrude refining unit comprises a hydrocracker for upgrading the long-chain HC and fractionating column that separates the products into different HC cuts. In this model, a simplifying assumption was made, i.e., C<sub>20+</sub> HC are cracked to smaller chains, as seen in the following equations.



For simplicity, all the C<sub>30+</sub> HC are lumped as C<sub>30</sub>.

The fractionation process's objective is to separate the HC into different cuts according to their boiling range, as seen in *Table 1*<sup>37,65,66</sup>.

**Table 1** Syncrude fractions

Fractions	Composition	Boiling Range (°F)
LPG	C <sub>2</sub> -C <sub>4</sub>	-127 – 31
Gasoline	C <sub>5</sub> -C <sub>12</sub>	82 – 408
Diesel Oil	C <sub>13</sub> -C <sub>18</sub>	442 – 595
Wax	C <sub>19+</sub>	+617

#### 4. RESEARCH OBJECTIVES

This work aims to retrofit and study the impact of replacing the ATR process of a pre-existing GTL plant with the CARGEN™ technology that composed of two-reactor system. In particular, the goal is to compare the retrofitted and CARGEN™ implemented GTL process with the ATR-based GTL process in terms of crucial metrics seen below at the same production capacity of 50,000 bbl/day:

- natural gas conversion
- water generation
- power and energy consumption
- direct and indirect CO<sub>2</sub> emissions.

This work builds on the previous studies conducted in a research collaboration by Gabriel et al.<sup>43,67</sup>, wherein the objective was to compare the performances of the benchmark reforming processes. The systematic approach adopted in this work includes:

*Step 1:* Re-development and validation of the ATR-based GTL process with the previous study<sup>43,68</sup>,

*Step 2:* Developing of the two-reactor CARGEN™-based GTL superstructure model on ASPEN Plus<sup>®</sup>,

*Step 3:* Comparing the performances of the two flowsheets and studying the differences in terms of the key metrics,

*Step 4:* Performing a heat integration pinch analysis and analytically developing a heat exchanger network in order to minimize heating and cooling utilities and determine the total energy requirement of each plant,

This work's outcome demonstrates the improvement achieved in terms of water, CO<sub>2</sub>, power, and energy by retrofitting the existing GTL process plant with the novel CARGENT™ technology.



## 5. DEVELOPMENT OF THE ASPEN PLUS® FLOWSHEET OF THE GTL MODEL

This section describes the ASPEN Plus® model for the production of gasoline from natural gas through a GTL superstructure consisting of the following three main blocks as highlighted earlier:<sup>36</sup>

- Reforming unit for the production of syngas
- FT unit for the conversion of syngas to long-chain HC
- Refinery for the cracking and fractionation of HC

### 5.1. ATR

The base case model developed in the current work is based on the instructions and details presented in the process work of Gabriel et al.<sup>36</sup>. The CARGEN™-based GTL model is simulated using a debottlenecking approach such that the only difference between the two models is the reforming unit, whereas the other units remain the same with minimal differences. The flowsheets of the ATR and CARGEN™-based models are provided in *Figure 18* and *Figure 19*. The properties of the natural gas feedstock used in this model are provided in *Table 2*.

**Table 2** Natural gas feedstock properties

Component	Mole Fraction (%)
CO <sub>2</sub>	0.59
N <sub>2</sub>	0.08
CH <sub>4</sub>	95.39
C <sub>2</sub> H <sub>6</sub>	3.91
C <sub>3</sub> H <sub>8</sub>	0.03
Temperature (°F)	79
Pressure (Psia)	310

The feedstock conditions of high-pressure steam (HP steam) and oxygen are also provided in *Table 3*. Oxygen is assumed to come from an air separation unit (ASU).

**Table 3** Feedstock properties

	Temperature (°F)	Pressure (Psia)
HP Steam	437	370
Oxygen	95	17

### 5.1.1. Saturation

The natural gas fed to the GTL process facility is free from sulfur compounds like H<sub>2</sub>S and mercaptans and doesn't contain significant amounts of CO<sub>2</sub>. The dry natural gas is first compressed to 370 psia to meet the pre-reformer operational pressure and then heated to 300 °F<sup>36,69</sup>. It is then saturated to increase its water content in a saturator operating at

the same pressure as the pre-reformer. The saturator is modeled as a RADFRAC absorption column on ASPEN Plus®. Its wash water flowrate is set using a calculator block following the relation below.

$$\text{Wash Water} = 0.1 \times C_{1-DRY} \quad \text{Eq. 18}$$

where,

- Wash Water is the flowrate of the water to be fed to the saturator
- $C_{1-DRY}$  is the methane flowrate in the dry natural gas stream.

The column is simulated to have two stages. The unabsorbed water recovered from the saturation process is taken as wastewater to be purified, whereas the saturated natural gas is taken to the pre-reformer<sup>36</sup>. *Figure 8* details the saturation and pre-reformer section.

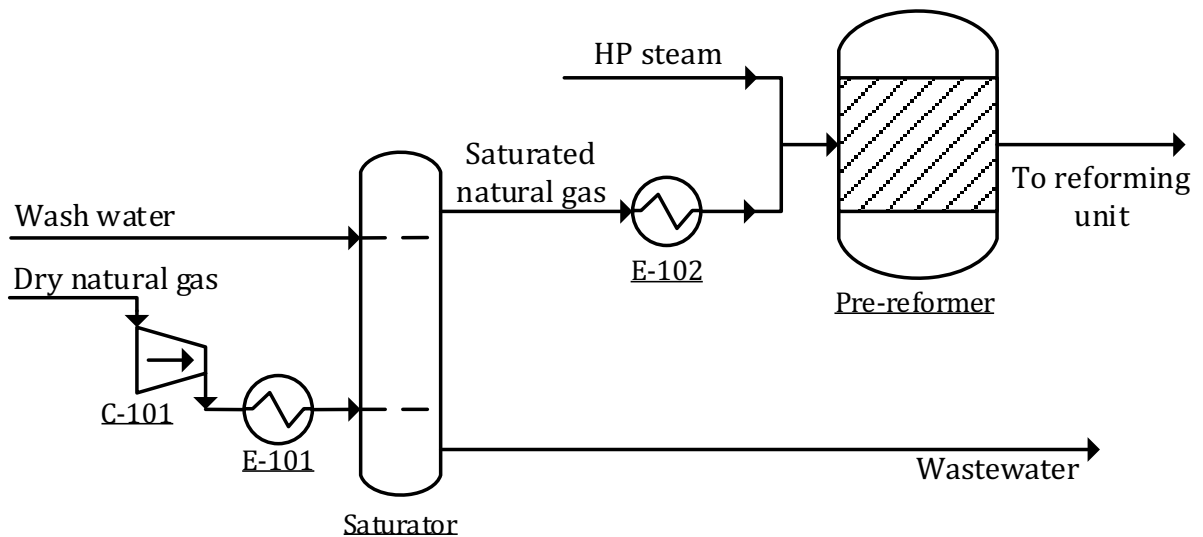


*Figure 8* Saturation and pre-reforming of natural gas

### 5.1.2. Pre-Reforming

Adiabatic pre-reforming is the steam reforming of HC to convert to lower HC like CH<sub>4</sub>, carbon oxides, and H<sub>2</sub> at a low temperature and high pressure.<sup>58</sup> Although this step is not essential, it is advantageous for the overall process as it reduces the risk of coking during the primary gas reforming process and improves the process economically<sup>70</sup>.

The pre-reformer pressure is set to 370 psia according to the industrial operational pressure of SRM. Since the feed is a natural gas and the target products are H<sub>2</sub> and CO, the inlet temperature range must be from 662 to 1022 °F. Additional steam must also be fed to the reactor to meet the steam to carbon atoms ratio range from 0.3 to 2<sup>70</sup>. This is set using the calculator feature, as seen in the relation below<sup>36</sup>.

$$HPSTEAM_1 = 0.4(C_{1-SAT} + 2C_{2-SAT} + 3C_{3-SAT}) - W_{1-i} \quad \text{Eq. 19}$$

where,

- HPSTEAM<sub>1</sub> is the steam flowrate to be fed to the pre-reformer
- C<sub>1-SAT</sub>, C<sub>2-SAT</sub>, and C<sub>3-SAT</sub> are the methane, ethane, and propane flowrates in the saturated natural gas stream, respectively
- W<sub>1-i</sub> is the flowrate of the water already present in the saturated natural gas stream.

The inlet feed temperature is set to 700 °F, while the H<sub>2</sub>O:C ratio is set to 0.4. The pre-reformer is simulated as an equilibrium RGIBBS reactor, which uses the concept of Gibbs free energy minimization to determine the product composition at equilibrium. Gibbs free energy is the total free energy in the system available to do useful or external work, and it

is a function of the temperature, pressure, and composition. The RGIBBS model can determine phase equilibrium without specifying a chemical reaction, and it is the only unit operation model on ASPEN Plus<sup>®</sup> that can handle solid-phase equilibria<sup>71</sup>.

### 5.1.3. Reforming

As stated earlier, two different reforming processes, ATR and CARGEN<sup>™</sup>, were modeled in this study. A detailed process description of ATR is presented in this section. The process description of the CARGEN<sup>™</sup> reforming process is provided in a later section.

ATR is the conversion of natural gas to syngas in the presence of oxygen and steam. It is operated adiabatically at a pressure of 435 psia with the reactor outlet temperature maintained at 1949 °F<sup>57</sup>.

Following industrial practice, an O:C ratio of 0.6 is required. This is done by co-feeding additional oxygen to maintain an overall ratio of 0.6<sup>36,57</sup>. A calculator block is used for this purpose. It is programmed as per the following mathematical equation.

$$O_{2-FRESH} = 0.6(C_1 + 2C_2 + \dots + 9C_9 + 10C_{10}) - O_{2-i} \quad \text{Eq. 20}$$

where,

- $O_{2-FRESH}$  is the flowrate of the additional oxygen to be fed
- $O_{2-i}$  is the flowrate of the oxygen initially present in the combined stream
- $C_1$  to  $C_{10}$  are the flowrates of methane to n-decane present in the combined stream. The flowrates of 'C<sub>11</sub>H<sub>24</sub>' to 'C<sub>30</sub>H<sub>62</sub>' are assumed to be negligible.

Additional HP steam is also fed through a design specification that varies its flowrate such that the reformer outlet maintains an H<sub>2</sub>:CO ratio of 2.15<sup>36,72</sup>. Maintaining this ratio is essential for the operation of commercial cobalt-based FT processes. However, it must be noted that although the steam flowrate was set using a design specification, it was ensured that the ATR required C:O<sub>2</sub>:H<sub>2</sub>O ratio of 1:0.6:0.1 was met by analytical hand calculation.

*Figure 9* shows the reforming, heat recovery, and water separation units in the ATR-based plant. Oxygen is first fed and compressed in a multistage compressor to a pressure of 435 psia. It is then fed to a heater, used to maintain the reformer outlet temperature at 1949 °F<sup>36</sup>. This is done through a design specification that varies the heater's outlet temperature, such that the outlet temperature of the reformer remains constant at 1949 °F.

Similar to the oxygen stream, the combined HP steam, pre-reformed gases, and the tail gas recycled back from the FT reactor (discussed in more detail in a later section) is also compressed to 435 psia and heated such that the reformer outlet temperature is maintained at 1949 °F. This combined stream is mixed with oxygen and fed to the reformer. Similar to the pre-reformer, ATR is modeled as an RGIBBS reactor. Finally, the reformer products are sent to a heat recovery, where they are cooled to 122 °F, and then flashed in a two-phase separator adiabatically to remove water from the stream.

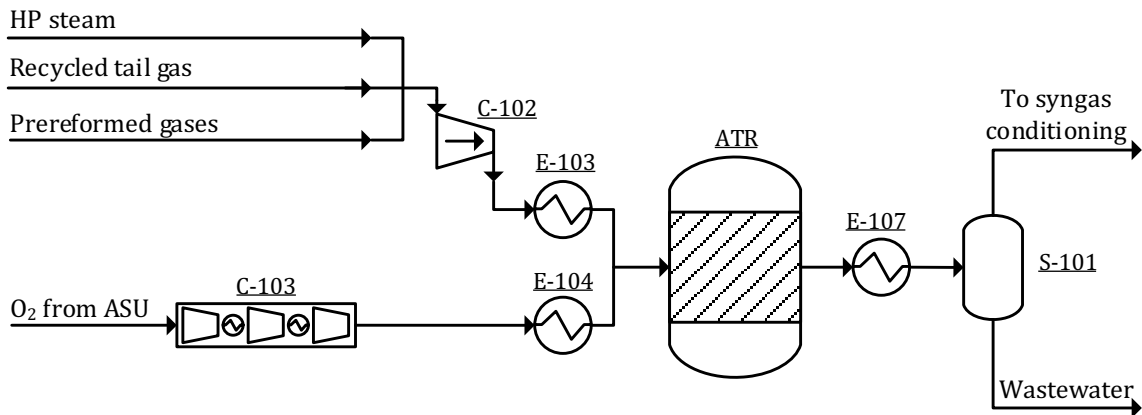


**Figure 9** Reforming unit, heat recovery, and water separation unit of an ATR-based GTL plant

#### 5.1.4. Syngas Conditioning

The vapor obtained from the flash tank after the reformer comprises  $\text{CO}_2$ ,  $\text{CO}$ ,  $\text{H}_2$ ,  $\text{N}_2$ , and water traces. Therefore, before feeding this stream to the FT reactor, it undergoes multiple separation stages known as conditioning as seen in *Figure 10*.

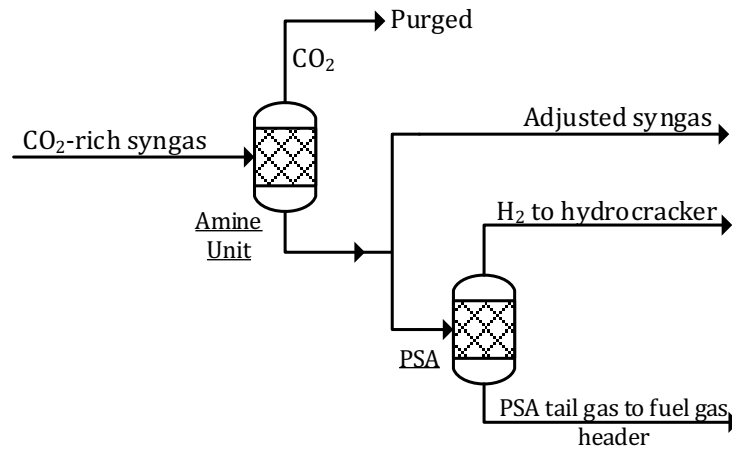


**Figure 10** ATR syngas conditioning unit

CO<sub>2</sub> is first removed from the stream in a CO<sub>2</sub> removal unit to reduce the overall inert concentration. This is done using a diethanolamine (DEA) based chemical absorption process. In this process, the CO<sub>2</sub>-rich syngas is fed to the bottom of an absorption column while the lean amine is fed counter currently from the top. CO<sub>2</sub> is then absorbed through chemical absorption. The CO<sub>2</sub>-free syngas leaves from the top of the absorption column while the rich amine stream leaves from the bottom. The rich amine stream is then taken to a stripping unit where CO<sub>2</sub> is removed to regenerate a lean amine stream. It is then recycled back to the absorption column<sup>36,65</sup>. The amine gas treatment is modeled on PROMAX<sup>®</sup>. However, it is not reported in this paper to maintain brevity in the discussion. In ASPEN Plus<sup>®</sup>, it is modeled as a black box using a separator and setting a 99.954% separation of CO<sub>2</sub> from the syngas stream<sup>36</sup>. In the case of ATR, the separated CO<sub>2</sub> is vented.

After CO<sub>2</sub> removal, the syngas obtained is adjusted by splitting the stream and sending it to a pressure swing absorption (PSA) unit to recover the H<sub>2</sub> from the stream, which is then used in the hydrocracking unit<sup>36</sup>. The split ratio is set using a design specification as follows.

$$H_{2-PSA} - 0.02CO_{FT} = 1 \quad \text{Eq. 21}$$

where,

- H<sub>2-PSA</sub> is the molar flowrate of H<sub>2</sub> in the stream taken to the PSA
- CO<sub>FT</sub> is the molar flowrate of the CO in the stream taken to the FT reactor



Similar to the amine unit, the PSA is simulated as a black box. An 87% recovery of H<sub>2</sub> with a purity of 99.99% is assumed as per the previous studies' guidelines<sup>36</sup>. Meanwhile, the PSA tail gas is sent to the fuel gas header.

### 5.1.5. Fischer-Tropsch Synthesis

In the FT process, syngas is converted into a range of HC via the following reaction<sup>73</sup>.



According to Eq. 22, the feed syngas ratio should approximately be around 2.15 to ensure optimal conversion for the cobalt-based catalyst used for the LTFT process<sup>74</sup>. The simulated FT unit utilizes a slurry bed reactor operating with a cobalt catalyst at a temperature of 428° F and a pressure of 363 psia<sup>64</sup>. To model this reaction, the product distribution was determined using the chain growth probability factor  $\alpha$ , which describes the total product spectrum in terms of carbon number and weight fractions<sup>75</sup>. For an  $\alpha$  value of 0.92, the stoichiometric coefficients for the FT reaction are provided in **Table 4**. For this high  $\alpha$  value, the product distribution is expected to be primarily paraffinic, ranging between C<sub>1</sub> and C<sub>100</sub>. However, to simplify modeling this reaction, the C<sub>30+</sub> components are lumped as C<sub>30</sub>H<sub>62</sub>. The FT reaction is modeled using an RSTOIC block with a 70% conversion of CO<sup>36</sup>.

**Table 4** Stoichiometric coefficients of the FT reaction

Component	Coefficient	Component	Coefficient
CO	-1.0005	C <sub>16</sub> H <sub>34</sub>	0.0018
H <sub>2</sub>	-2.0806	C <sub>17</sub> H <sub>36</sub>	0.0016
CH <sub>4</sub>	0.0064	C <sub>18</sub> H <sub>38</sub>	0.0015
C <sub>2</sub> H <sub>6</sub>	0.0055	C <sub>19</sub> H <sub>40</sub>	0.0014
C <sub>3</sub> H <sub>8</sub>	0.005	C <sub>20</sub> H <sub>42</sub>	0.0013
C <sub>4</sub> H <sub>10</sub>	0.0047	C <sub>21</sub> H <sub>44</sub>	0.0012
C <sub>5</sub> H <sub>12</sub>	0.0043	C <sub>22</sub> H <sub>46</sub>	0.0011
C <sub>6</sub> H <sub>14</sub>	0.004	C <sub>23</sub> H <sub>48</sub>	0.001
C <sub>7</sub> H <sub>16</sub>	0.0037	C <sub>24</sub> H <sub>50</sub>	0.0009
C <sub>8</sub> H <sub>18</sub>	0.0034	C <sub>25</sub> H <sub>52</sub>	0.0009
C <sub>9</sub> H <sub>20</sub>	0.0031	C <sub>26</sub> H <sub>54</sub>	0.0008
C <sub>10</sub> H <sub>22</sub>	0.0029	C <sub>27</sub> H <sub>56</sub>	0.0007
C <sub>11</sub> H <sub>24</sub>	0.0027	C <sub>28</sub> H <sub>58</sub>	0.0007
C <sub>12</sub> H <sub>26</sub>	0.0025	C <sub>29</sub> H <sub>60</sub>	0.0006
C <sub>13</sub> H <sub>28</sub>	0.0023	C <sub>30</sub> H <sub>62</sub>	0.0106
C <sub>14</sub> H <sub>30</sub>	0.0021	H <sub>2</sub> O	1
C <sub>15</sub> H <sub>32</sub>	0.0019		

As seen in *Figure 11*, the adjusted syngas is first compressed and heated to the FT reactor's conditions. The FT reactor products are sent to a flash tank to separate the vapor and liquid phases. The flash tank is operated adiabatically at the pressure of the FT reactor. The liquid phase obtained, known as the FT wax, is dominated by long-chain HC (C<sub>15</sub> to C<sub>30</sub>), while unreacted CO and H<sub>2</sub> dominate the vapor phase along with H<sub>2</sub>O and HC. Therefore, the

vapor phase must be treated before taking the syngas to the hydrocracker. This is done by reducing the stream's temperature to 60 °F and feeding it to a three-phase separator. The light gases, known as FT tail gas ( $H_2$  and  $CO$ ), are obtained from the top of the flash tank. It is then split into two streams at a 1:1 ratio, where half is sent to the fuel header while the other half is recycled back to the reformer.

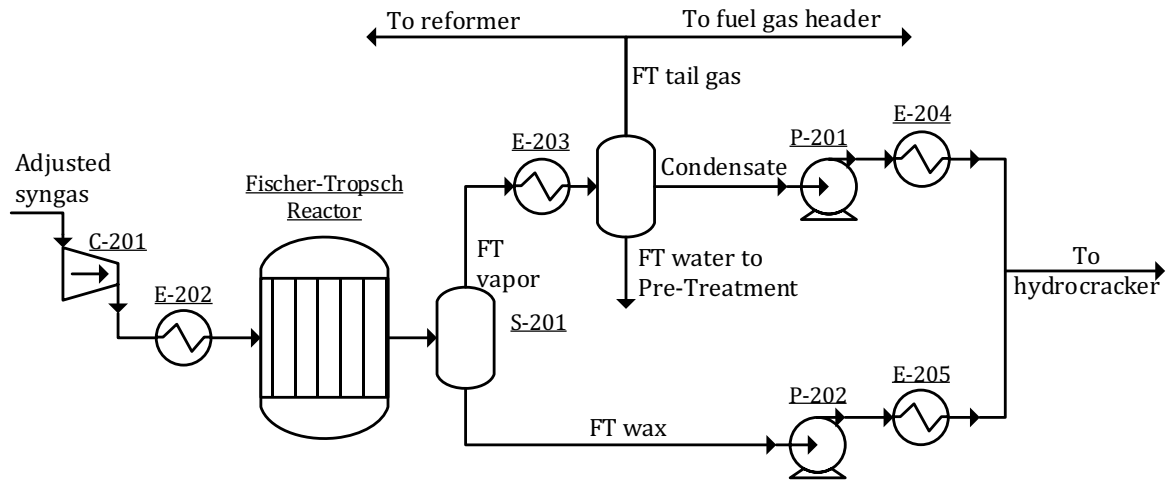


*Figure 11 FT synthesis and product recovery*

Meanwhile, the FT water leaving from the bottom of the flash tank is sent to the water pre-treatment unit. Finally, the condensate rich in HC leaves from the center of the three-phase separator. The FT wax and condensate are then compressed to a pressure of 1015 psia and heated to the temperature of the hydrocracker<sup>36</sup>.

### 5.1.6. Refinery

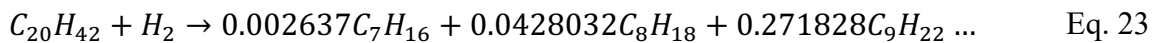
The refinery is constituted of two processes; hydrocracking and fractionation. In the hydrocracker, the long-chain HC are cracked into smaller chains using  $H_2$  from the PSA.

Depending on the hydrocracking operating conditions, the product composition varies between LPG, gasoline, diesel oil, and wax<sup>65</sup>.

The FT wax, FT condensate, and the H<sub>2</sub> obtained from the PSA are fed into the hydrocracker. These are also co-fed with the heavy and light HC recycled from the fractionation unit. The hydrocracker is operated isothermally at 662 °F and 1015 psia modeled using an RSTOIC reactor with a 65% conversion per pass<sup>36</sup>. For simplification, it is assumed that all the C<sub>20+</sub> HC are cracked into smaller chain molecules. The stoichiometric coefficients for the hydrocracking of C<sub>20</sub> and C<sub>21</sub> are provided in

Hydrocarbon	C20H42	C21H44
C7H16	0.002637	0.002637
C8H18	0.042803	0.042803
C9H20	0.271828	0.271828
C10H22	1.365466	0.682733
C11H24	0.271828	0.682733
C12H26	0.042803	0.271828
C13H28	0.002637	0.042803
C14H30		0.002637

For example, using the stoichiometric coefficients provided, the hydrocracking of C<sub>20</sub>H<sub>42</sub> is as follows.

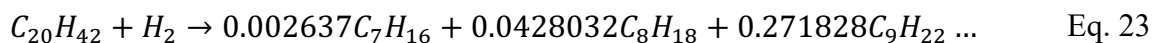


<sup>36,37</sup>. These coefficients are repeated for even and odd carbon number HC<sup>36,37</sup>.

**Table 5** Stoichiometric coefficients for the hydrocracking reactions

Hydrocarbon	C <sub>20</sub> H <sub>42</sub>	C <sub>21</sub> H <sub>44</sub>
C <sub>7</sub> H <sub>16</sub>	0.002637	0.002637
C <sub>8</sub> H <sub>18</sub>	0.042803	0.042803
C <sub>9</sub> H <sub>20</sub>	0.271828	0.271828
C <sub>10</sub> H <sub>22</sub>	1.365466	0.682733
C <sub>11</sub> H <sub>24</sub>	0.271828	0.682733
C <sub>12</sub> H <sub>26</sub>	0.042803	0.271828
C <sub>13</sub> H <sub>28</sub>	0.002637	0.042803
C <sub>14</sub> H <sub>30</sub>		0.002637

For example, using the stoichiometric coefficients provided, the hydrocracking of C<sub>20</sub>H<sub>42</sub> is as follows.



The hydrocracker products are then taken to a heat exchanger for heat recovery, where they are cooled to 400 °F. It is then followed by a vapor-liquid separation unit known as a hot separator to recover the H<sub>2</sub> from the product stream for recycling. The separator is operated adiabatically at a pressure of 55 psia<sup>36</sup>. During this separation, some HC leave from the top stream of the flash tank with the H<sub>2</sub>. Therefore, the separation efficiency is improved by further cooling down the stream and feeding into a second flash tank, a cold separator, operated at 122 °F and 55 psia.

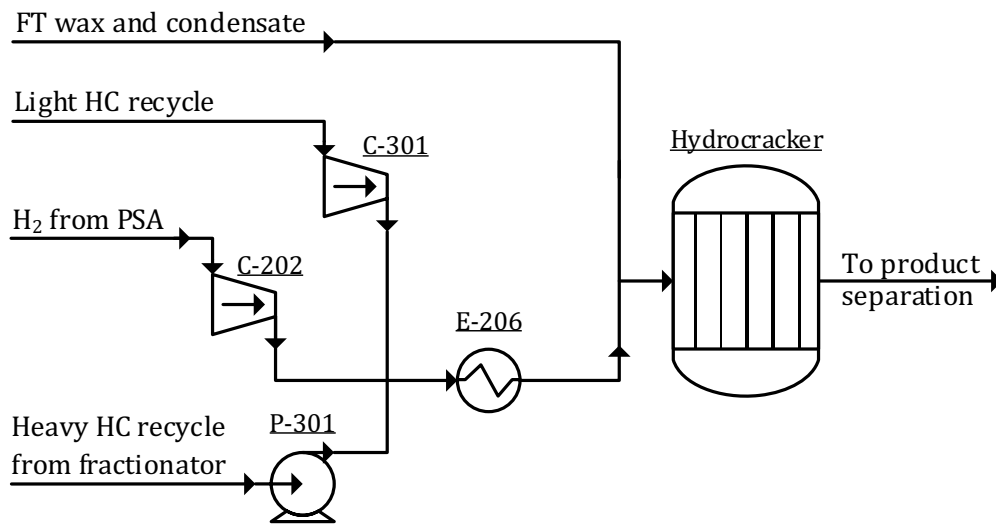


**Figure 12** Hydrocracking unit of the GTL plant

To prevent an inert gas buildup, some of the  $H_2$  obtained from the cold separator top stream is removed and combined with  $H_2$  gas obtained from the PSA and fed back to the hydrocracker. Meanwhile, the bottom streams of the cold and hot separators are mixed and taken to the fractionator<sup>36</sup>, as shown in *Figure 13*.

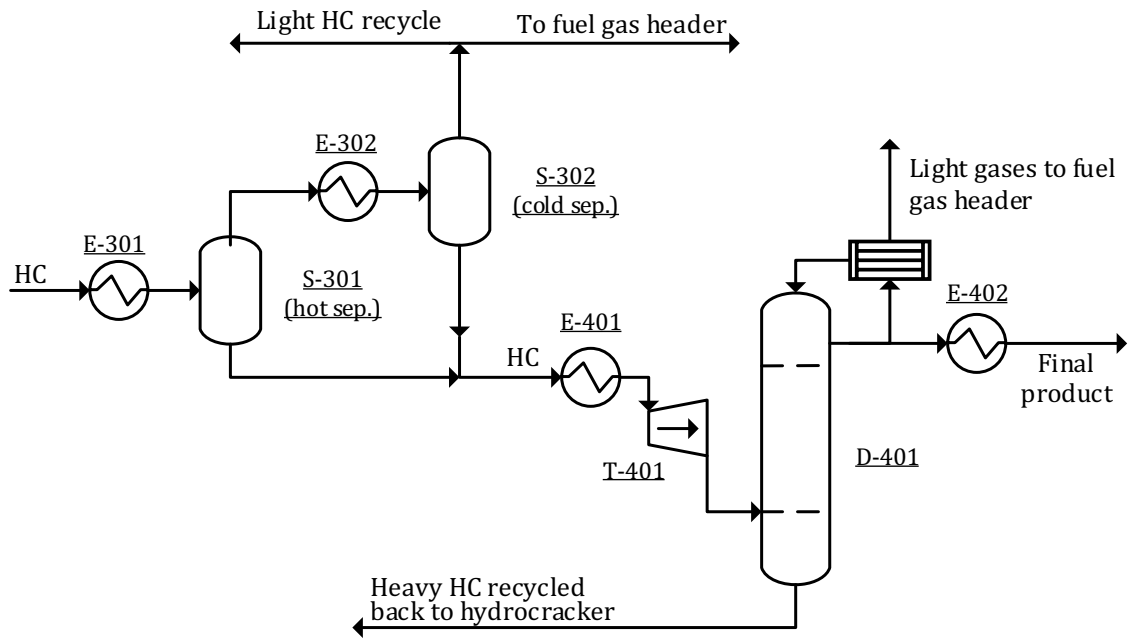


**Figure 13** Hydrocracking product recovery and fractionation

The HC are heated to 733 °F and fed to the bottom of the fractionation column. The column is modeled as a RADFRAC. It is operated at a pressure of 55 psia with a 0.1 psia pressure drop and a distillate to feed ratio of 0.27. It is designed to have 45 stages based on industrial practice<sup>76</sup>.

The heavy HC are obtained from the bottom of the fractionation column, dominated by C<sub>13+</sub> molecules. This stream is pumped and heated to the hydrocracker's operating conditions and recycled back for further cracking<sup>36</sup>. The lighter components rise to the top of the column forming both vapor and distillate products. This is done by specifying a partial-vapor-liquid condenser at a temperature of 302 °F. The vapor obtained is dominated by water and H<sub>2</sub> with HC traces, mainly those in the LPG range. This stream

is known as “lights” and is taken to the fuel gas header. Meanwhile, the distillate product obtained is dominated by C<sub>5</sub> to C<sub>12</sub> HC, known as gasoline. This product is the desired cut, and therefore it is taken to a heat recovery unit where it is cooled down to 122 °F and then obtained as the final product<sup>36,65</sup>.

### 5.1.7. Water Pre-Treatment Unit

In the GTL plant, water is obtained from multiple sources, mainly the saturator, the reformer, and the Fischer Tropsch reactor. Before treating this water, it is necessary to remove the organic contaminants in the stream. This is done through a wastewater pre-treatment unit detailed in *Figure 14*, where contaminated water is sent to a distillation column that removes some of the organic components.

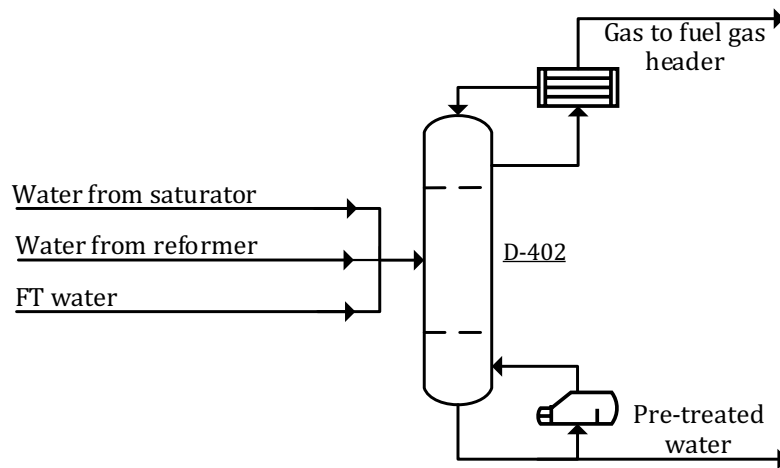


**Figure 14** Water pre-treatment unit

It is modeled using a RADFRAC column comprising of 4 stages. It is operated at 20 psia with a pressure drop of 0.1 psia. Also, a reflux ratio of 0.5 is specified with a distillate



flowrate of 15 lb/mol. The contaminants leaving from the top of the column are taken as fuel to the fuel gas header<sup>36</sup>. Meanwhile, the water is taken for further treatment, which is beyond the scope of this work.

### 5.1.8. Fuel Gas Header and Flaring

As stated in earlier sections, light gases from different GTL plant units are taken as fuel gas to the header. Unreacted CO and H<sub>2</sub> dominate it in addition to small amounts of HC. To flare the fuel gas, it must first be combusted. This is done by feeding the fuel gas to a combustion chamber operated isothermally at 2000 °F at atmospheric pressure in the presence of air. The fuel gas undergoes complete combustion through its reaction with oxygen, in which CO, H<sub>2</sub>, and HC are converted to CO<sub>2</sub> and water, which is finally flared<sup>77</sup>.

This is shown in *Figure 15* below.

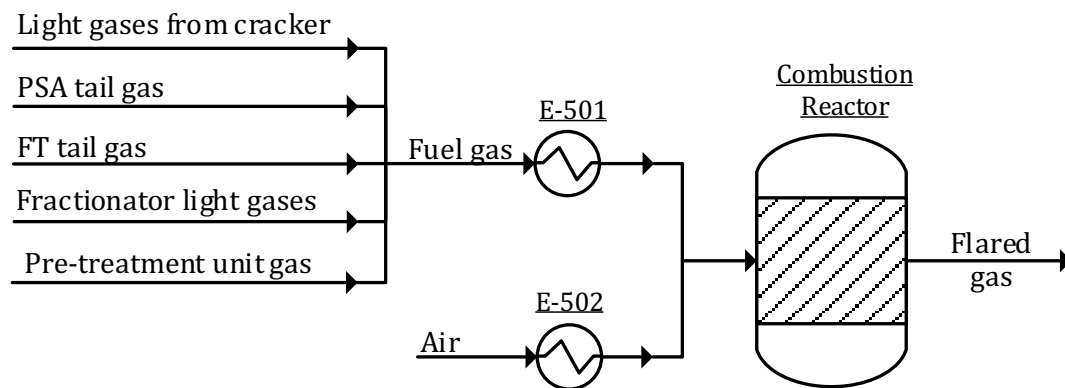


*Figure 15* Fuel gas combustion unit

## 5.2. CARGEN™

The retrofitted model is developed through debottlenecking approach; wherein, the ATR unit is replaced with the two-reactor CARGEN™ setup and with minimal changes to the other units of the plant. This section provides a process description of the CARGEN™ reforming section along with the additional modifications required upon replacing ATR.

### 5.2.1. Reforming

As seen earlier, natural gas is first saturated, pre-reformed, and combined with recycled tail gas. Unlike ATR, no additional steam is needed in the CARGEN™ process as the oxygen feed controls the syngas ratio. This is done using a design specification that manipulates the oxygen stream flowrate such that the syngas obtained from the reformer has a ratio of 2.15. Similar to ATR, it was ensured that the C: CO<sub>2</sub>: O<sub>2</sub> ratio of 1:1:0.1 was met to satisfy the CARGEN™ feed ratio requirement. Therefore, the oxygen stream is first compressed to 363 psia in a multistage compressor and heated to 788 °F. Meanwhile, CO<sub>2</sub> is fed to the CARGEN™ reactor at a ratio of CO<sub>2</sub>:C of 1:1.

Therefore, this process requires a constant and fresh source of CO<sub>2</sub>. It can be obtained by recycling the CO<sub>2</sub> stream received from the amine unit. In ATR, the CO<sub>2</sub> obtained is purged. However, in the CARGEN™ setup, this CO<sub>2</sub> is recycled back and mixed with additional fresh CO<sub>2</sub> to meet the CO<sub>2</sub>:C ratio of 1:1. The flowrate of the extra CO<sub>2</sub> is set through a calculator block, per the following mathematical correlation.

$$CO'_{2-Fresh} = C'_1 + 2C'_2 + \dots + 9C'_9 + 10C'_{10} - CO'_{2-i} \quad \text{Eq. 24}$$

where,

- $CO'_{2-Fresh}$  is the flowrate of the additional CO<sub>2</sub> to be fed to the reactor
- $C'_1$  to  $C'_{10}$  are the flowrates of methane to n-decane present in the pre-reformed gases and the recycled tail gas. The flowrates of 'C<sub>11</sub>H<sub>24</sub>' and 'C<sub>30</sub>H<sub>62</sub>' are assumed to be negligible.
- $CO'_{2-i}$  is the flowrate of the recycled CO<sub>2</sub> stream coming from the amine unit.

The recycled CO<sub>2</sub> is combined with the recycled FT tail gas and the pre-reformed gases. It is then compressed to 363 psia and heated to 788 °F. The CO<sub>2</sub> feedstock is assumed to be separated and obtained from the flare<sup>77</sup>. The properties of the flared gas are provided in *Table 6* below.

**Table 6** Flare gas properties

Component	Mole Fraction (%)
CO <sub>2</sub>	7.86
N <sub>2</sub>	71.60
H <sub>2</sub> O	15.84
O <sub>2</sub>	4.70
Temperature (°F)	2000
Pressure (Psia)	362

Therefore, this stream is at atmospheric pressure and must be cooled before compression. First, it is fed to a heat exchanger where its temperature is cooled to 79 °F. Then, it is

compressed in a multistage compressor to 363 psia with a stage cooler temperature set to 788 °F. This scheme of operation is presented in *Figure 16*.

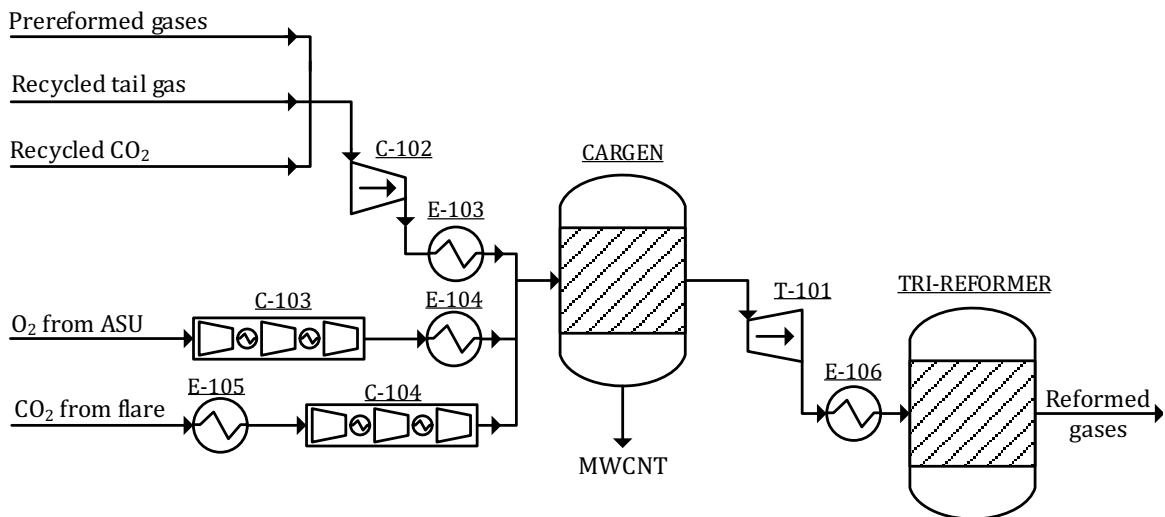


**Figure 16** Reforming unit of a CARGEN<sup>TM</sup>-based GTL plant

The streams are then mixed and fed to the CARGEN<sup>TM</sup> reactor. It is modeled as an equilibrium RGIBBS reactor operating adiabatically at 363 psia. Additionally, a constraint is set to ensure that the reactant product temperature does not exceed the maximum temperature range (1148 °F) of the CARGEN<sup>TM</sup> process<sup>19,59</sup>.

Most importantly, the reactor is designed to produce two phases, solid and vapor, obtained from two different product streams, as seen in *Figure 16*. In reality, both solid and gas products would be received in one stream and sent to an electrostatic separator from the fluidized bed reactor (or moving bed reactor), which recovers the solid carbon and catalyst and sends the unreacted gases to the tri-reformer. However, for modeling and simplification purposes, it is assumed that the solid and vapor phases are obtained from

the reactor in two separate streams. This is done by specifying the possible products and their valid phases to each outlet stream on ASPEN Plus®.

The vapor phase is then expanded to 290 psia and heated to 1508 °F to meet the tri-reformer operational temperature that is assumed to operate isothermally<sup>20</sup>. As stated earlier, the syngas ratio obtained from the reformer is maintained at 2.15 through a design specification that varies the inlet oxygen flowrate. Finally, the reformed gases are taken to heat recovery and water separation, similar to ATR.

### 5.2.2. Syngas Conditioning

As seen in ATR, the syngas must be conditioned before the FT reaction. However, instead of purging the CO<sub>2</sub>, it is recycled back to the reactor.

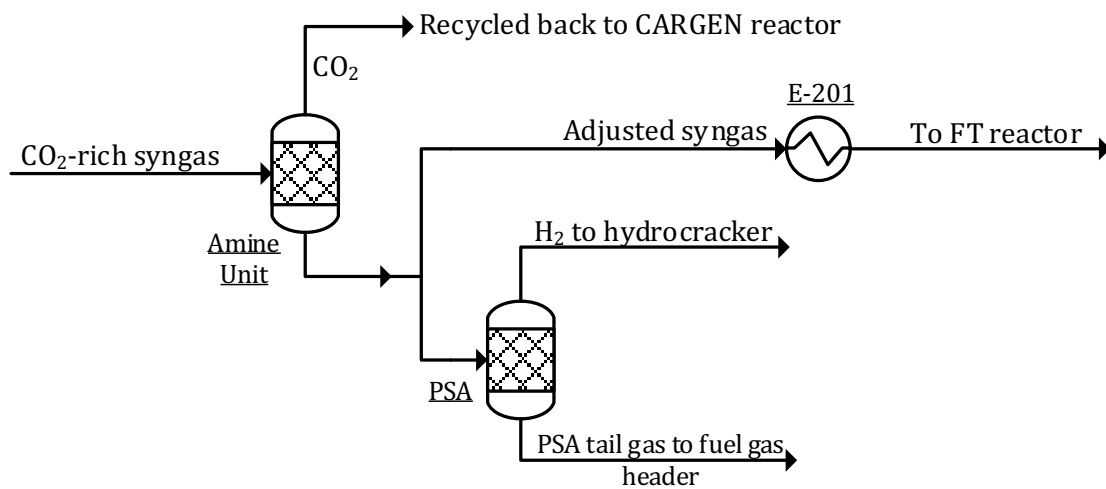


*Figure 17 CARGEN™ syngas conditioning*

The syngas obtained from the CARGEN™ setup has a 50% higher steam content than that obtained from ATR. Therefore, to avoid dew temperature issues in the pre-FT reactor compression, the adjusted syngas is heated. This heater is used to increase the adjusted syngas' temperature to 130 °F (higher than the stream dew temperature). The adjusted syngas is then taken to the FT synthesis unit, and the remainder of the process is carried out as seen in ATR. The syngas conditioning unit of the CARGEN™-based process is provided in *Figure 17*.

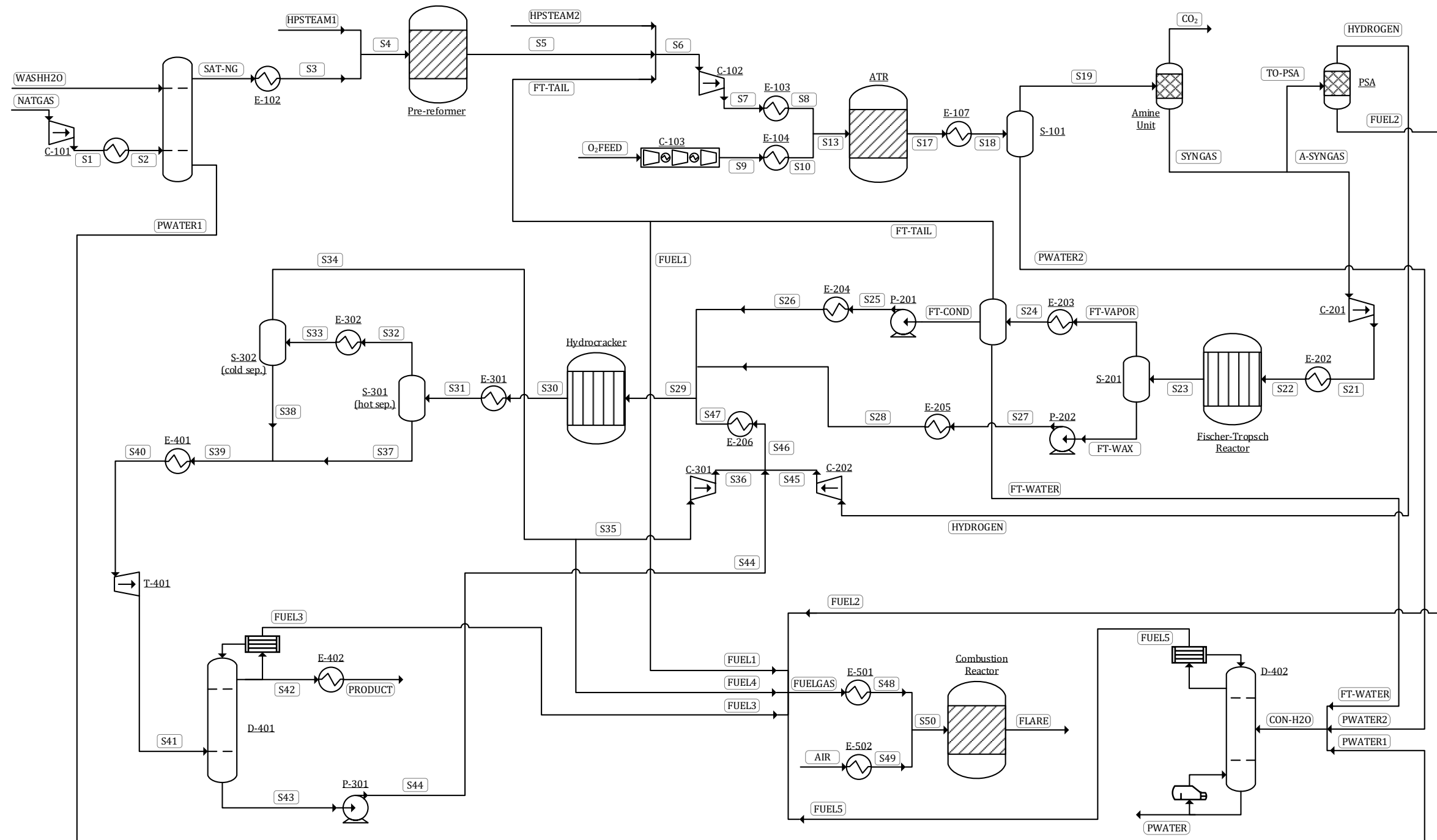
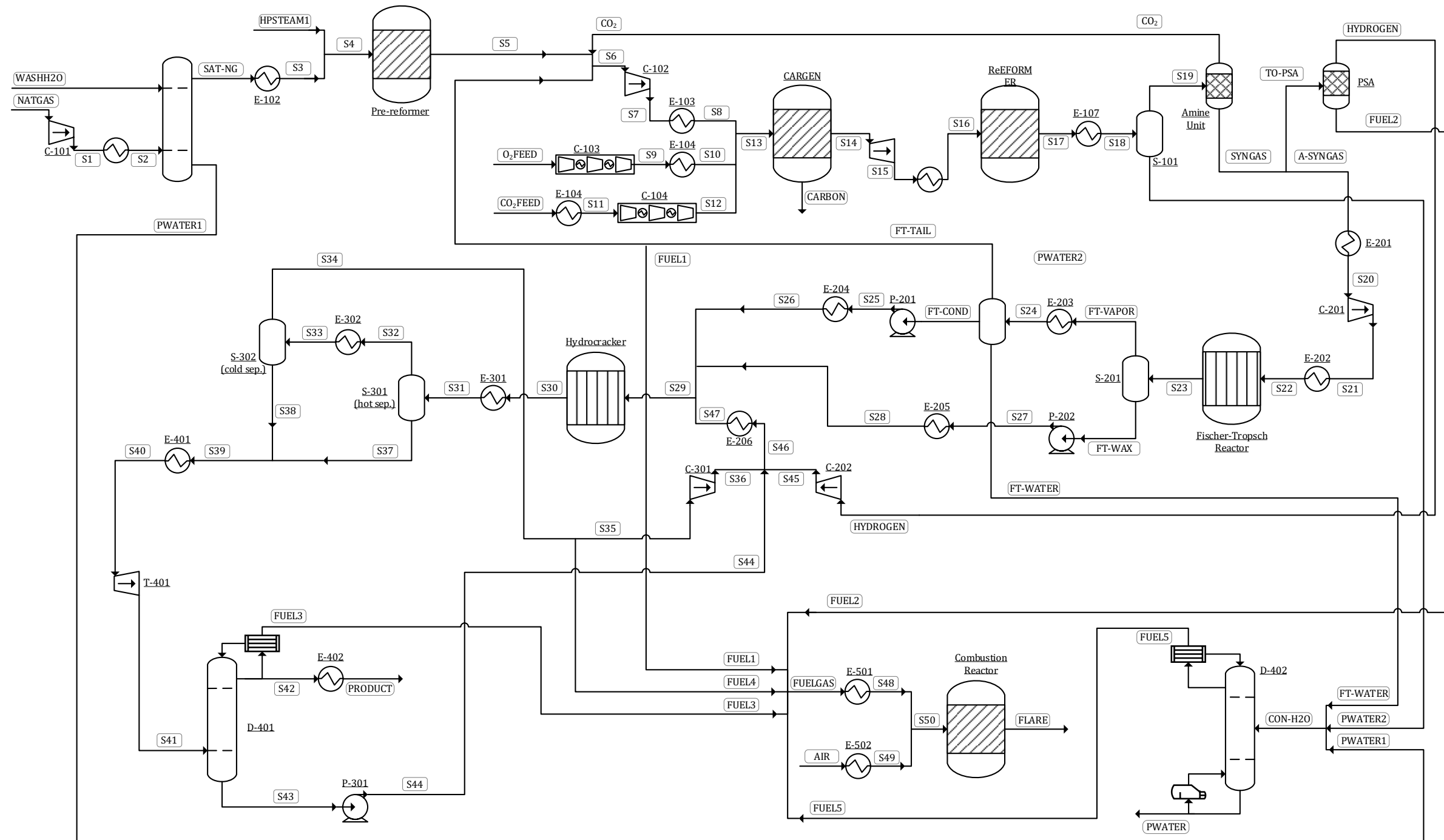


Figure 18 ATR-based GTL plant flowsheet



*Figure 19 CARGEN™-based GTL plant flowsheet*



## 6. RESULTS AND DISCUSSION

In this section, the model convergence of the developed ATR and CARGEN<sup>TM</sup>-based GTL processes will be validated by looking at the flowsheet balance report generated by ASPEN Plus<sup>®</sup>. The ATR-based model will then be validated by comparing its results to Gabriel et al.<sup>36</sup> work in terms of mass balance and key performance indicators (KPI) to confirm their agreement with the literature data. The ATR-based and CARGEN<sup>TM</sup>-based process results were then studied and compared in terms of natural gas conversion, CO<sub>2</sub> emissions, water generation, oxygen consumption, and power utilization. Finally, the heat integration pinch analysis results will be presented to compare the energy utilization of each developed model.

### 6.1. Validation of Model Convergence

For each developed model, ASPEN Plus<sup>®</sup> provides a flowsheet balance report that summarizes each component's overall input and output flowrates along with the relative difference between them and how much of each component is generated. This provides a clear insight into the generated model's validity to ensure that it has successfully converged as the overall simulation is in mass balance.

The ATR-based model flowsheet balance results are provided in *Table 7*.

**Table 7** ATR-based model flowsheet balance

Components Lbmol/hr	In	Out	Generation	Relative difference
CO	0.00000	0.784034	0.842108	$0.740712 \times 10^{-1}$
CO <sub>2</sub>	345.796	21450.9	21105.1	$0.468664 \times 10^{-9}$
H <sub>2</sub> O	28742.1	104996.	76253.7	$-0.192406 \times 10^{-5}$
H <sub>2</sub>	0.00000	3.40008	3.53475	$0.396083 \times 10^{-1}$
O <sub>2</sub>	87741.1	28497.8	-59243.4	$0.124388 \times 10^{-15}$
N <sub>2</sub>	195666	195666	$0.130795 \times 10^{-12}$	$0.144618 \times 10^{-8}$
CH <sub>4</sub>	55907.6	0.619505	-55906.9	$0.194045 \times 10^{-6}$
C <sub>2</sub> H <sub>6</sub>	2291.63	0.488656	-2291.14	$0.317924 \times 10^{-6}$
C <sub>3</sub> H <sub>8</sub>	17.5828	2.06551	-15.5167	$0.363018 \times 10^{-4}$
C <sub>4</sub> H <sub>10</sub>	0.00000	8.39062	8.39117	$0.648309 \times 10^{-4}$
C <sub>5</sub> H <sub>12</sub>	0.00000	25.5404	25.5407	$0.121537 \times 10^{-4}$
C <sub>6</sub> H <sub>14</sub>	0.00000	59.5175	59.5175	$0.421204 \times 10^{-6}$
C <sub>7</sub> H <sub>16</sub>	0.00000	98.8839	98.8837	$-0.280546 \times 10^{-5}$
C <sub>8</sub> H <sub>18</sub>	0.00000	126.334	126.333	$-0.355335 \times 10^{-5}$
C <sub>9</sub> H <sub>20</sub>	0.00000	159.386	159.385	$-0.306210 \times 10^{-5}$
C <sub>10</sub> H <sub>22</sub>	0.00000	265.856	265.855	$-0.169019 \times 10^{-5}$
C <sub>11</sub> H <sub>24</sub>	0.00000	289.189	289.189	$-0.133455 \times 10^{-5}$
C <sub>12</sub> H <sub>26</sub>	0.00000	272.025	272.024	$-0.109711 \times 10^{-5}$
C <sub>13</sub> H <sub>28</sub>	0.00000	259.772	259.771	$-0.271185 \times 10^{-5}$
C <sub>14</sub> H <sub>30</sub>	0.00000	324.338	259.771	$-0.123248 \times 10^{-5}$
C <sub>15</sub> H <sub>32</sub>	0.00000	758.562	758.561	$-0.136955 \times 10^{-5}$
C <sub>16</sub> H <sub>34</sub>	0.00000	215.986	215.987	$0.148071 \times 10^{-5}$
C <sub>17</sub> H <sub>36</sub>	0.00000	91.6598	91.6601	$0.237664 \times 10^{-5}$

*Table 7 Continued*

Components Lbmol/hr	In	Out	Generation	Relative difference
C <sub>18</sub> H <sub>38</sub>	0.00000	67.3039	67.3047	0.127888×10 <sup>-4</sup>
C <sub>19</sub> H <sub>40</sub>	0.00000	61.5967	61.6061	0.153670×10 <sup>-3</sup>
C <sub>20</sub> H <sub>42</sub>	0.00000	0.635672×10 <sup>-4</sup>	0.217922×10 <sup>-4</sup>	-0.657178
C <sub>21</sub> H <sub>44</sub>	0.00000	0.280459×10 <sup>-8</sup>	-0.277538×10 <sup>-4</sup>	-9896.84
C <sub>22</sub> H <sub>46</sub>	0.00000	0.194961×10 <sup>-12</sup>	-0.184943×10 <sup>-4</sup>	-0.948614×10 <sup>+8</sup>
C <sub>23</sub> H <sub>48</sub>	0.00000	0.307123×10 <sup>-17</sup>	-0.111448×10 <sup>-4</sup>	0.00000
C <sub>24</sub> H <sub>50</sub>	0.00000	0.00000	-0.685003×10 <sup>-5</sup>	0.00000
C <sub>25</sub> H <sub>52</sub>	0.00000	0.402005×10 <sup>-18</sup>	-0.481122×10 <sup>-5</sup>	0.00000
C <sub>26</sub> H <sub>54</sub>	0.00000	0.936084×10 <sup>-18</sup>	-0.284934×10 <sup>-5</sup>	0.00000
C <sub>27</sub> H <sub>56</sub>	0.00000	0.526784×10 <sup>-35</sup>	-0.158958×10 <sup>-5</sup>	0.00000
C <sub>28</sub> H <sub>58</sub>	0.00000	0.603967×10 <sup>-38</sup>	-0.117873×10 <sup>-5</sup>	0.00000
C <sub>29</sub> H <sub>60</sub>	0.00000	0.526476×10 <sup>-38</sup>	-0.738425×10 <sup>-6</sup>	0.00000
C <sub>30</sub> H <sub>62</sub>	0.00000	0.163755×10 <sup>-17</sup>	-0.889183×10 <sup>-5</sup>	0.00000
C	0.00000	0.00000	0.00000	0.00000

Looking at the relative difference results for each component, it is seen that they mostly fall below 10<sup>-3</sup>. However, the relative differences of C<sub>21</sub>H<sub>44</sub> and C<sub>22</sub>H<sub>46</sub> have much higher values. It must be noted that although these two relative differences are high, their outlet flowrates are very low (less than 10<sup>-8</sup>) and therefore do not affect the convergence of the model. The high relative difference, in this case, is due to the large size and complication of the model and the presence of multiple recycle streams. Overall, this is an excellent indication of the accuracy and success of the ATR-based developed model.

The following table shows the flowsheet balance results of the CARGEN<sup>TM</sup>-based model.

**Table 8** CARGEN<sup>TM</sup>-based model flowsheet balance

Components Lbmol/hr	In	Out	Generation	Relative difference
CO	0.00000	0.69056	0.590845	-0.144573
CO <sub>2</sub>	57195.2	20648.4	-36548.3	-0.259516×10 <sup>-4</sup>
H <sub>2</sub> O	43372.7	193036	149663	-0.967192×10 <sup>-8</sup>
H <sub>2</sub>	0.00000	3.27437	2.66653	-0.185638
O <sub>2</sub>	50651.0	12356.7	-38294.3	0.179561×10 <sup>-15</sup>
N <sub>2</sub>	188171	188171	-0.844935×10 <sup>-10</sup>	0.448424×10 <sup>-10</sup>
CH <sub>4</sub>	90115.4	2.41457	-90113.3	-0.315526×10 <sup>-5</sup>
C <sub>2</sub> H <sub>6</sub>	3693.80	0.401252	-3693.40	-0.350074×10 <sup>-6</sup>
C <sub>3</sub> H <sub>8</sub>	28.3412	1.69262	-26.6497	-0.419915×10 <sup>-4</sup>
C <sub>4</sub> H <sub>10</sub>	0.00000	6.86837	6.86711	-0.181977×10 <sup>-3</sup>
C <sub>5</sub> H <sub>12</sub>	0.00000	21.1886	21.1871	-0.698935×10 <sup>-4</sup>
C <sub>6</sub> H <sub>14</sub>	0.00000	51.1779	51.1762	-0.341816×10 <sup>-4</sup>
C <sub>7</sub> H <sub>16</sub>	0.00000	89.4754	89.4739	-0.172707×10 <sup>-4</sup>
C <sub>8</sub> H <sub>18</sub>	0.00000	119.818	119.817	-0.455505×10 <sup>-5</sup>
C <sub>9</sub> H <sub>20</sub>	0.00000	155.114	155.114	-0.242712×10 <sup>-5</sup>
C <sub>10</sub> H <sub>22</sub>	0.00000	261.749	261.749	-0.140837×10 <sup>-5</sup>
C <sub>11</sub> H <sub>24</sub>	0.00000	285.382	285.381	-0.141199×10 <sup>-5</sup>
C <sub>12</sub> H <sub>26</sub>	0.00000	268.651	268.650	-0.177631×10 <sup>-5</sup>
C <sub>13</sub> H <sub>28</sub>	0.00000	256.625	254.624	-0.201704×10 <sup>-5</sup>
C <sub>14</sub> H <sub>30</sub>	0.00000	320.448	320.447	-0.118698×10 <sup>-5</sup>
C <sub>15</sub> H <sub>32</sub>	0.00000	749.497	749.496	-0.203420×10 <sup>-5</sup>

**Table 8 Continued**

Components Lbmol/hr	In	Out	Generation	Relative difference
C <sub>16</sub> H <sub>34</sub>	0.00000	213.405	213.404	-0.428867×10 <sup>-5</sup>
C <sub>17</sub> H <sub>36</sub>	0.00000	90.5662	90.5643	-0.211259×10 <sup>-4</sup>
C <sub>18</sub> H <sub>38</sub>	0.00000	66.5016	66.5003	-0.201622×10 <sup>-4</sup>
C <sub>19</sub> H <sub>40</sub>	0.00000	60.8865	60.8699	-0.274094×10 <sup>-3</sup>
C <sub>20</sub> H <sub>42</sub>	0.00000	0.638781E <sup>-4</sup>	-0.258603×10 <sup>-3</sup>	-5.04839
C <sub>21</sub> H <sub>44</sub>	0.00000	0.283801E <sup>-8</sup>	-0.297758×10 <sup>-3</sup>	-104919
C <sub>22</sub> H <sub>46</sub>	0.00000	0.198508E <sup>-12</sup>	-0.272984×10 <sup>-3</sup>	-0.137518×10 <sup>+10</sup>
C <sub>23</sub> H <sub>48</sub>	0.00000	0.329203E <sup>-17</sup>	-0.248197×10 <sup>-3</sup>	0.00000
C <sub>24</sub> H <sub>50</sub>	0.00000	0.00000	-0.223395×10 <sup>-3</sup>	0.00000
C <sub>25</sub> H <sub>52</sub>	0.00000	0.634569E <sup>-18</sup>	-0.223405×10 <sup>-3</sup>	0.00000
C <sub>26</sub> H <sub>54</sub>	0.00000	0.00000	-0.198590×10 <sup>-3</sup>	0.00000
C <sub>27</sub> H <sub>56</sub>	0.00000	0.557704E <sup>-35</sup>	-0.173771×10 <sup>-3</sup>	0.00000
C <sub>28</sub> H <sub>58</sub>	0.00000	0.116217E <sup>-17</sup>	-0.173774×10 <sup>-3</sup>	0.00000
C <sub>29</sub> H <sub>60</sub>	0.00000	0.130959E <sup>-37</sup>	-0.148950×10 <sup>-3</sup>	0.00000
C <sub>30</sub> H <sub>62</sub>	0.00000	0.00000	-0.263148×10 <sup>-2</sup>	0.00000
C	0.00000	95375.4	95375.4	0.00000

Like ATR, the component relative differences in the CARGEN<sup>TM</sup>-based model mostly fall below 10<sup>-3</sup> except for C<sub>21</sub>H<sub>44</sub> and C<sub>22</sub>H<sub>46</sub>. As seen earlier, although the relative differences are high, the outlet flowrates are very low, which does not affect the model convergence. Overall, the developed model is accurate and has successfully converged.

Based on a preliminary comparison between the two flowsheet balance tables, the most significant differences between the two models are:

- The CH<sub>4</sub> inlet flowrate is lower in the ATR-based model
- The CO<sub>2</sub> generation in the ATR-based model is positive, indicating that ATR is a net producer of CO<sub>2</sub> in terms of direct emissions. Meanwhile, the CO<sub>2</sub> generated in the CARGEN<sup>TM</sup>-based model is negative, meaning that the plant is a net consumer of CO<sub>2</sub>
- The ATR-based model has a lower generation of H<sub>2</sub>O
- The CARGEN<sup>TM</sup>-based model produces a significant amount of carbon, unlike the ATR-based model, which has no generation.

These findings will be explained and discussed in more detail in the sections 6.2 and 6.3.

## **6.2. ATR-based Model Validation**

After validating the model's convergence, the ATR-based GTL process will first be further confirmed by comparing its results to those obtained from Gabriel et al.<sup>36</sup>. Starting with the mass balance results, *Table 9* compares the differences in the feed and product stream mass flowrates in addition to the percentage difference between them. For comparison purposes, it is assumed that the fuel gas is the product stream in this model.

**Table 9** Comparison of the literature and reproduced model mass balance results

<b>Stream (lb/hr)</b>	Literature (Gabriel et al. <sup>36</sup> )	ATR Model (Current Model)	% Difference
<b>Input</b>			
Saturator Water Feed	102,381	97,542	4.73%
HP Steam	455,267	402,681	11.55%
Natural Gas Feed	953,276	952,115	0.12%
Oxygen Feed	1,171,340	1,107,593	5.44%
<b>Output</b>			
GTL Product	531,019	542,415	-2.15%
Carbon Dioxide	371,674	310,426	16.48%
Fuel Gas	377,893	382,481	-1.21%
Pretreated Water	1,410,540	1,324,610	6.09%

The results in this table indicate almost similar mass balance results. This similarity is highlighted through the percentage differences as they mostly fall below 10% except for HP steam requirement and CO<sub>2</sub> output, which are below 20%. While the generated model results are in great agreement with those of the literature, the high percentage difference seen in some of the streams is attributed to the complexity and interconnectivity of the simulation units, leading to a cumulative error throughout the model. The results are further verified by comparing the KPI results as seen in *Figure 20*. The comparison was made in terms of the amount of natural gas consumed, amount of net water produced, direct CO<sub>2</sub> emissions, and the amount of oxygen consumed per barrel of GTL. The percentage difference between the two models is provided.

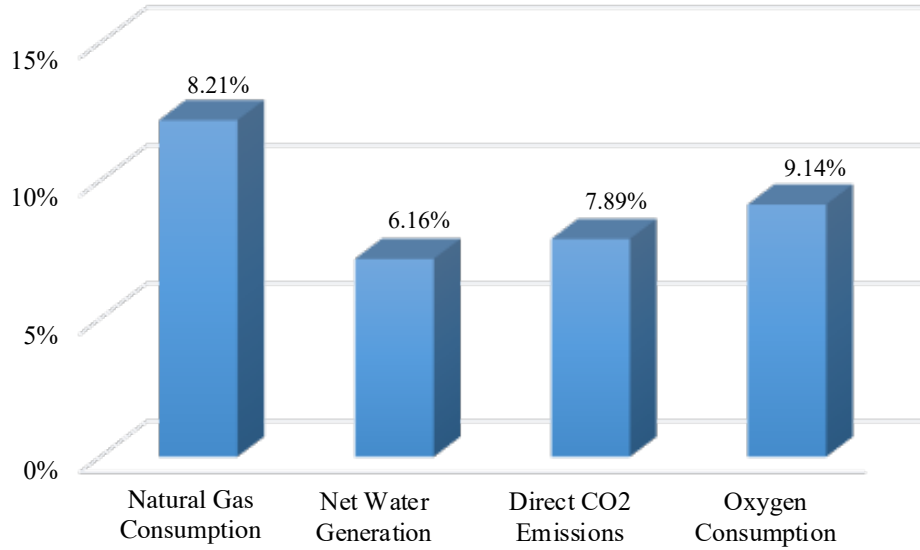


**Figure 20** Comparison of the literature and reproduced ATR model KPI results

The simulated model results are in reasonable agreement with the literature results with an error margin of less than 15% in all cases.

### 6.3. Comparison of ATR and CARGEN™ KPI Results

To evaluate the performance of the CARGEN™ process, its benchmark indicators are compared to those of the modeled ATR-based process to determine the effect of replacing the ATR unit with a CARGEN™ unit. The targeted indicators are the natural gas requirement, the net water generation, direct and indirect CO<sub>2</sub> emissions, oxygen consumption, syngas conversion, and the amount of MWCNT's produced. In *Figure 21* and *Figure 22*, a comparison of the KPI results along with their percentage difference is provided.



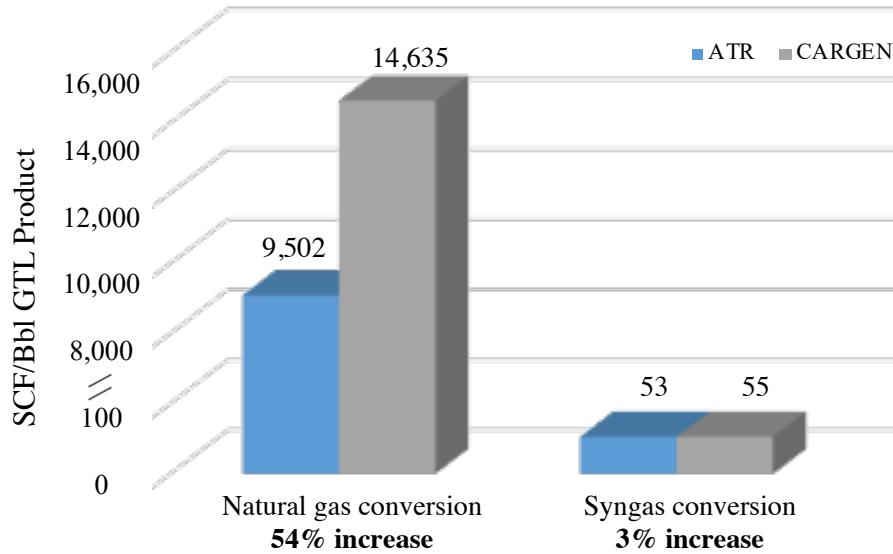


**Figure 21** Comparison of the ATR-based and CARGEN<sup>TM</sup>-based model natural gas and syngas conversion

From the provided results, it is seen that the CARGEN<sup>TM</sup>-based process requires 54% more natural gas per barrel of GTL, which is agreement with the molar flow rate data reported in *Table 7* and *Table 8*. This is because the CARGEN<sup>TM</sup> technology produces two products (MWCNT and syngas), whereas the ATR reactor produces only syngas. Therefore, more natural gas is needed in the CARGEN<sup>TM</sup> process, as it contributes to the production of both syngas and MWCNT.

As for the syngas conversion, both processes have a similar conversion as expected, as changing the reforming process used does not affect the FT process, and the same amount of syngas is required for producing a barrel of GTL. This further proves that replacing an ATR unit with a CARGEN<sup>TM</sup> unit can be done with minimal downtime as the only change

taking place in the GTL plant is in the reforming section, while everything else remains unchanged.

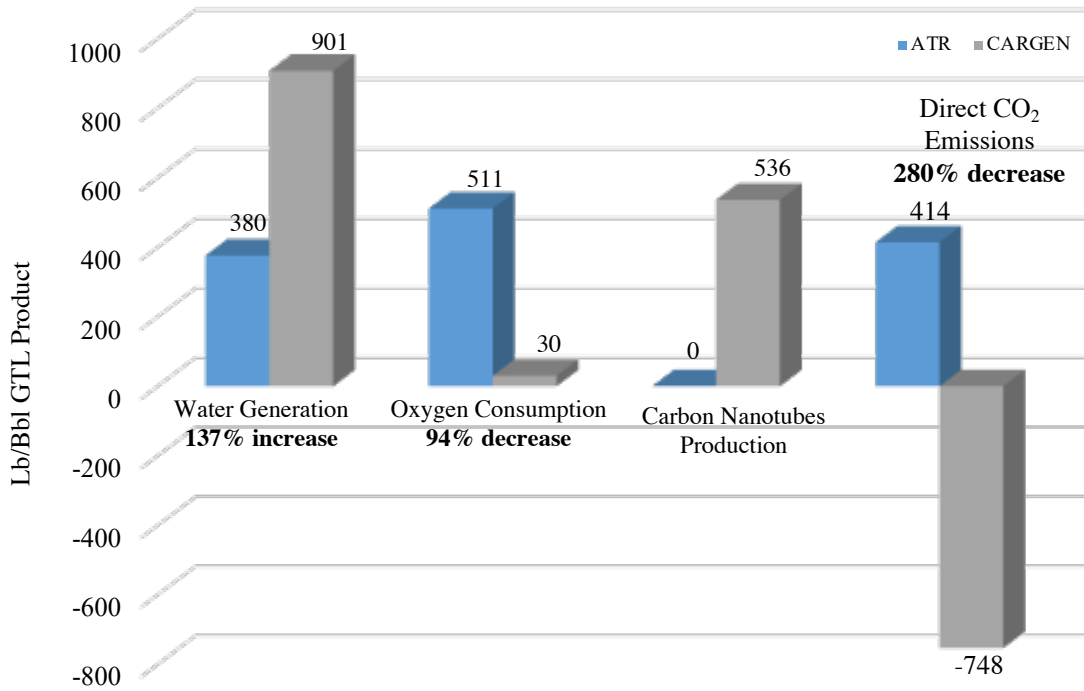


**Figure 22** Comparison of the ATR-based and CARGEN<sup>TM</sup>-based water generation, oxygen consumption, carbon nanotubes production, and direct CO<sub>2</sub> emissions

Meanwhile, it is seen that the overall generation of water in the CARGEN<sup>TM</sup>-based process is 137% more than that of the ATR-based process, which is also confirmed by the numbers reported in *Table 7* and *Table 8*. This is due to the shift in the equilibrium toward water and carbon formation in the CARGEN<sup>TM</sup> reactor via the following predominant reactions.





While this is considered a disadvantage as a significant amount of HC is wasted in its conversion to water, this water can be recycled into the GTL process after pre-treatment or used for irrigation and other purposes. The Oryx GTL plant also reports a similar practice to reduce the demand for water desalination<sup>78</sup>.

In terms of oxygen consumption, the CARGENTM process shows a 94% reduction in its oxygen feed requirement due to the low C:O<sub>2</sub> ratio compared to the ATR process. This highly improves the plant's economy, as it reduces the need for a continuous oxygen source while also reducing the ASU operating cost.

A significant difference between the two processes, as stated earlier, is the production of MWCNT. Through the CARGENTM process, 536 lb of MWCNT are produced per barrel of GTL. This offers a great advantage to the GTL process as through replacing the ATR unit, the plant becomes more eco-friendly while also forming a valuable product, MWCNT, which brings in a very high revenue into the plant.

Another significant effect of replacing the CARGENTM unit with ATR is the significant drop in CO<sub>2</sub> emissions. In fact, by switching to CARGENTM, the overall GTL process goes from being a net producer of CO<sub>2</sub> to a net consumer in terms of its direct emissions. While the ATR reactor produces large amounts of CO<sub>2</sub> flared into the atmosphere, the CO<sub>2</sub> produced from the CARGENTM reactor setup is recycled while also utilizing additional

CO<sub>2</sub> from external sources to meet the C:CO<sub>2</sub> ratio of 1:1. Therefore, by switching to CARGEN™ technology, the direct CO<sub>2</sub> emissions drop from 414 to -748 lb of CO<sub>2</sub> per barrel of GTL. However, it must be noted that the CARGEN™-based GTL process does produce CO<sub>2</sub>; however, it consumes a lot more than it generates, thus making it an overall net consumer. This is also consistent with the life cycle assessment results published in our previous work<sup>19</sup>.

#### **6.4. Power Utilization**

To compare the power utilization, all the compressors, pumps, and turbines are considered. *Table 10* summarizes each plant's total power requirement in addition to the indirect CO<sub>2</sub> emissions produced from the power requirement as obtained from ASPEN Plus®. Furthermore, the ASU power requirement is calculated using a factor of 245 kWh/ton O<sub>2</sub>.

Looking at the total power requirement, it is seen that the CARGEN™-based process requires around 15% less power than ATR. Although the CARGEN™-based process has additional compression requirements due to the higher natural gas flowrates, the low C:O<sub>2</sub> ratio required in the CARGEN reactor reduces the need for a continuous source of oxygen and thus reduces the power requirement of the air separation unit in addition to the oxygen compression.

**Table 10** Comparison of the power requirement in the developed GTL models

Unit	Power (MW)	
	ATR	CARGEN™
C-101	4.6	7.4
C-102	18.2	37.9
C-103	72.6	3.8
C-104	-	152.8
C-201	9.0	24.4
C-202	0.7	0.8
C-301	0.3	0.3
P-201	0.2	0.2
P-202	0.4	0.4
P-301	1.5	1.5
T-101	-	-38.1
T-401	-0.1	-0.1
ASU	126.9	7.1
<b>Total</b>	<b>234.3</b>	<b>198.4</b>
<b>Indirect CO<sub>2</sub> emissions from power generation (lb CO<sub>2</sub>/Bbl GTL)</b>	<b>152.9</b>	<b>130.4</b>
<b>% Difference</b>	<b>-14.7 %</b>	

According to the United States Environmental Protection Agency (EPA), the emission factor for power generation is 0.000707 Mtons of CO<sub>2</sub> emissions per kWh<sup>77</sup>. This is equivalent to 153 lb of indirect CO<sub>2</sub> emissions per bbl of GTL generated from the ATR-

based process and 130 lb of CO<sub>2</sub> emissions per bbl in the CARGEN<sup>TM</sup>-based process, as seen in *Table 10*.

The power requirement of the CARGEN<sup>TM</sup>-based process must be further reduced. Therefore, the operation of the CARGEN<sup>TM</sup> two-reactor setup at lower pressures investigating can be investigated. This is a possible solution for the reduction in the power requirement. However, since limited practical information is known about the operation of CARGEN<sup>TM</sup>, such as coke formation in the reactor, it was chosen to operate at a high pressure following the practice of industrial reformers.

### **6.5. Heat Integration and Energy Targeting**

This section compares the heat requirement and generation in the developed models through a thermal pinch analysis to determine the minimum heating and cooling requirement. The pinch design method (PDM) known as pinch analysis is a method outlined by Linnhoff *et al.*<sup>79</sup> for the development of heat exchanger networks through matching hot and cold streams. The key elements of pinch analysis are<sup>79</sup>:

- decomposing the heat recovery problem at the pinch temperature
- developing separate heat exchanger networks below and above the thermal pinch
- starting the network near the pinch as this is where the problem is the most constrained (limited degrees of freedom to match the hot and cold streams)

- assigning exchangers for process streams first, then process to process units, and finally installing utility exchangers where necessary to reach the stream target temperature
- using the stream heat capacity rules (CP rules) to decide on matching between cold and hot streams
- splitting the process streams wherever the CP rules are not applicable
- maximizing the heat exchange duty for each match to minimize the number of units needed

After performing the heat integration, a cascade diagram will be developed. This diagram is an algebraic approach to determine the minimum heating and cooling utilities required.<sup>79</sup>

Using the pinch analysis, a heat exchanger network (HEN) was analytically developed for each plant. For simplicity, the heaters of the multistage compressors, distillation reboilers, and condensers were not considered. *Table 11* and *Table 12* summarize the hot and cold process streams data.

**Table 11** Stream data for ATR-based GTL process

Stream	Supply Temperature (°F)	Target Temperature (°F)	Heat Duty (MBtu/hr)
S1	111	300	110,515
SAT-NG	218	700	344,568
S7	578	940	482,158
S9	212	940	200,225
S17	1,950	122	-3,969,691
S21	141	428	412,412
FT-VAPOR	428	122	-1,105,089
S25	124	662	61,958
S27	430	662	67,246
S30	662	400	-261,488
S32	403	150	-5,869
S39	400	733	441,599
S42	302	122	-58,254
FUELGAS	121	2,000	552,949
AIR	86	2,000	3,625,495
S45	668	662	-4,007

**Table 12** Stream data for CARGEN<sup>TM</sup>-based GTL process

Stream	Supply temperature (°F)	Target temperature (°F)	Heat duty (MBtu/hr)
S1	111	300	179,804
SAT-NAG	218	700	559,020
S7	509	788	703,503
S9	212	788	8,751



*Table 12 Continued*

Stream	Supply temperature (°F)	Target temperature (°F)	Heat duty (MBtu/hr)
CO <sub>2</sub> -FEED	2,000	79	-1,313,221
S15	965	1,508	1,794,973
S17	1,508	122	-6,272,484
A-SYNGAS	122	130	18,206
S21	184	428	379,388
FT-VAPOR	428	122	-1,142,964
S25	124	662	62,031
S27	430	662	65,449
S30	662	400	-258,275
S32	403	150	-5,694
S39	400	733	436,083
S42	302	122	-57,244
FUELGAS	119	2,000	734,948
AIR	86	2,000	3,465,403
S45	668	662	-4,534

This data was then used to develop the composite curves (CC) for each process, as seen in *Figure 23* and *Figure 24*.

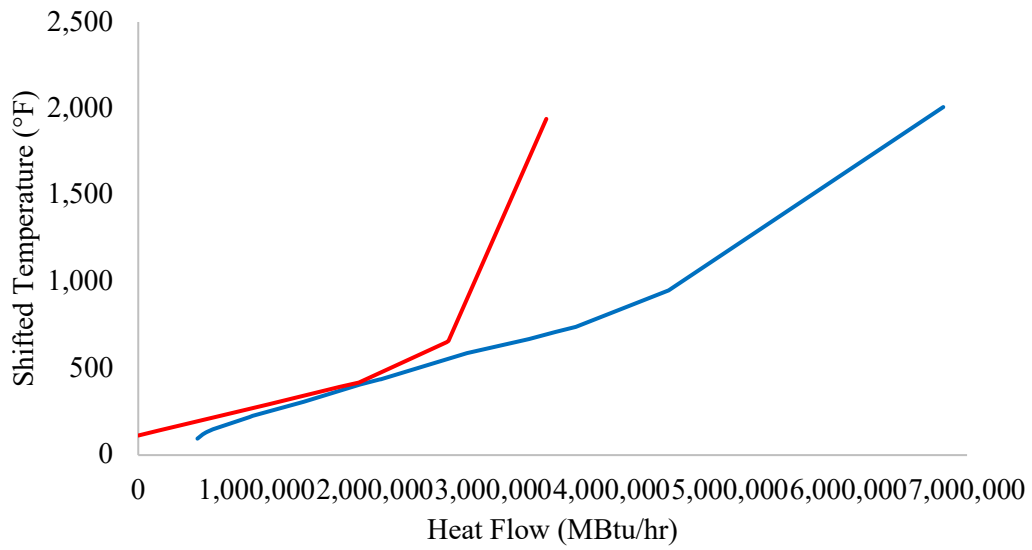


**Figure 23** ATR-based model composite curve

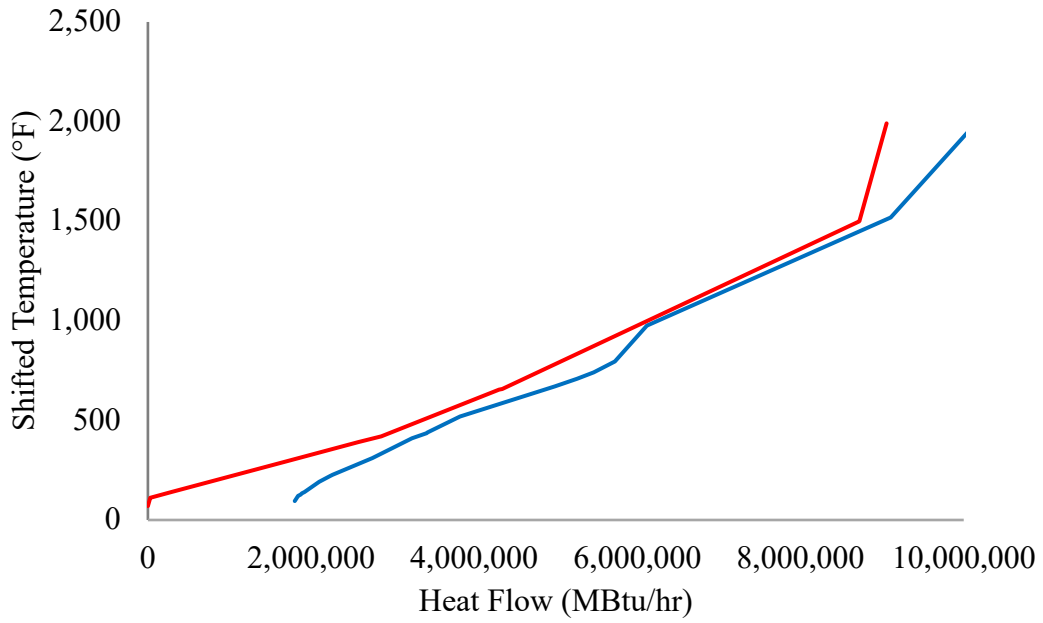


**Figure 24** CARGEN™-based process composite curve

The HEN for each process was then developed, as seen in Figure 25 to Figure 28. The

HEN was developed based on the outlined steps given by Linnhoff *et al.*<sup>80</sup>,

where,

- HE represents the counterclockwise heat exchanger
- H represents the heaters that uses an external utility
- C represents the coolers that use external utilities

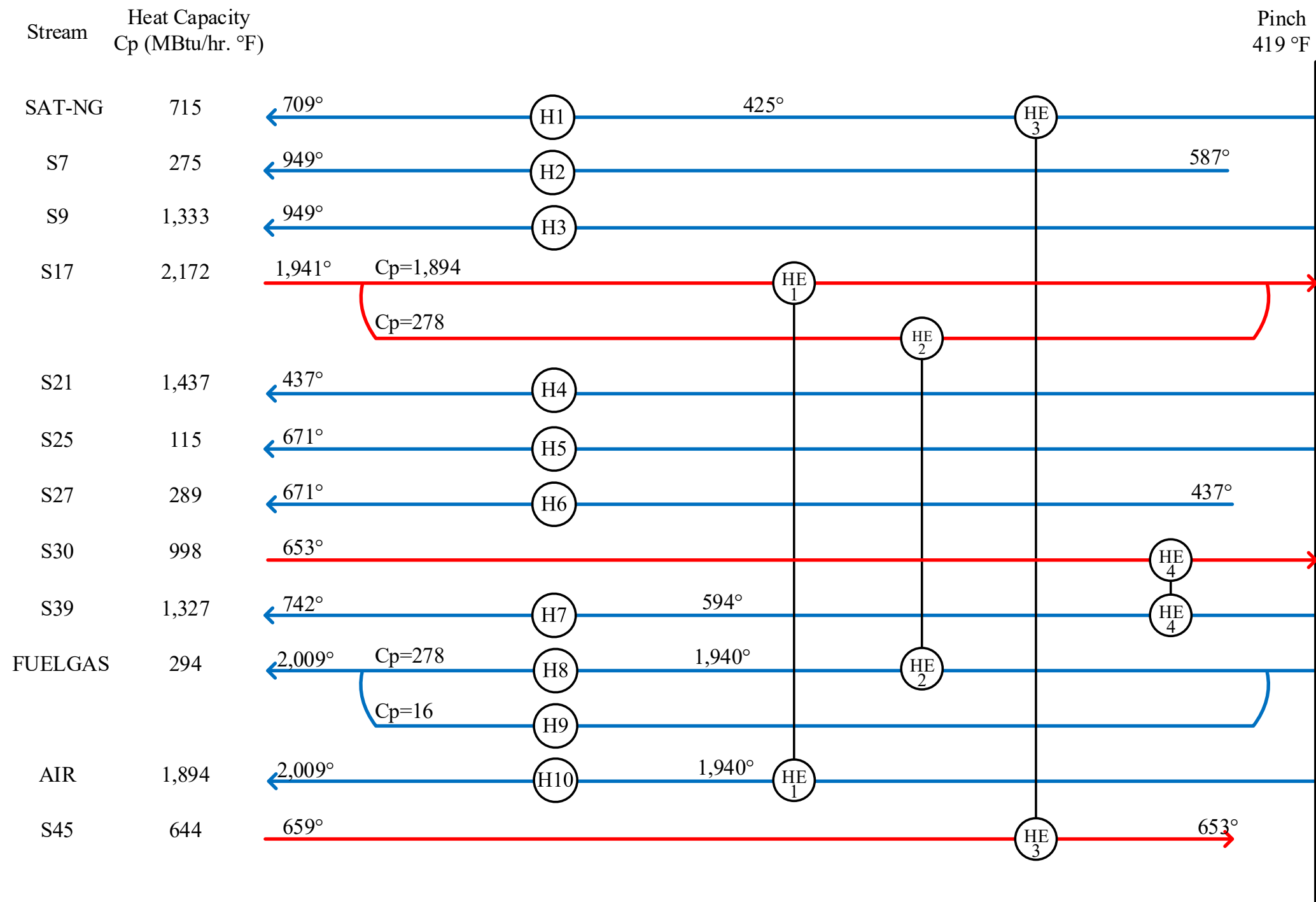


Figure 25 Heat exchanger network of the ATR-based model – above the pinch

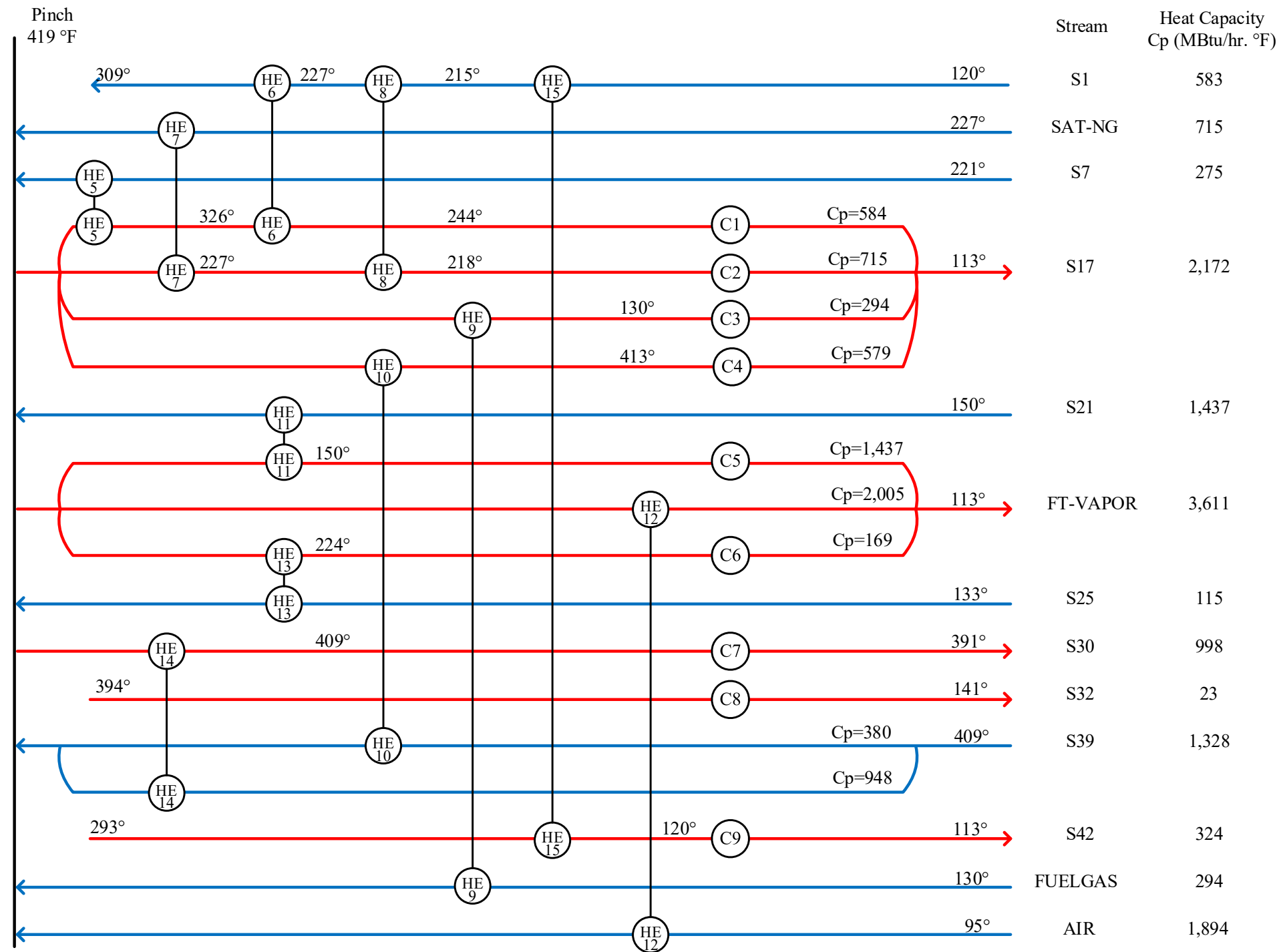


Figure 26 Heat exchanger network of the ATR-based model – below the pinch

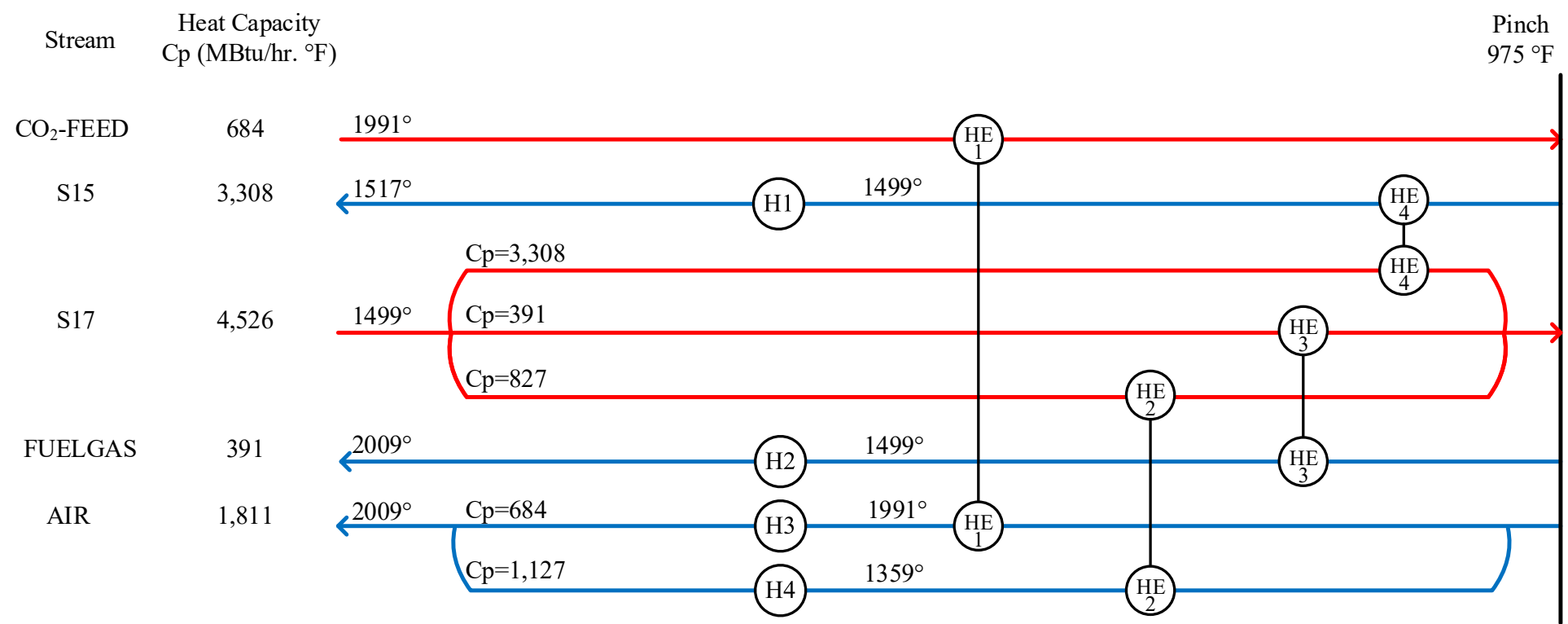


Figure 27 Heat exchanger network of the CARGEN™-based model – above the pinch

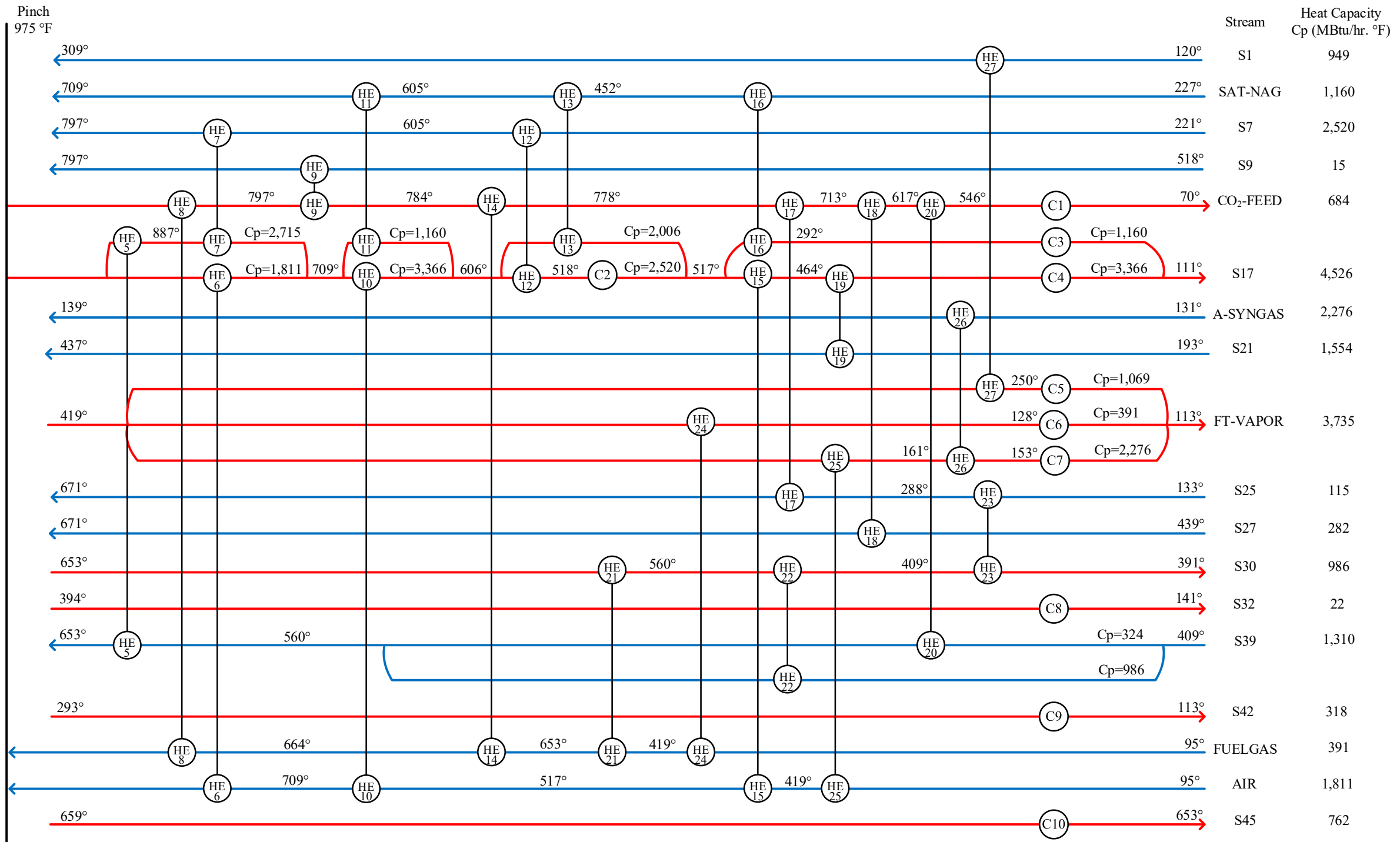


Figure 28 Heat exchanger network of the CARGEN™-based model –below the pinch

Figure 25 to Figure 28 show the stream matching and splitting according to the CP rules. This network helps in reducing the energy requirement in the plant where heat is transferred from the hot (red) streams to the cold (blue) streams to reduce the need for hot and cold streams. The HEN unit specifications are also detailed in Table 13 and

Table 14 below.

**Table 13** Summary of ATR-based GTL model heat exchanger network specifications

Heat exchanger	Heat duty (MBtu/hr)	Temperature (°F)			
		Cold stream		Hot stream	
		Inlet	Outlet	Inlet	Outlet
HE1	2,882,252	419	1,940	1,941	419
HE2	422,790	419	1,940	1,941	419
HE3	4,007	419	425	659	653
HE4	233,543	419	742	653	419
HE5	54,457	221	419	419	326
HE6	47,787	227	309	326	244
HE7	137,215	227	419	419	227
HE8	6,804	215	227	227	218
HE9	84,967	130	419	419	130
HE10	3,680	409	419	419	413
HE11	386,545	150	419	419	150
HE12	613,720	95	419	419	113
HE13	32,917	133	419	419	224
HE14	9,191	409	419	419	409
HE15	55,924	120	215	293	120



**Table 14** Summary of CARGEN<sup>TM</sup>-based GTL model heat exchanger network specifications

Heat exchanger	Heat duty (MBtu/hr)	Temperature (°F)			
		Cold stream		Hot stream	
		Inlet	Outlet	Inlet	Outlet
HE1	694,956	975	1,991	1,991	975
HE2	433,664	975	1,359	1,499	975
HE3	1,735,426	975	1,499	1,499	975
HE4	205,002	975	1,499	1,499	975
HE5	238,088	560	653	975	887
HE6	480,537	709	975	975	709
HE7	482,508	605	797	887	709
HE8	121,279	664	975	975	797
HE9	8,751	518	797	797	784
HE10	348,218	517	709	709	606
HE11	120,020	605	709	709	606
HE12	220,995	221	605	606	518
HE13	178,214	452	605	606	517
HE14	4,323	653	664	784	778
HE15	176,843	419	517	517	464
HE16	260,786	227	452	517	292
HE17	44,205	439	671	778	713
HE18	65,449	439	671	713	617
HE19	379,388	193	437	464	111
HE20	48,990	409	560	617	546
HE21	91,444	419	543	653	560
HE22	149,005	409	560	560	409
HE23	17,827	133	288	409	391

**Table 14** *Continued*

Heat exchanger	Heat duty (MBtu/hr)	Temperature (°F)			
		Cold stream		Hot stream	
		Inlet	Outlet	Inlet	Outlet
HE24	113,601	95	419	419	128
HE25	586,620	95	419	419	161
HE26	18,206	131	139	161	153
HE27	179,804	120	309	419	250

As it can be seen from *Table 13* and *Table 14*, the CARGEN<sup>TM</sup>-based GTL process has a lot more heat exchangers than the ATR-based process. This is due to the presence of more streams in the CARGEN<sup>TM</sup>-based process and the high pinch temperature which increases the number of constraints when developing the HEN. Therefore, this requires more complex stream splitting in order to satisfy the heating and cooling requirements. Moreover, it is noticed that streams with higher CP values such as streams S17 and FT-VAPOR are split a lot more than those of lower CP values as their high capacity offers a bigger chance for heat transfer.

Moreover, *Table 15* and

*Table 16* summarize the external cooling and heating utilities required.

**Table 15** Summary of external cooling duties and specifications for each model

	ATR			CARGEN™		
	Heat duty (MBtu/hr)	Temperature (°F)		Heat duty (Mbtu/hr)	Temperature (°F)	
		In	Out		In	Out
C1	76,285	244	113	325,270	546	70
C2	74,773	218	113	2,946	518	517
C3	5,098	130	113	207,482	292	111
C4	173,582	413	113	802,366	464	111
C5	53,188	150	113	147,212	250	113
C6	18,719	224	113	5,979	128	113
C7	18,754	409	391	91,541	153	113
C8	5,869	394	141	5,694	394	141
C9	2,330	120	113	57,244	293	113
C10	-	-	-	4,534	659	653
<b>Total</b>	<b>428,599 MBtu/hr</b>			<b>1,650,270 MBtu/hr</b>		

**Table 16** Summary of external heating duties and specifications for each model

	ATR			CARGEN™		
	Heat duty (Mbtu/hr)	Temperature (°F)		Heat duty (Mbtu/hr)	Temperature (°F)	
		In	Out		In	Out
H1	203,346	425	709	59,547	1,499	1,517
H2	482,158	587	949	199,300	1,499	2,009
H3	145,768	419	949	12,305	1,991	2,009
H4	25,867	419	437	732,260	1,359	2,009
H5	29,041	419	671	-	-	-
H6	67,246	437	659	-	-	-
H7	195,184	594	742	-	-	-

**Table 16 Continued**

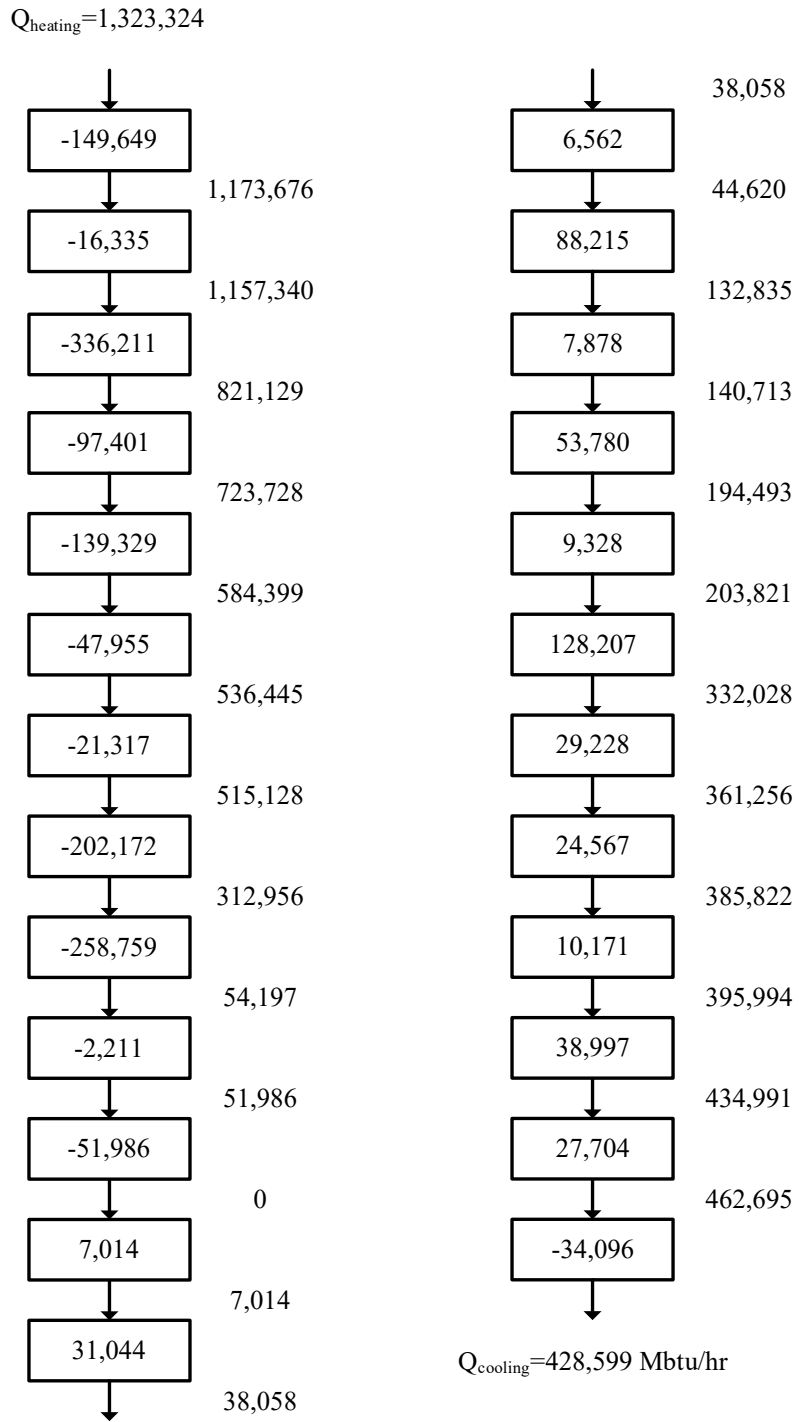
	ATR			CARGEN™		
	Heat duty (Mbtu/hr)	Temperature (°F)		Heat duty (Mbtu/hr)	Temperature (°F)	
		In	Out		In	Out
H8	18,999	1,940	2,009	-	-	-
H9	26,192	419	2,009	-	-	-
H10	129,523	1,940	2,009	-	-	-
<b>Total</b>	<b>1,323,324 MBtu/hr</b>			<b>1,003,412 MBtu/hr</b>		

Table 17 summarizes the heat duties of the reactors and distillation column reboilers and condensers. Note that positive heat duty indicates endothermicity while negative heat duty indicates exothermicity.

**Table 17 Process unit heat duties of each model before integration**

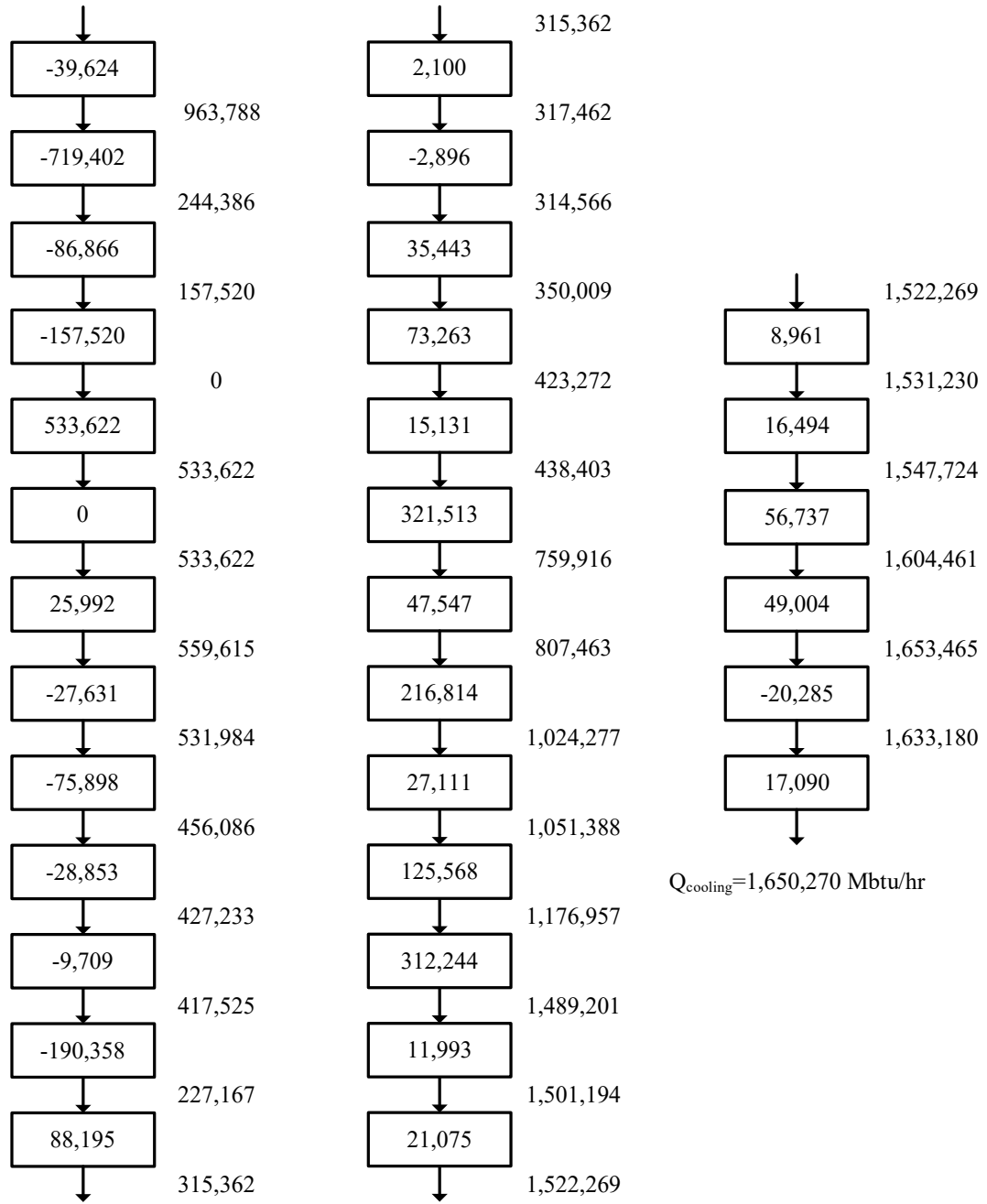
Unit	Heat duty (MBtu/hr)	
	ATR	CARGEN™
Pre-reformer	0	0
Reformer	0	4,342,253
CARGEN™ reactor	-	0
FT reactor	-3,098,794	-3,061,429
Hydrocracker	-19,076	-18,828
Combustion chamber	-4,889,410	-7,085,129
D-401 Condenser	-32,2481	-317,042
D-402 Reboiler	-283	-1,267
D-402 Condenser	129,417	258,727
PSA	-119	-142
Amine unit	-2,596	-14,917

The cascade diagrams were then developed as seen in *Figure 29* and *Figure 30* in addition to the grand composite curves (GCC) for each process in *Figure 31* and *Figure 32*. The GCC provides a graphical representation of the heat surplus available in the process.



**Figure 29** Cascade diagram of the ATR-based GTL plant

$Q_{\text{heating}} = 1,003,412 \text{ Mbtu/hr}$



$Q_{\text{cooling}} = 1,650,270 \text{ Mbtu/hr}$

**Figure 30** Cascade diagram of the CARGEN™-based GTL plant

As it can be seen from *Figure 29* and *Figure 30*, the cascade diagram provides the minimum cooling and heating utilities required. It must be noted that these values are the same as those obtained from the HEN which indicates that the developed network is correct.

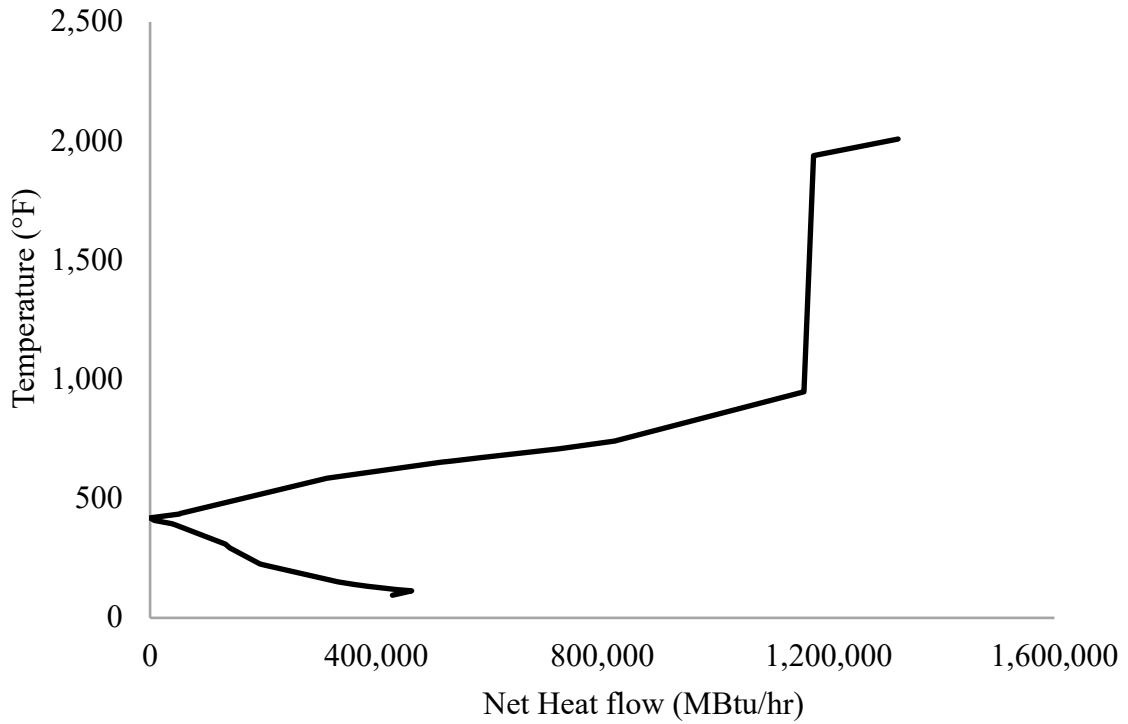


**Figure 31** Grand composite curve of the ATR-based GTL plant before integration



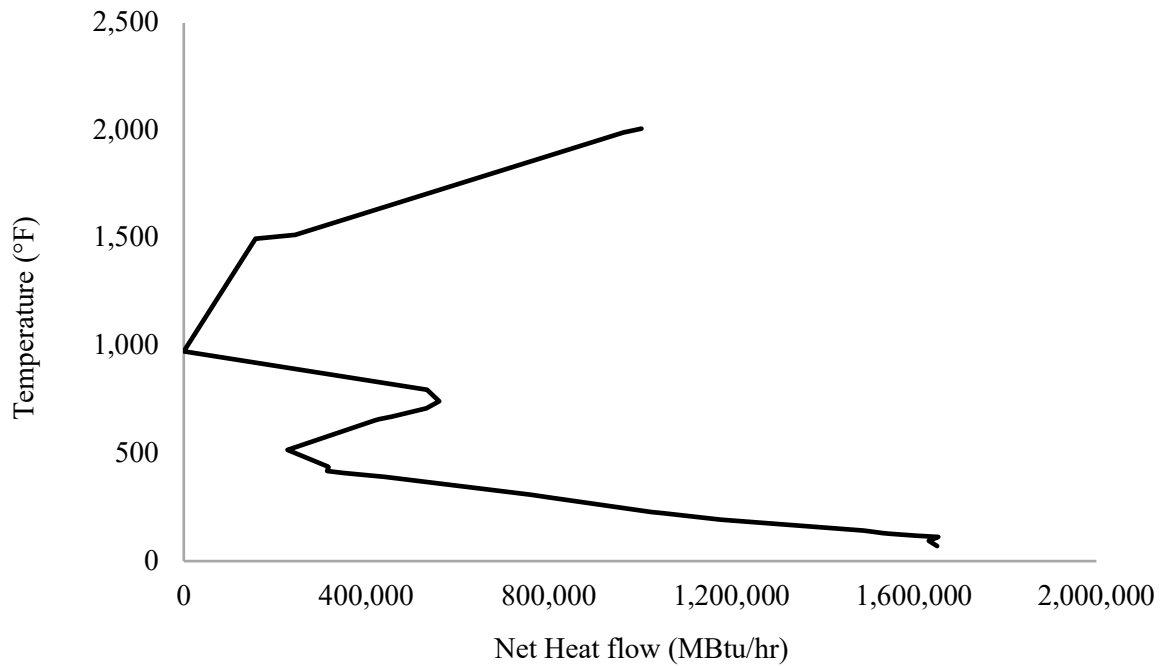


**Figure 32** Grand composite curve of the CARGEN™-based GTL plant before integration

Looking at the GCC, it is seen that for both processes, there are no “pockets” above the pinch and that the process acts as a net heat sink. This sink can be satisfied by external heating utilities or by integrating exothermic reactors above the pinch. As seen in *Table 17*, the combustion chamber is an exothermic reactor with a high heat duty (-7,085,129 MBtu/hr) available at 2000 °F. Therefore, this reactor can be used to satisfy the heating requirement completely. The red arrow in *Figure 33* and

*Figure 34* represents the exothermic combustion chamber energy used to meet heating requirement in the GTL plant.

Meanwhile, under the pinch, a small pocket is seen in the ATR-based process. This pocket acts as a self-sufficient process to process heat transfer. Similarly, in the CARGEN<sup>TM</sup>-based process GCC, one large pocket and a smaller pocket are seen. These pockets are represented by blue lines. Pockets can also be used to satisfy the distillation column duties. However, the distillation column's reboiler and condenser temperatures fall below the pocket temperature (<500 °F). Therefore, to satisfy the energy requirement below the pinch, an external cooling utility can be used or integrating with an endothermic reactor. From the data obtained in *Table 17*, the only endothermic reactor available in both GTL plants is the FT reactor. However, its endothermic energy is available at a temperature higher than that of the cooling requirement, which means it cannot be used. Therefore, this process's cooling requirement can only be satisfied using external cooling utilities such as cooling water or a refrigerant. *Figure 33* and

*Figure 34* represent the GCC of the GTL plants after integration.

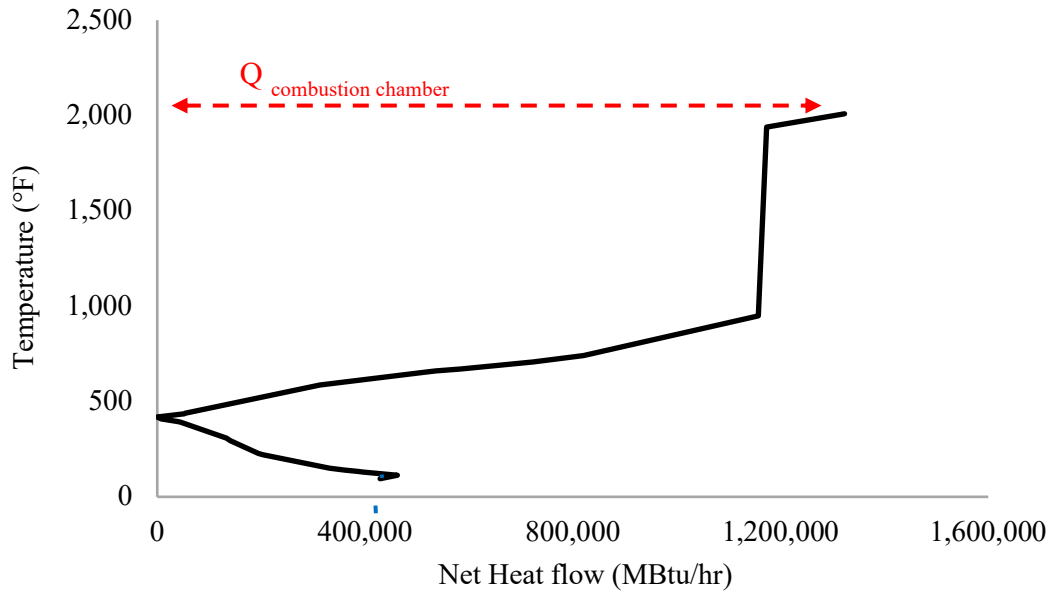


**Figure 33** Grand composite curve of the ATR-based GTL plant after integration

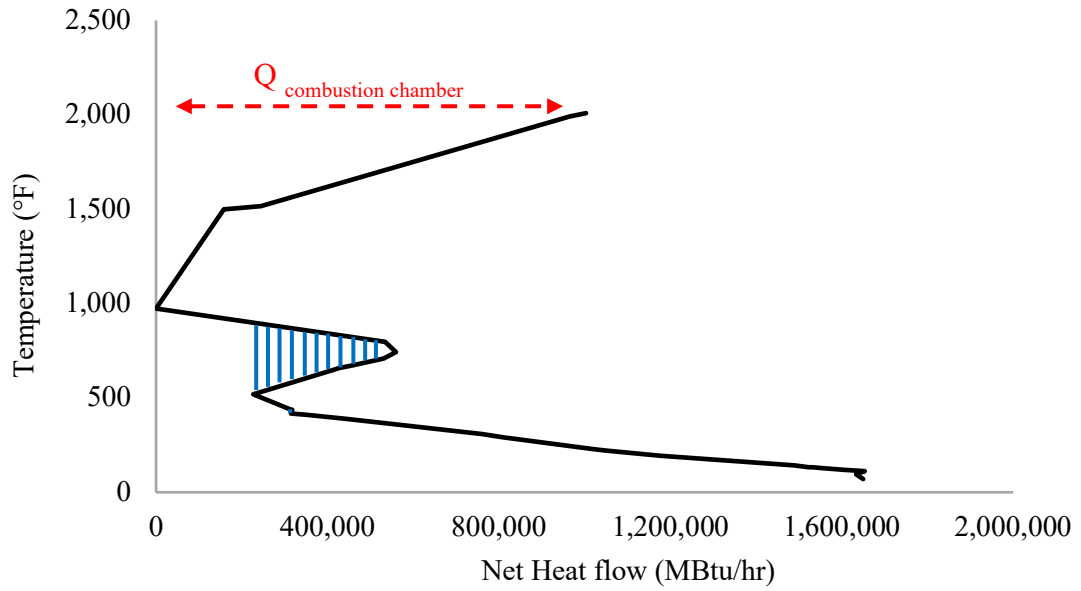


**Figure 34** Grand composite curve of the ATR-based GTL plant after integration

After satisfying the heat requirements, the process can be further integrated to reduce the overall plant energy requirement and reduce indirect emissions by satisfying the plant's endothermic energies. *Table 18* summarizes the unsatisfied endothermic units in each plant. The indirect CO<sub>2</sub> emissions from energy requirement are calculated using the emission factor of 0.0053 Mtons of CO<sub>2</sub> per therm<sup>77</sup>.

**Table 18** Total energy requirement and CO<sub>2</sub> emissions before and after integration

Unit	Heat duty (MBtu/hr)	
	ATR	CARGEN™
Before integration		
Reformer	0	4,342,253
D-402 Reboiler	129,417	258,727
Cooling utility	428,599	1,650,270

**Table 18** Continued

<b>Total energy required</b>	<b>558,016</b>	<b>6,251,250</b>
<b>Indirect CO<sub>2</sub> emissions from energy generation (lb CO<sub>2</sub>/Bbl GTL)</b>	<b>272</b>	<b>3,080</b>
<b>% Difference</b>	<b>288%</b>	
After integration		
Cooling utility	428,599	1,650,270
<b>Total energy required</b>	<b>428,417</b>	<b>1,650,270</b>
<b>Indirect CO<sub>2</sub> emissions from energy generation (lb CO<sub>2</sub>/Bbl GTL)</b>	<b>210</b>	<b>813</b>
<b>% Difference</b>	<b>288%</b>	

Looking at the total energy required before integration, a drastic increase is seen in the CARGEN™-based plant. This is attributed mainly to the high endothermic requirement of the reformer in the CARGEN™-based GTL plant, leading to a dramatic increase in the indirect CO<sub>2</sub> emissions. This can be highly mitigated by satisfying the endothermic energies with the excess heat from the combustion chamber as done in the GCC. However, as seen earlier, the cooling requirement remains unsatisfied. Therefore, after integration, the total energy required is reduced, as seen in *Table 18*.

Looking at the indirect CO<sub>2</sub> emissions, it is seen that the CARGEN™-based plant has a 288% higher value.

## **6.6. Overall CO<sub>2</sub> Emissions**

After determining the amount of direct and indirect CO<sub>2</sub> emissions from each GTL plant, the overall emissions can be determined. The diagram below summarizes the CO<sub>2</sub> emissions generated.

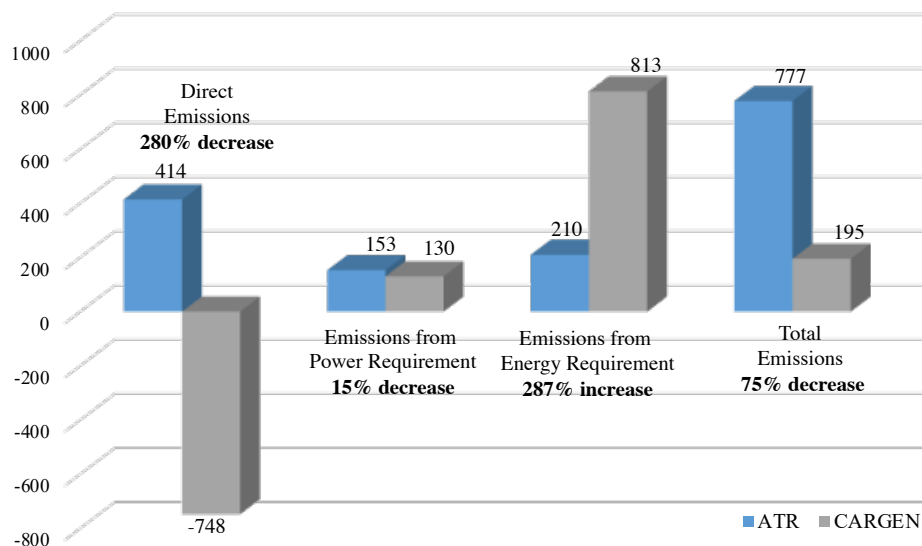


**Figure 35** Comparison of the ATR-based and CARGEN<sup>TM</sup>-based direct and indirect CO<sub>2</sub> emissions

Although the CARGEN<sup>TM</sup>-based process leads to a 287% spike is seen in the energy requirement which in turn also increased the indirect CO<sub>2</sub> emissions, the overall emissions are significantly reduced. This is due to the high CO<sub>2</sub>:CH<sub>4</sub> ratio required in the CARGEN reactor which makes the process a net consumer in terms of the direct emissions in addition to the reduction in the power requirement. As a result, it is seen that the CARGEN<sup>TM</sup>-based GTL plant produces around 75% less emissions compared to the ATR-based plant.

### 6.7. Summary of Results

The following table summarizes the KPI results obtained from this work.

**Table 19** KPI results summary

KPI	ATR	CARGEN™	% Difference
Natural gas requirement [SCF/bbl GTL]	9,502	14,635	54%
Net water [lb/bbl GTL]	380	901	137%
Total CO <sub>2</sub> emissions [lb/bbl GTL]	777	195	-73%
Oxygen [lb/bbl GTL]	524	30	-94%
Syngas conversion [SCF/bbl GTL]	53	55	3%
MWCNT produced [lb/bbl GTL]	0	536	-

## 7. CONCLUSIONS AND RECOMMENDATIONS FOR FUTURE WORK

This thesis demonstrates the economics and the process engineering implementation of the CARGEN technology. CARGEN technology is shown to replace the commercial ATR process as utilized in the commercial GTL process plants. The CARGEN technology add significant value to the GTL plant, both in terms of sustainability (reduction of CO<sub>2</sub> footprint) and economics of the process. In particular, as the CARGEN technology utilizes CO<sub>2</sub> as a feedstock, it heavily reduces the net CO<sub>2</sub> emission from the GTL facility by 75%. Earlier studies have demonstrated that the POX and ATR based GTL processes have similar carbon footprint and their operation is completely dependent on the operation expertise. However, this work shows that although the overall GTL process remains same except the reforming unit, there are great implications in the overall water-energy-CO<sub>2</sub> dynamics of the process plant due to incorporation of the CARGEN technology. Not only does CARGEN technology enables CO<sub>2</sub> conversion, it also co-produces an additional product in the form of solid carbon. The experimental work from our previous publications had demonstrated that the solid carbon produced from CARGEN technology is multi-walled carbon nanotubes (MWCNTs) quality, which is a product of great market value and demand as the application ranges from micro-elements like microscopes, batteries, to building and structural materials like cement, steel, rubber, etc.



In terms of quantitative comparison, CARGEN technology requires 61% more natural gas (approx. 5,500 SCF/bbl GTL) compared to ATR based GTL plant due to the co-production of around 500 lb of CNTs/bbl GTL for the case-study of 50,000 bbl/day GTL products. Moreover, CARGEN™ leads to a significant reduction in the oxygen requirement by 94% (approx. 480 lb O<sub>2</sub>/bbl GTL) compared to the benchmark ATR-based GTL plant. The consumption of more natural gas and CO<sub>2</sub> also leads to the production of 140% more water. In conjunction with the reported industry practice, the production of large amount of clean water is highly beneficial for the irrigation purposes.

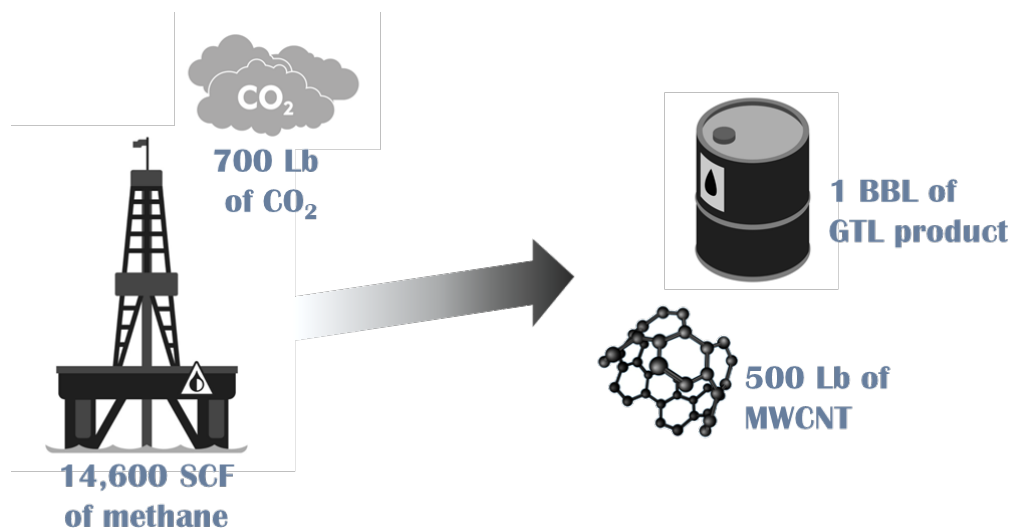


*Figure 36 Conversion of greenhouse gases to fuels and MWCNT*

In terms of the sensitivity of the implementation of the CARGEN™ technology on the other process units within the GTL plant, following differences are identified:

- (a) 3% change in the synthesis conversion
- (b) 2% change in the hydrocracker duty

(c) 2% change in the energy requirement of the fractionation unit

Therefore, the incorporation of the CARGEN™ technology in an existing GTL process plant result in significant improvements in the water-energy-CO<sub>2</sub> nexus of the overall process plant as demonstrated in the work done in this thesis.

## 8. RECOMMENDATIONS FOR FUTURE WORK

This work demonstrates the uniqueness and novelty in the CARGEN<sup>TM</sup> process. This technology can be also further improved and expanded on, and this will be addressed in our future work.

- Studying the effect of different CARGEN reactor feed ratios and operating conditions of the ratio of syngas produced and MWCNT formation
- Improving the accuracy of the analysis through modeling an ASU, PSA, and amine unit in order to get more insight on the effect of CARGEN<sup>TM</sup> on the energy and power requirement
- Exploring options for providing a continuous source of CO<sub>2</sub> feed such as carbon capture
- Integrating the CARGEN<sup>TM</sup>-based GTL plant with a midstream natural gas processing plant
- Integrating the CARGEN<sup>TM</sup> process with industrial plants to produce chemicals such as methanol, acetic acid, and dimethyl carbonate
- Performing a detailed techno-economic analysis of the plant

## REFERENCES

1. Charts – Data & Statistics - IEA. Accessed February 18, 2021.  
<https://www.iea.org/data-and-statistics/charts?type=pie>
2. 2020 Edition of the GECF Global Gas Outlook 2050. Accessed May 28, 2021.  
[https://www.gecf.org/\\_resources/files/flipbook/ggo2020fb/#2](https://www.gecf.org/_resources/files/flipbook/ggo2020fb/#2)
3. Lavoie J-M. Review on dry reforming of methane, a potentially more environmentally-friendly approach to the increasing natural gas exploitation. *Frontiers in chemistry*. 2014;2:81.
4. ELbashir NO; E-HME; KH. *Natural Gas Processing from Midstream to Downstream*. Wiley
5. Elbashir N, Challiwala MS, Ghouri MM, Linke P, El-Halwagi M. Modeling Development of a Combined Methane Fixed Bed Reactor Reformer. In: *Qatar Foundation Annual Research Conference Proceedings*. Vol 2016. HBKU Press Qatar; 2016:EESP2384.
6. Challiwala MS, Ghouri MM, Linke P, El-Halwagi MM, Elbashir NO. A combined thermo-kinetic analysis of various methane reforming technologies: Comparison

- with dry reforming. *Journal of CO2 Utilization*. 2017;17:99-111. doi:10.1016/j.jcou.2016.11.008
7. Abusrafa AE, Challiwala MS, Wilhite BA, Elbashir NO. Thermal assessment of a micro fibrous fischer tropesch fixed bed reactor using computational fluid dynamics. *Processes*. 2020;8(10). doi:10.3390/pr8101213
  8. Abusrafa AE, Challiwala MS, Choudhury HA, Wilhite BA, Elbashir NO. Experimental Verification of 2-Dimensional Computational Fluid Dynamics Modeling of Supercritical Fluids Fischer Tropsch Reactor Bed. *Catalysis Today*. Published online 2019. doi:<https://doi.org/10.1016/j.cattod.2019.05.027>
  9. Wu T, Huang Z, Zhang WG, Fang JH, Yin Q. Physical and chemical properties of GTL - Diesel fuel blends and their effects on performance and emissions of a multicylinder DI compression ignition engine. *Energy and Fuels*. 2007;21(4):1908-1914. doi:10.1021/ef0606512
  10. Sajjad H, Masjuki HH, Varman M, et al. Engine combustion, performance and emission characteristics of gas to liquid (GTL) fuels and its blends with diesel and bio-diesel. *Renewable and Sustainable Energy Reviews*. 2014;30:961-986. doi:10.1016/j.rser.2013.11.039
  11. David A. Wood. A Review of an Industry Offering Several Routes for Monetizing Natural Gas. Accessed July 24, 2020.

<http://www.dwasolutions.com/images/GTLReviewArticleJune2012DWoodetalJNGSENov2012.pdf>

12. Elbashir NO; E-HME; KH. *Natural Gas Processing from Midstream to Downstream*. Wiley
13. Martínez DY, Jiménez-Gutiérrez A, Linke P, Gabriel KJ, Noureldin MMB, El-Halwagi MM. Water and energy issues in gas-to-liquid processes: Assessment and integration of different gas-reforming alternatives. *ACS Sustainable Chemistry and Engineering*. 2014;2(2):216-225. doi:10.1021/sc4002643
14. Noureldin MMB, Elbashir NO, Gabriel KJ, El-Halwagi MM. A process integration approach to the assessment of CO<sub>2</sub> fixation through dry reforming. *ACS Sustainable Chemistry and Engineering*. 2015;3(4):625-636. doi:10.1021/sc5007736
15. Challiwala MS, Wilhite BA, Ghouri MM, Elbashir NO. Multi-Dimensional Modeling of a Microfibrous Entrapped Cobalt Catalyst Fischer-Tropsch Reactor Bed. *AIChE Journal*. 2017;[under rev(5):1723-1731. doi:10.1002/aic.16053
16. Challiwala MS, Ghouri MM, Linke P, El-Halwagi MM, Elbashir NO. A combined thermo-kinetic analysis of various methane reforming technologies: Comparison with dry reforming. *Journal of CO<sub>2</sub> Utilization*. 2017;17:99-111. doi:10.1016/j.jcou.2016.11.008

17. Challiwala M, Afzal S, Choudhury H, Sengupta D, El-Halwagi M, Elbashir N. Alternative Pathways for CO<sub>2</sub> Utilization via Dry Reforming of Methane. In: ; 2020:253-272. doi:10.1201/9780429243608-14
18. Martínez DY, Jiménez-Gutiérrez A, Linke P, Gabriel KJ, Noureldin MMB, El-Halwagi MM. Water and energy issues in gas-to-liquid processes: assessment and integration of different gas-reforming alternatives. *ACS Sustainable Chemistry & Engineering*. 2013;2(2):216-225.
19. Challiwala M, Afzal S, Choudhury H, Sengupta D, El-Halwagi M, Elbashir N. Alternative Pathways for CO<sub>2</sub> Utilization via Dry Reforming of Methane. In: ; 2020:253-272. doi:10.1201/9780429243608-14
20. Elbashir NO, Challiwala MS, Sengupta D, El-Halwagi MM. System and method for carbon and syngas production. Property WI, Organization, eds. Published online 2018.
21. Elbashir N, Challiwala MS, Ghouri MM, Linke P, El-Halwagi M. Modeling Development of a Combined Methane Fixed Bed Reactor Reformer. In: *Qatar Foundation Annual Research Conference Proceedings*. Vol 2016. HBKU Press Qatar; 2016:EESP2384.
22. Challiwala MS, Ghouri MM, Linke P, El-Halwagi MM, Elbashir NO. A combined thermo-kinetic analysis of various methane reforming technologies: Comparison

- with dry reforming. *Journal of CO2 Utilization*. 2017;17:99-111. doi:10.1016/j.jcou.2016.11.008
23. Abusrafa AE, Challiwala MS, Choudhury HA, Wilhite BA, Elbashir NO. Experimental verification of 2-dimensional computational fluid dynamics modeling of supercritical fluids Fischer Tropsch reactor bed. *Catalysis Today*. 2020;343:165-175.
24. Challiwala MS, Ghouri MM, Sengupta D, El-Halwagi MM, Elbashir NO. A Process Integration Approach to the Optimization of CO2 Utilization via Tri-Reforming of Methane. In: *Computer Aided Chemical Engineering*. Vol 40. Elsevier B.V.; 2017:1993-1998. doi:10.1016/B978-0-444-63965-3.50334-2
25. Afzal S, Sengupta D, Sarkar A, El-Halwagi M, Elbashir N. Optimization Approach to the Reduction of CO2 Emissions for Syngas Production Involving Dry Reforming. *ACS Sustainable Chemistry and Engineering*. 2018;6(6):7532-7544. doi:10.1021/acssuschemeng.8b00235
26. Noureldin MMB, Elbashir NO, El-Halwagi MM, McFerrin A. Optimization and Selection of Reforming Approaches for Syngas Generation from Natural/Shale Gas. Published online 2013. doi:10.1021/ie402382w
27. Oyama ST, Hacıoğlu P, Gu Y, Lee D. Dry reforming of methane has no future for hydrogen production: Comparison with steam reforming at high pressure in



- standard and membrane reactors. *International Journal of Hydrogen Energy*. 2012;37(13):10444-10450. doi:10.1016/j.ijhydene.2011.09.149
28. Challiwala MS, Choudhury HA, Sengupta D, El-Halwagi MM, Elbashir NO. Turning CO<sub>2</sub> into Carbon Nanotubes. *Chemical Engineering Progress*. Published online October 2020:9-10.
  29. Challiwala M, Choudhury HA, Elbashir NO. Regeneration & Activation of Dry Reforming of Methane Catalysts Using CO<sub>2</sub>. Published online 2019.
  30. Challiwala MS, Ghouri MM, Linke P, El-Halwagi MM, Elbashir NO. A combined thermo-kinetic analysis of various methane reforming technologies: Comparison with dry reforming. *Journal of CO<sub>2</sub> Utilization*. 2017;17:99-111. doi:10.1016/j.jcou.2016.11.008
  31. Challiwala M, Afzal S, Choudhury HA, Sengupta D, El-halwagi M, Elbashir NO. Alternative pathways for CO<sub>2</sub> utilization for enhanced methane dry reforming technology. In: *Advances in Carbon Management Technologies*. ; 2019.
  32. Pearl GTL - overview | Shell Global. Accessed December 8, 2020. <https://www.shell.com/about-us/major-projects/pearl-gtl/pearl-gtl-an-overview.html#vanity-aHR0cHM6Ly93d3cuc2h1bGwuY29tL2dsb2JhbC9hYm91dHN0ZWxsL21ham9yLXByb2plY3RzLTlvcGVhcmwvb3ZlcnZpZXcuaHRtbA>

33. Oryx GTL. Accessed December 8, 2020. <https://qp.com.qa/en/QPActivities/Pages/SubsidiariesAndJointVenturesDetails.aspx?aid=37>
34. Gabriel KJ, Linke P, Jiménez-Gutiérrez A, Martínez DY, Noureldin M, El-Halwagi MM. Targeting of the water-energy nexus in gas-to-liquid processes: A comparison of syngas technologies. *Industrial and Engineering Chemistry Research*. 2014;53(17):7087-7102. doi:10.1021/ie4042998
35. Martínez DY, Jiménez-Gutiérrez A, Linke P, Gabriel KJ, Noureldin MMB, El-Halwagi MM. Water and energy issues in gas-to-liquid processes: Assessment and integration of different gas-reforming alternatives. *ACS Sustainable Chemistry and Engineering*. 2014;2(2):216-225. doi:10.1021/sc4002643
36. Gabriel KJ, Linke P, Jiménez-Gutiérrez A, Martínez DY, Noureldin M, El-Halwagi MM. Targeting of the water-energy nexus in gas-to-liquid processes: A comparison of syngas technologies. *Industrial and Engineering Chemistry Research*. 2014;53(17):7087-7102. doi:10.1021/ie4042998
37. Bao B, El-Halwagi MM, Elbashir NO. Simulation, integration, and economic analysis of gas-to-liquid processes. *Fuel Processing Technology*. 2010;91(7):703-713. doi:10.1016/j.fuproc.2010.02.001

38. Jang WJ, Shim JO, Kim HM, Yoo SY, Roh HS. A review on dry reforming of methane in aspect of catalytic properties. *Catalysis Today*. 2019;324:15-26. doi:10.1016/j.cattod.2018.07.032
39. Wang Y, Yao L, Wang S, Mao D, Hu C. Low-temperature catalytic CO<sub>2</sub> dry reforming of methane on Ni-based catalysts: A review. *Fuel Processing Technology*. 2018;169:199-206. doi:10.1016/j.fuproc.2017.10.007
40. Aramouni NAK, Touma JG, Tarboush BA, Zeaiter J, Ahmad MN. Catalyst design for dry reforming of methane: Analysis review. *Renewable and Sustainable Energy Reviews*. 2018;82:2570-2585. doi:10.1016/j.rser.2017.09.076
41. Wang Q, Yan BH, Jin Y, Cheng Y. Investigation of dry reforming of methane in a dielectric barrier discharge reactor. *Plasma Chemistry and Plasma Processing*. 2009;29(3):217-228. doi:10.1007/s11090-009-9173-3
42. Afzal S, Sengupta D, Sarkar A, El-Halwagi M, and, Elbashir N. Optimization Approach to the Reduction of CO<sub>2</sub> Emissions for Syngas Production Involving Dry Reforming. *ACS Sustainable Chemistry & Engineering*. 2018;6(6):7532-7544. doi:10.1021/acssuschemeng.8b00235
43. Nouredin MMB, Elbashir NO, Gabriel KJ, El-Halwagi MM. A process integration approach to the assessment of CO<sub>2</sub> fixation through dry reforming. *ACS*

- Sustainable Chemistry and Engineering*. 2015;3(4):625-636.  
doi:10.1021/sc5007736
44. Özkara-Aydınoğlu Ş. Thermodynamic equilibrium analysis of combined carbon dioxide reforming with steam reforming of methane to synthesis gas. *International Journal of Hydrogen Energy*. 2010;35(23):12821-12828.  
doi:10.1016/j.ijhydene.2010.08.134
45. Nematollahi B, Rezaei M, Lay EN, Khajenoori M. Thermodynamic analysis of combined reforming process using Gibbs energy minimization method: In view of solid carbon formation. *Journal of Natural Gas Chemistry*. 2012;21(6):694-702.  
doi:10.1016/S1003-9953(11)60421-0
46. Song C, Pan W. Tri-reforming of Natural Gas Using CO<sub>2</sub> in Flue Gas of Power Plants without CO<sub>2</sub> Pre-separation for Production of Synthesis Gas with Desired H<sub>2</sub>/CO Ratios Solid Deposition on Metal Surfaces from Heated Fuels and Hydrocarbons View project Tri-reforming of methane: a novel concept for catalytic production of industrially useful synthesis gas with desired H<sub>2</sub>/CO ratios \$. Published online 2002. doi:10.1007/978-1-4615-0773-4\_18
47. Lee SH, Cho W, Ju WS, Cho BH, Lee YC, Baek YS. Tri-reforming of CH<sub>4</sub> using CO<sub>2</sub> for production of synthesis gas to dimethyl ether. In: *Catalysis Today*. Vol 87. Elsevier; 2003:133-137. doi:10.1016/j.cattod.2003.10.005

48. Pino L, Vita A, Cipiti F, Laganà M, Recupero V. Hydrogen production by methane tri-reforming process over Ni-ceria catalysts: Effect of La-doping. *Applied Catalysis B: Environmental*. 2011;104(1-2):64-73. doi:10.1016/j.apcatb.2011.02.027
49. Majewski AJ, Wood J. Tri-reforming of methane over Ni@SiO<sub>2</sub> catalyst. *International Journal of Hydrogen Energy*. 2014;39(24):12578-12585. doi:10.1016/j.ijhydene.2014.06.071
50. Kang JS, Kim DH, Lee SD, Hong SI, Moon DJ. Nickel-based tri-reforming catalyst for the production of synthesis gas. *Applied Catalysis A: General*. 2007;332(1):153-158. doi:10.1016/j.apcata.2007.08.017
51. Baltrusaitis J, Luyben WL. Methane Conversion to Syngas for Gas-to-Liquids (GTL): Is Sustainable CO<sub>2</sub> Reuse via Dry Methane Reforming (DMR) Cost Competitive with SMR and ATR Processes? *ACS Sustainable Chemistry and Engineering*. 2015;3(9):2100-2111. doi:10.1021/acssuschemeng.5b00368
52. Luyben WL. Design and control of the dry methane reforming process. *Industrial and Engineering Chemistry Research*. 2014;53(37):14423-14439. doi:10.1021/ie5023942
53. Song C, Pan W. Tri-reforming of Natural Gas Using CO<sub>2</sub> in Flue Gas of Power Plants without CO<sub>2</sub> Pre-separation for Production of Synthesis Gas with Desired

H<sub>2</sub>/CO Ratios Solid Deposition on Metal Surfaces from Heated Fuels and Hydrocarbons View project Tri-reforming of methane: a novel concept for catalytic production of industrially useful synthesis gas with desired H<sub>2</sub>/CO ratios \$. Published online 2002. doi:10.1007/978-1-4615-0773-4\_18

54. Chatla A, Ghouri MM, El Hassan OW, Mohamed N, Prakash A V., Elbashir NO. An experimental and first principles DFT investigation on the effect of Cu addition to Ni/Al<sub>2</sub>O<sub>3</sub> catalyst for the dry reforming of methane. *Applied Catalysis A: General*. 2020;602:117699. doi:10.1016/j.apcata.2020.117699
55. Omran A, Yoon SH, Khan M, Ghouri M, Chatla A, Elbashir N. Mechanistic Insights for Dry Reforming of Methane on Cu/Ni Bimetallic Catalysts: DFT-Assisted Microkinetic Analysis for Coke Resistance. *Catalysts*. 2020;10(9):1043. doi:10.3390/catal10091043
56. Liu CJ, Ye J, Jiang J, Pan Y. Progresses in the preparation of coke resistant Ni-based catalyst for steam and CO<sub>2</sub> reforming of methane. *ChemCatChem*. 2011;3(3):529-541. doi:10.1002/cctc.201000358
57. De Klerk, A. Fischer–Tropsch Refinin.pdf.
58. De Klerk, A. Fischer–Tropsch Refinin.pdf.

59. Lutz AE, Bradshaw RW, Bromberg L, Rabinovich A. Thermodynamic analysis of hydrogen production by partial oxidation reforming. *International Journal of Hydrogen Energy*. 2004;29(8):809-816. doi:10.1016/j.ijhydene.2003.09.015
60. Sherif SA, Goswami • D Yogi, Stefanakos EK, Steinfeld A. Handbook of Hydrogen Energy EDITED BY.
61. Dry ME. FT catalysts. *Studies in Surface Science and Catalysis*. 2004;152:533-600. doi:10.1016/s0167-2991(04)80464-6
62. Perego C, Bortolo R, Zennaro R. Gas to liquids technologies for natural gas reserves valorization: The Eni experience. *Catalysis Today*. 2009;142(1-2):9-16. doi:10.1016/j.cattod.2009.01.006
63. Anderson, B R. Fischer-Tropsch synthesis. Published online 1984.
64. Jager B, Espinoza R. Advances in low temperature Fischer-Tropsch synthesis. *Catalysis Today*. 1995;23(1):17-28. doi:10.1016/0920-5861(94)00136-P
65. Kidnay, Arthur J & Parrish WR. Fundamentals of Natural Gas Processing mechanical engineering. *Mechanical Engineering*. Published online 2006.
66. 6 Fluid characterisation. In: *Developments in Petroleum Science*. Vol 47. Elsevier; 1998:209-252. doi:10.1016/S0376-7361(98)80028-9

67. Martínez DY, Jiménez-Gutiérrez A, Linke P, et al. Water and energy issues in gas-to-liquid processes: assessment and integration of different gas-reforming alternatives. *ACS Sustainable Chemistry & Engineering*. 2013;2(2):216-225. doi:10.1021/sc4002643
68. Martínez DY, Jiménez-Gutiérrez A, Linke P, et al. Water and energy issues in gas-to-liquid processes: assessment and integration of different gas-reforming alternatives. *ACS Sustainable Chemistry & Engineering*. 2013;2(2):216-225. doi:10.1021/sc4002643
69. Aasberg-petersen BK, Nielsen CS, Dybkjær I, Perregaard J. Large Scale Methanol Production from Natural Gas.
70. Christensen TS. Adiabatic prereforming of hydrocarbons - An important step in syngas production. *Applied Catalysis A: General*. 1996;138(2):285-309. doi:10.1016/0926-860X(95)00302-9
71. *Aspen Plus* ® *Aspen Plus User Guide*.; 1981.
72. Perego C, Bortolo R, Zennaro R. Gas to liquids technologies for natural gas reserves valorization: The Eni experience. *Catalysis Today*. 2009;142(1-2):9-16. doi:10.1016/j.cattod.2009.01.006



73. Dry ME. High quality diesel via the Fischer-Tropsch process - A review. *Journal of Chemical Technology and Biotechnology*. 2002;77(1):43-50. doi:10.1002/jctb.527
74. Dry ME. High quality diesel via the Fischer-Tropsch process - A review. *Journal of Chemical Technology and Biotechnology*. 2002;77(1):43-50. doi:10.1002/jctb.527
75. Davis BH, Ocelli ML. *Advances in Fischer-Tropsch Synthesis, Catalysts, and Catalysis*.; 1934.
76. Fuels and Fuel Technology: A Summarized Manual - Wilfrid Francis, Martin C. Peters - Google Books. Accessed June 25, 2020. [https://books.google.com.qa/books?id=Zz8fAwAAQBAJ&pg=PA207&lpg=PA207&dq=number+of+trays+in+fractionating+columns+typically+used+in+industry&source=bl&ots=4WYO36sRTb&sig=ACfU3U0V3SQC-\\_BQ23kmf7wdpCwafINUDA&hl=en&sa=X&ved=2ahUKEwimjtip3\\_LpAhXbm nIEHWYrBGcQ6AEwCnoECAkQAQ#v=onepage&q=number of trays in fractionating columns typically used in industry&f=false](https://books.google.com.qa/books?id=Zz8fAwAAQBAJ&pg=PA207&lpg=PA207&dq=number+of+trays+in+fractionating+columns+typically+used+in+industry&source=bl&ots=4WYO36sRTb&sig=ACfU3U0V3SQC-_BQ23kmf7wdpCwafINUDA&hl=en&sa=X&ved=2ahUKEwimjtip3_LpAhXbm nIEHWYrBGcQ6AEwCnoECAkQAQ#v=onepage&q=number of trays in fractionating columns typically used in industry&f=false)
77. *Air Pollution Control Technology Fact Sheet EPA-CICA Fact Sheet Flare*.
78. SUSTAINABILITY REPORTS – ORYX GTL. Accessed March 7, 2021. <https://oryxgtl.com.qa/sustainability-reports/>

79. Linnhoff B, Flower JR. Synthesis of heat exchanger networks: I. Systematic generation of energy optimal networks. *AIChE Journal*. 1978;24(4):633-642. doi:10.1002/aic.690240411
  
80. Gundersen T. Heat Integration: Targets and Heat Exchanger Network Design. In: *Handbook of Process Integration (PI): Minimisation of Energy and Water Use, Waste and Emissions*. Elsevier Inc.; 2013:129-167. doi:10.1533/9780857097255.2.129

## APPENDIX A

### UNIT SPECIFICATIONS

The following section summarizes the ASPEN Plus<sup>®</sup> unit specifications of the reactors, columns, PSA, and amine unit for ATR-based and CARGEN<sup>™</sup>-based GTL models.

## 8.1. Simulation Properties

Select components

Component ID	Type	Component name	Alias
CO	Conventional	CARBON-MONOXIDE	CO
CO2	Conventional	CARBON-DIOXIDE	CO2
H2O	Conventional	WATER	H2O
H2	Conventional	HYDROGEN	H2
AR	Conventional	ARGON	AR
O2	Conventional	OXYGEN	O2
N2	Conventional	NITROGEN	N2
H3N	Conventional	AMMONIA	H3N
CH4	Conventional	METHANE	CH4
C2H6	Conventional	ETHANE	C2H6
C3H8	Conventional	PROPANE	C3H8
C4H10-1	Conventional	N-BUTANE	C4H10-1
C5H12-1	Conventional	N-PENTANE	C5H12-1
C6H14-1	Conventional	N-HEXANE	C6H14-1
C7H16-1	Conventional	N-HEPTANE	C7H16-1
C8H18-1	Conventional	N-OCTANE	C8H18-1
C9H20-1	Conventional	N-NONANE	C9H20-1
C10H22-1	Conventional	N-DECANE	C10H22-1
C11H24	Conventional	N-UNDECANE	C11H24
C12H26	Conventional	N-DODECANE	C12H26
C13H28	Conventional	N-TRIDECANE	C13H28
C14H30	Conventional	N-TETRADECANE	C14H30
C15H32	Conventional	N-PENTADECANE	C15H32
C16H34	Conventional	N-HEXADECANE	C16H34
C17H36	Conventional	N-HEPTADECANE	C17H36
C18H38	Conventional	N-OCTADECANE	C18H38
C19H40	Conventional	N-NONADECANE	C19H40
C20H42	Conventional	N-EICOSANE	C20H42
C21H44	Conventional	N-HENEICOSANE	C21H44
C22H46	Conventional	N-DOCOSANE	C22H46
C23H48	Conventional	N-TRICOSANE	C23H48
C24H50	Conventional	N-TETRACOSANE	C24H50
C25H52	Conventional	N-PENTACOSANE	C25H52
C26H54	Conventional	N-HEXACOSANE	C26H54
C27H56	Conventional	N-HEPTACOSANE	C27H56
C28H58	Conventional	N-OCTACOSANE	C28H58
C29H60	Conventional	N-NONACOSANE	C29H60
C30H62	Conventional	N-TRIACONTANE	C30H62
C	Conventional	CARBON-GRAPHITE	C

*Figure 37 Simulation Component Selection*

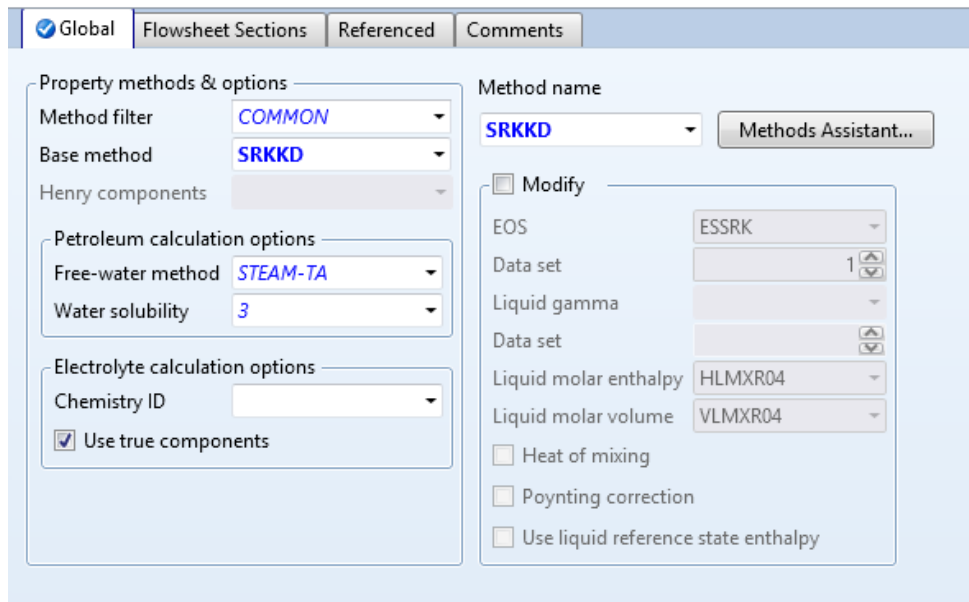


*Figure 38 simulation property method selection*

## 8.2. Saturator

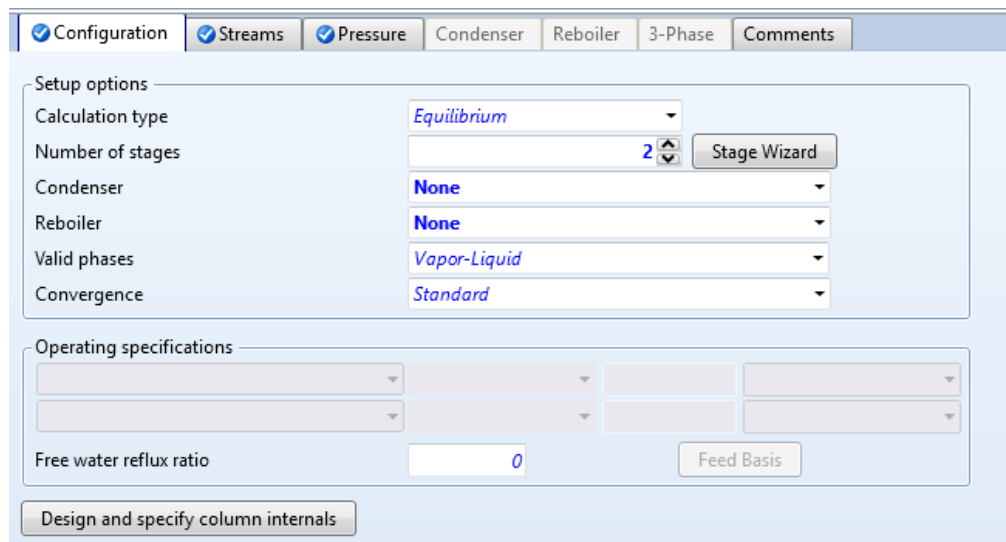


*Figure 39 Saturator configuration*

Configuration		Streams		Pressure		Condenser	Reboiler	3-Phase	Comments
Feed streams									
Name	Stage	Convention							
WASHH2O	1	Above-Stage							
S2	2	On-Stage							
Product streams									
Name	Stage	Phase	Basis	Flow	Units	Flow Ratio	Feed Specs		
SAT-NG	1	Vapor	Mole		lbmol/hr		Feed basis		
PWATER1	2	Liquid	Mole		lbmol/hr		Feed basis		
Pseudo streams									
Name	Pseudo Stream Type	Stage	Internal Phase	Reboiler Phase	Reboiler Conditions	Pumparound ID	Pumparound Conditions	Flow	Units

Figure 40 Saturator stream specifications

Configuration		Streams		Pressure		Condenser	Reboiler	3-Phase	Comments
View <span>Top / Bottom</span>									
Top stage / Condenser pressure									
Stage 1 / Condenser pressure				370	psia				
Stage 2 pressure (optional)									
<input checked="" type="radio"/> Stage 2 pressure					psia				
<input type="radio"/> Condenser pressure drop					psi				
Pressure drop for rest of column (optional)									
<input checked="" type="radio"/> Stage pressure drop					psi				
<input type="radio"/> Column pressure drop					psi				

Figure 41 Saturator pressure specification

### 8.3. Pre-Reformer

Specifications Products Assign Streams Inerts Restricted Equilibrium PSD Utility Comments

Calculation option  
 Calculate phase equilibrium and chemical equilibrium

Operating conditions  
 Pressure 370 psia  
 Temperature F  
 Heat Duty 0 Btu/hr

Phases  
 Maximum number of fluid phases 1  
 Maximum number of solid solution phases 0  
 Include vapor phase  
 Merge all CISOLID species into the first CISOLID substream

Figure 42 Pre-reformer specifications

Specifications Products Assign Streams Inerts Restricted Equilibrium PSD Utility Comments

RGibbs considers all components as products  
 Identify possible products  
 Define phases in which products appear

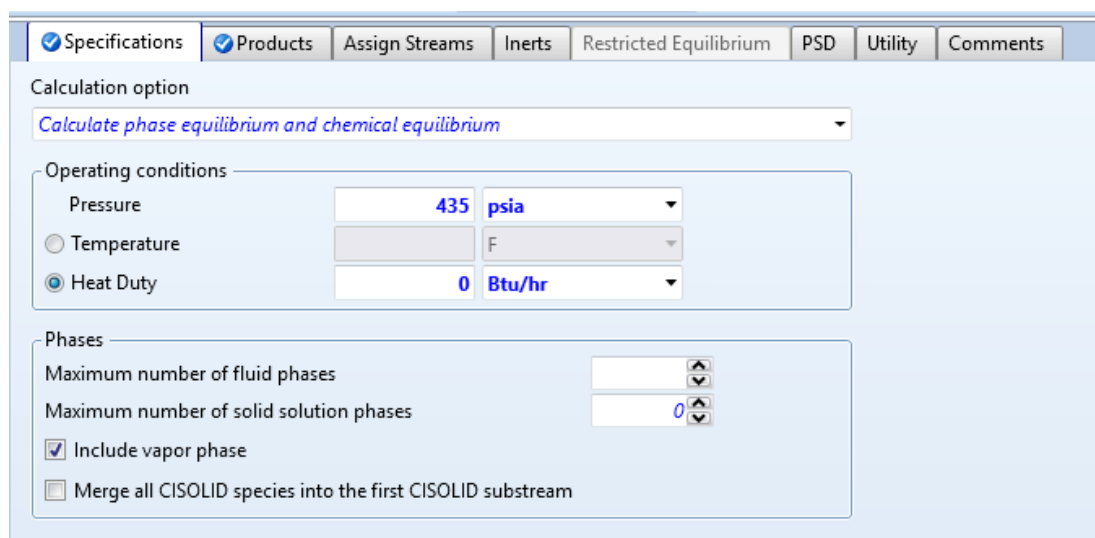
Hydrate-check Rigorous

Products

Component	Valid phases
CO	Mixed
H2O	Mixed
CO2	Mixed
H2	Mixed
AR	Mixed
O2	Mixed
N2	Mixed
CH4	Mixed

Figure 43 Pre-reformer product specifications

## 8.4. Autothermal Reformer



Specifications    Products   Assign Streams   Inerts   Restricted Equilibrium   PSD   Utility   Comments

Calculation option  
*Calculate phase equilibrium and chemical equilibrium*

Operating conditions

Pressure   435   psia

Temperature   F

Heat Duty   0   Btu/hr

Phases

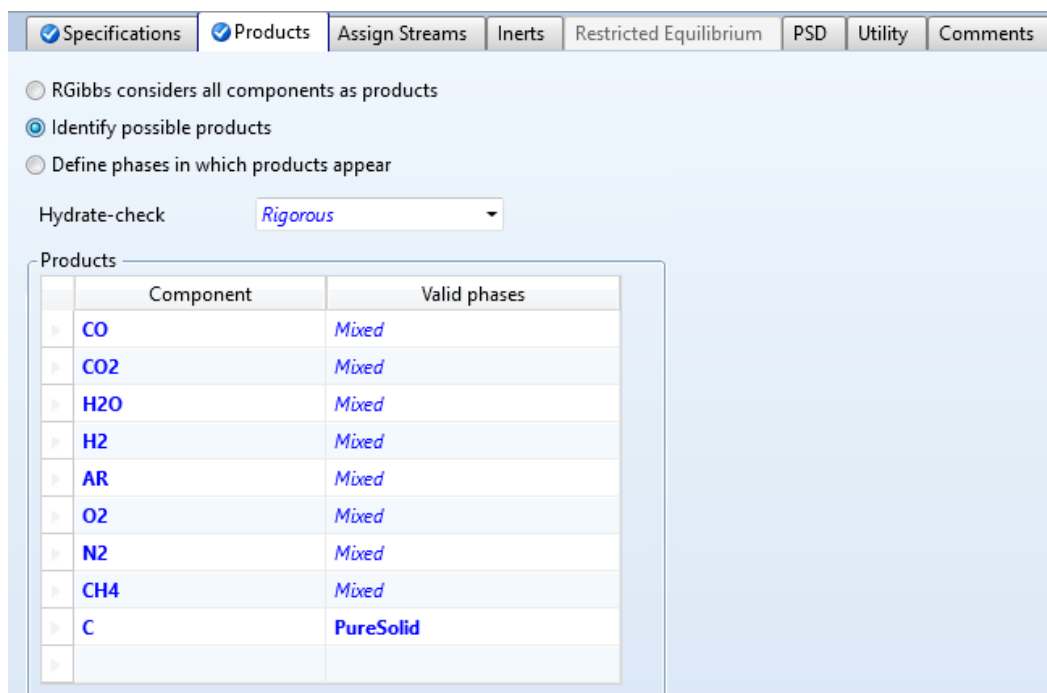
Maximum number of fluid phases   [ ]

Maximum number of solid solution phases   0

Include vapor phase

Merge all CISOLID species into the first CISOLID substream

Figure 44 ATR specifications



Specifications    Products   Assign Streams   Inerts   Restricted Equilibrium   PSD   Utility   Comments

RGibbs considers all components as products

Identify possible products

Define phases in which products appear

Hydrate-check   *Rigorous*

Products

Component	Valid phases
CO	Mixed
CO2	Mixed
H2O	Mixed
H2	Mixed
AR	Mixed
O2	Mixed
N2	Mixed
CH4	Mixed
C	PureSolid

Figure 45 ATR products



## 8.5. FT Reactor

The screenshot shows a software interface for configuring an FT reactor. At the top, there is a horizontal menu with several tabs: 'Specifications' (checked), 'Streams', 'Reactions' (checked), 'Combustion', 'Heat of Reaction' (checked), 'Selectivity', 'PSD', 'Component Attr.', 'Utility', and 'Comments'. Below the menu, the 'Operating conditions' section is visible. It contains several input fields and dropdown menus: 'Flash Type' with dropdowns for 'Temperature' and 'Pressure'; 'Temperature' with a text input '428' and a unit dropdown 'F'; 'Pressure' with a text input '363' and a unit dropdown 'psia'; 'Duty' with a text input and a unit dropdown 'Btu/hr'; and 'Vapor fraction' with a text input. Below this, the 'Valid phases' section has a dropdown menu currently set to 'Vapor-Liquid'.

**Figure 46** FT reaction specifications

Reaction No.

Reactants

Component	Coefficient
CO	-1.0005
H2	-2.0806

Products

Component	Coefficient
C6H14-1	0.004
C7H16-1	0.0037
C8H18-1	0.0034
C9H20-1	0.0031
C10H22-1	0.0029
C11H24	0.0027
C12H26	0.0025
C13H28	0.0023
C14H30	0.0021
C15H32	0.0019
C16H34	0.0018
C17H36	0.0016
C18H38	0.0015
C19H40	0.0014
C20H42	0.0013
C21H44	0.0012
C22H46	0.0011
C23H48	0.001
C24H50	0.0009
C25H52	0.0009
C26H54	0.0008
C27H56	0.0007
C28H58	0.0007
C29H60	0.0006
C30H62	0.0106
H2O	1

Products generation

Molar extent  lbmol/hr

Fractional conversion  of component

*Figure 47 FT reaction stoichiometry*

## 8.6. Hydrocracker

Specifications | Streams | **Reactions** | Combustion | Heat of Reaction | Selectivity | PSD | Component Attr. | Utility | Comments

Operating conditions

Flash Type: Temperature Pressure

Temperature: 662 F

Pressure: 1015 psia

Duty: Btu/hr

Vapor fraction:

Valid phases: Vapor-Liquid

Figure 48 Hydrocracker reaction specifications

Run No.	Specification type	Molar extent	Units	Fractional conversion	Fractional Conversion of Component	Stoichiometry
1	Free conversion		kmol/hr	0.05	C20H42	C20H42 + HC → 0.002898 C16H16 (MIXED) + 0.042802 C8H18 (MIXED) + 0.271827 C10H20 (MIXED) + 1.35547 C14H22 (MIXED) + 0.271827 C19H40 (MIXED) + 0.042802 C12H26 (MIXED) + 0.002898 C13H28 (MIXED)
2	Free conversion		kmol/hr	0.05	C21H44	C21H44 + HC → 0.002898 C16H16 (MIXED) + 0.042802 C8H18 (MIXED) + 0.271827 C10H20 (MIXED) + 0.042733 C18H42 (MIXED) + 0.042733 C15H34 (MIXED) + 0.271827 C19H40 (MIXED) + 0.042802 C12H26 (MIXED) + 0.002898 C14H30 (MIXED)
3	Free conversion		kmol/hr	0.05	C22H46	C22H46 + HC → 0.002898 C16H16 (MIXED) + 0.042802 C8H18 (MIXED) + 0.271827 C10H20 (MIXED) + 1.35547 C14H22 (MIXED) + 0.271827 C19H40 (MIXED) + 0.042802 C12H26 (MIXED) + 0.002898 C13H28 (MIXED)
4	Free conversion		kmol/hr	0.05	C23H48	C23H48 + HC → 0.002898 C16H16 (MIXED) + 0.042802 C8H18 (MIXED) + 0.271827 C10H20 (MIXED) + 0.042733 C17H40 (MIXED) + 0.042733 C14H32 (MIXED) + 0.271827 C19H40 (MIXED) + 0.042802 C12H26 (MIXED) + 0.002898 C14H30 (MIXED)
5	Free conversion		kmol/hr	0.05	C24H50	C24H50 + HC → 0.002898 C16H16 (MIXED) + 0.042802 C10H42 (MIXED) + 0.271827 C11H24 (MIXED) + 1.35547 C14H22 (MIXED) + 0.271827 C19H40 (MIXED) + 0.042802 C12H26 (MIXED) + 0.002898 C13H28 (MIXED)
6	Free conversion		kmol/hr	0.05	C25H52	C25H52 + HC → 0.002898 C16H16 (MIXED) + 0.042802 C10H42 (MIXED) + 0.271827 C11H24 (MIXED) + 0.042733 C18H44 (MIXED) + 0.042733 C15H36 (MIXED) + 0.271827 C19H40 (MIXED) + 0.042802 C12H26 (MIXED) + 0.002898 C14H30 (MIXED)
7	Free conversion		kmol/hr	0.05	C26H54	C26H54 + HC → 0.002898 C16H16 (MIXED) + 0.042802 C11H26 (MIXED) + 0.271827 C12H28 (MIXED) + 1.35547 C14H22 (MIXED) + 0.271827 C19H40 (MIXED) + 0.042802 C12H26 (MIXED) + 0.002898 C14H30 (MIXED)
8	Free conversion		kmol/hr	0.05	C27H56	C27H56 + HC → 0.002898 C16H16 (MIXED) + 0.042802 C11H26 (MIXED) + 0.271827 C12H28 (MIXED) + 0.042733 C18H44 (MIXED) + 0.042733 C15H36 (MIXED) + 0.271827 C19H40 (MIXED) + 0.042802 C12H26 (MIXED) + 0.002898 C14H30 (MIXED)
9	Free conversion		kmol/hr	0.05	C28H58	C28H58 + HC → 0.002898 C16H16 (MIXED) + 0.042802 C12H30 (MIXED) + 0.271827 C13H30 (MIXED) + 1.35547 C14H22 (MIXED) + 0.271827 C19H40 (MIXED) + 0.042802 C12H26 (MIXED) + 0.002898 C14H30 (MIXED)
10	Free conversion		kmol/hr	0.05	C29H60	C29H60 + HC → 0.002898 C16H16 (MIXED) + 0.042802 C12H30 (MIXED) + 0.271827 C13H30 (MIXED) + 0.042733 C18H44 (MIXED) + 0.042733 C15H36 (MIXED) + 0.271827 C19H40 (MIXED) + 0.042802 C12H26 (MIXED) + 0.002898 C14H30 (MIXED)
11	Free conversion		kmol/hr	0.05	C30H62	C30H62 + HC → 0.002898 C16H16 (MIXED) + 0.042802 C13H32 (MIXED) + 0.271827 C14H32 (MIXED) + 1.35547 C14H22 (MIXED) + 0.271827 C19H40 (MIXED) + 0.042802 C12H26 (MIXED) + 0.002898 C14H30 (MIXED)

Figure 49 Hydrocracker reaction stoichiometry

## 8.7. Fractionating Column

Configuration | **Streams** | Pressure | Condenser | Reboiler | 3-Phase | Comments

Setup options

Calculation type: Equilibrium

Number of stages: 45

Condenser: Partial-Vapor-Liquid

Reboiler: None

Valid phases: Vapor-Liquid

Convergence: Standard

Operating specifications

Distillate to feed ratio: Mole 0.326

Free water reflux ratio: 0

Design and specify column internals

Figure 50 Fractionating column specifications

Configuration   Streams   Pressure   Condenser   Reboiler   3-Phase   Comments										
Feed streams										
Name	Stage	Convention								
S41	45	On-Stage								
Product streams										
Name	Stage	Phase	Basis	Flow	Units	Flow Ratio	Feed Specs			
S43	45	Liquid	Mole		lbmol/hr		Feed basis			
S42	1	Liquid	Mole		lbmol/hr		Feed basis			
FUEL3	1	Vapor	Mole		lbmol/hr		Feed basis			
Pseudo streams										
Name	Pseudo Stream Type	Stage	Internal Phase	Reboiler Phase	Reboiler Conditions	Pumparound ID	Pumparound Conditions	Flow	Units	

**Figure 51** Fractionating column Stream Specifications

Configuration   Streams   Pressure   Condenser   Reboiler   3-Phase   Comments										
View <span>Top / Bottom</span>										
Top stage / Condenser pressure										
Stage 1 / Condenser pressure			30		psia					
Stage 2 pressure (optional)										
<input checked="" type="radio"/> Stage 2 pressure					psia					
<input type="radio"/> Condenser pressure drop					psi					
Pressure drop for rest of column (optional)										
<input checked="" type="radio"/> Stage pressure drop			0.1		psi					
<input type="radio"/> Column pressure drop					psi					

**Figure 52** Fractionating column pressure specifications

Configuration	Streams	Pressure	Condenser	Reboiler	3-Phase	Comments
<b>Condenser specification</b>						
<input checked="" type="radio"/> Temperature		<input type="text" value="302"/> <input type="text" value="F"/>				
<input type="radio"/> Distillate vapor fraction		<input type="text" value="Mole"/> <input type="text"/>				
<b>Subcooling specification</b>						
<input type="text" value="Subcooled temperature"/>		<input type="text"/> <input type="text" value="F"/>				
<input checked="" type="radio"/> Both reflux and liquid distillate are subcooled						
<input type="radio"/> Only reflux is subcooled						
<b>Utility specification</b>						
<input type="text" value="Utility"/>		<input type="text"/>				

**Figure 53** Fractionating column condenser specifications

## 8.8. Water Pre-Treatment Unit

Configuration	Streams	Pressure	Condenser	Reboiler	3-Phase	Comments
<b>Setup options</b>						
Calculation type		<input type="text" value="Equilibrium"/>				
Number of stages		<input type="text" value="4"/>		<input type="button" value="Stage Wizard"/>		
Condenser		<input type="text" value="Partial-Vapor"/>				
Reboiler		<input type="text" value="Kettle"/>				
Valid phases		<input type="text" value="Vapor-Liquid"/>				
Convergence		<input type="text" value="Standard"/>				
<b>Operating specifications</b>						
<input type="text" value="Distillate rate"/>		<input type="text" value="Mole"/>		<input type="text" value="20"/> <input type="text" value="lbmol/hr"/>		
<input type="text" value="Reflux ratio"/>		<input type="text" value="Mole"/>		<input type="text" value="0.8"/> <input type="text"/>		
Free water reflux ratio		<input type="text" value="0"/>		<input type="button" value="Feed Basis"/>		
<input type="button" value="Design and specify column internals"/>						

**Figure 54** Water pre-treatment unit specifications

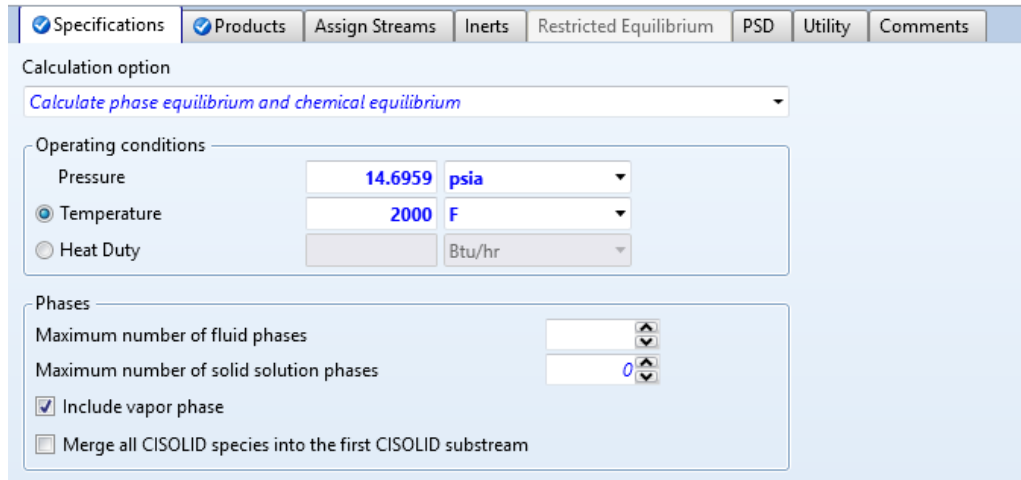
Configuration		Streams		Pressure		Condenser		Reboiler		3-Phase		Comments	
Feed streams													
	Name	Stage	Convention										
▶	CONH2O	2	Above-Stage										
Product streams													
	Name	Stage	Phase	Basis	Flow	Units	Flow Ratio	Feed Specs					
▶	FUEL5	1	Vapor	Mole		lbmol/hr		Feed basis					
▶	PWATER	4	Liquid	Mole		lbmol/hr		Feed basis					
Pseudo streams													
	Name	Pseudo Stream Type	Stage	Internal Phase	Reboiler Phase	Reboiler Conditions	Pumparound ID	Pumparound Conditions	Flow	Units			

*Figure 55 Water pre-treatment unit stream specifications*

Configuration		Streams		Pressure		Condenser		Reboiler		3-Phase		Comments	
View													
Top / Bottom													
Top stage / Condenser pressure													
Stage 1 / Condenser pressure													
20 psia													
Stage 2 pressure (optional)													
<input checked="" type="radio"/> Stage 2 pressure													
<input type="radio"/> Condenser pressure drop													
Pressure drop for rest of column (optional)													
<input checked="" type="radio"/> Stage pressure drop													
<input type="radio"/> Column pressure drop													

*Figure 56 Water pre-treatment unit pressure specifications*

## 8.9. Combustion Unit and Flaring



Specifications    Products   Assign Streams   Inerts   Restricted Equilibrium   PSD   Utility   Comments

Calculation option  
 Calculate phase equilibrium and chemical equilibrium

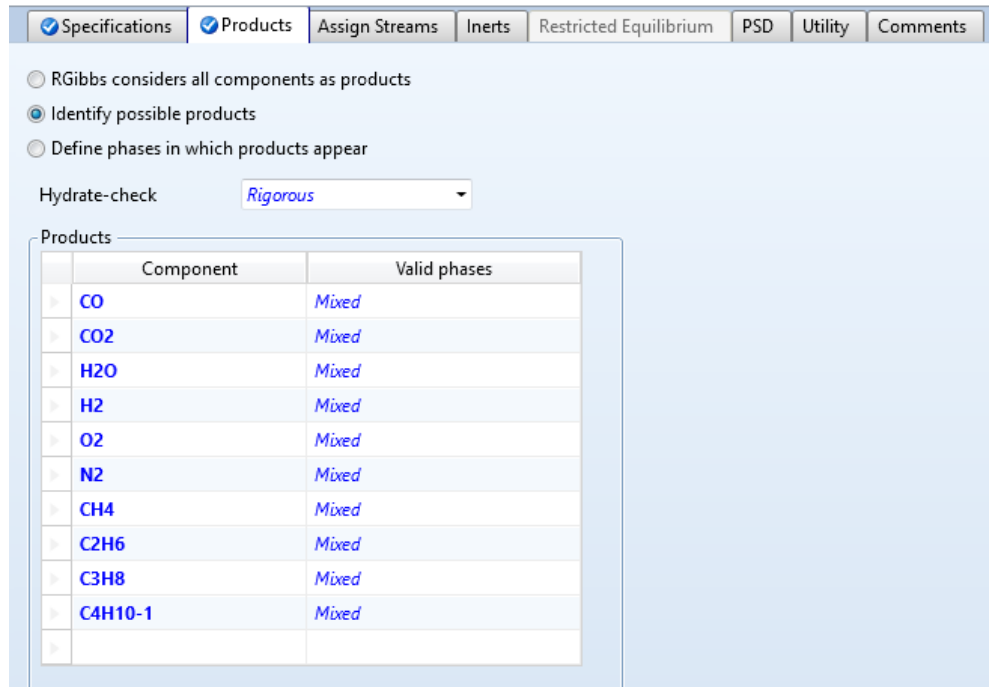
Operating conditions

Pressure: 14.6959 psia  
 Temperature: 2000 F  
 Heat Duty: Btu/hr

Phases

Maximum number of fluid phases: [ ]  
 Maximum number of solid solution phases: 0  
 Include vapor phase  
 Merge all CISOLID species into the first CISOLID substream

*Figure 57 Combustion unit specifications*



RGibbs considers all components as products  
 Identify possible products  
 Define phases in which products appear

Hydrate-check: Rigorous

Products

Component	Valid phases
CO	Mixed
CO2	Mixed
H2O	Mixed
H2	Mixed
O2	Mixed
N2	Mixed
CH4	Mixed
C2H6	Mixed
C3H8	Mixed
C4H10-1	Mixed

*Figure 58 Combustion unit reaction specifications*

## 8.10. Amine Unit Specifications

Outlet stream conditions

Outlet stream: **CO2**

Substream: **MIXED**

Component ID	Specification	Basis	Value	Units
CO	Split fraction		0	
CO2	Split fraction		0.99954	
H2O	Split fraction		0	
H2	Split fraction		0	
AR	Split fraction		0	
O2	Split fraction		0	
N2	Split fraction		0	
H3N	Split fraction		0	
CH4	Split fraction		0	
C2H6	Split fraction		0	
C3H8	Split fraction		0	
C4H10-1	Split fraction		0	
C5H12-1	Split fraction		0	
C6H14-1	Split fraction		0	
C7H16-1	Split fraction		0	
C8H18-1	Split fraction		0	
C9H20-1	Split fraction		0	
C10H22-1	Split fraction		0	
C11H24	Split fraction		0	
C12H26	Split fraction		0	
C13H28	Split fraction		0	
C14H30	Split fraction		0	
C15H32	Split fraction		0	
C16H34	Split fraction		0	
C17H36	Split fraction		0	
C18H38	Split fraction		0	
C19H40	Split fraction		0	
C20H42	Split fraction		0	
C21H44	Split fraction		0	
C22H46	Split fraction		0	
C23H48	Split fraction		0	
C24H50	Split fraction		0	
C25H52	Split fraction		0	
C26H54	Split fraction		0	
C27H56	Split fraction		0	
C28H58	Split fraction		0	
C29H60	Split fraction		0	
C30H62	Split fraction		0	
C	Split fraction			

Figure 59 Amine unit specifications



## 8.11. PSA

Outlet stream conditions

Outlet stream: **HYDROGEN**

Substream: **MIXED**

Component ID	Specification	Basis	Value	Units
> CO	Split fraction		0.0001	
> CO2	Split fraction		0.0001	
> H2O	Split fraction		0.0001	
> H2	Split fraction		0.87	
> AR	Split fraction		0.0001	
> O2	Split fraction		0.0001	
> N2	Split fraction		0.0001	
> H3N	Split fraction		0.0001	
> CH4	Split fraction		0.0001	
> C2H6	Split fraction		0.0001	
> C3H8	Split fraction		0.0001	
> C4H10-1	Split fraction		0.0001	
> C5H12-1	Split fraction		0.0001	
> C6H14-1	Split fraction			
> C7H16-1	Split fraction			
> C8H18-1	Split fraction			
> C9H20-1	Split fraction			
> C10H22-1	Split fraction			
> C11H24	Split fraction			
> C12H26	Split fraction			
> C13H28	Split fraction			
> C14H30	Split fraction			
> C15H32	Split fraction			
> C16H34	Split fraction			
> C17H36	Split fraction			
> C18H38	Split fraction			
> C19H40	Split fraction			
> C20H42	Split fraction			
> C21H44	Split fraction			
> C22H46	Split fraction			
> C23H48	Split fraction			
> C24H50	Split fraction			
> C25H52	Split fraction			
> C26H54	Split fraction			
> C27H56	Split fraction			
> C28H58	Split fraction			
> C29H60	Split fraction			
> C30H62	Split fraction			
> C	Split fraction			

Figure 60 PSA unit specifications

## 8.12. CARGEN

Specifications  
  Products  
  Assign Streams  
 Inerts  
 Restricted Equilibrium  
 PSD  
 Utility  
 Comments

Calculation option  
 Calculate phase equilibrium and chemical equilibrium

Operating conditions

Pressure    25 bar  
 Temperature    F  
 Heat Duty    0 Btu/hr

Phases

Maximum number of fluid phases    [ ]  
 Maximum number of solid solution phases    0  
 Include vapor phase  
 Merge all CISOLID species into the first CISOLID substream

*Figure 61 CARGEN Specifications*

RGibbs considers all components as products  
 Identify possible products  
 Define phases in which products appear

Hydrate-check    Rigorous

Products

Component	Valid phases
CO	Mixed
CO2	Mixed
H2O	Mixed
H2	Mixed
AR	Mixed
O2	Mixed
N2	Mixed
CH4	Mixed
C	PureSolid

*Figure 62 CARGEN product specifications*

### 8.13. Reformer

Specifications Products Assign Streams Inerts Restricted Equilibrium PSD Utility Comments

Calculation option  
 Calculate phase equilibrium and chemical equilibrium

Operating conditions  
 Pressure: 20 bar  
 Temperature: 1508 F  
 Heat Duty: Btu/hr

Phases  
 Maximum number of fluid phases: 1  
 Maximum number of solid solution phases: 0  
 Include vapor phase  
 Merge all CISOLID species into the first CISOLID substream

*Figure 63 Reformer specifications*

Specifications Products Assign Streams Inerts Restricted Equilibrium PSD Utility Comments

RGibbs considers all components as products  
 Identify possible products  
 Define phases in which products appear

Hydrate-check: Rigorous

Products

Component	Valid phases
CO	Mixed
CO2	Mixed
H2O	Mixed
H2	Mixed
AR	Mixed
O2	Mixed
N2	Mixed
CH4	Mixed
C	PureSolid

*Figure 64 Reformer product specifications*

APPENDIX B  
MASS BALANCE

This appendix provides a detailed mass balance of all the process streams in the ATR-based and the CARGEN<sup>TM</sup>-based GTL plants.

Table 20 ATR-based GTL model mass balance

Stream	NATGAS	S1	S2	WASHH2O	SAT-NG	PWATER1	HPSTEAM1	S3	S4	HPSTEAM2	S5	S6	S7
Temperature (F)	79	660	300	230	218	217	437	700	645	437	638	527	578
Pressure (Psia)	310	1015	370	435	370	370	370	370	370	370	370	363	435
Mass Flows (Lb/hr)	952112.25	559426.60	952112.25	97541.62	1002672.57	46981.30	371927.67	1002672.57	1374600.24	30753.74	1374600.24	1763376.87	1763376.87
CO	-	340.96	-	-	-	-	-	-	-	-	101.72	255683.28	255683.28
CO <sub>2</sub>	14738.30	4.33E-01	14738.30	-	14736.61	1.69	-	14736.61	14736.61	-	56074.58	56144.66	56144.66
H <sub>2</sub> O	-	554.49	-	97541.62	50583.02	46958.60	371927.67	50583.02	422510.68	30753.74	388602.11	422426.91	422426.91
H <sub>2</sub>	-	2488.05	-	-	-	-	-	-	-	-	3053.45	45620.16	45620.16
O <sub>2</sub>	-	-	-	-	-	-	-	-	-	-	5.16E-30	-	-
N <sub>2</sub>	1272.05	1.58	1272.05	-	1272.05	1.62E-03	-	1272.05	1272.05	-	1272.05	2517.06	2517.06
CH <sub>4</sub>	868616.42	66.70	868616.42	-	868596.53	19.89	-	868596.53	868596.53	-	925496.32	952870.44	952870.44
C <sub>2</sub> H <sub>6</sub>	66734.60	28.08	66734.60	-	66733.50	1.10	-	66733.50	66733.50	-	-	3483.03	3483.03
C <sub>3</sub> H <sub>8</sub>	750.88	78.82	750.88	-	750.87	1.41E-02	-	750.87	750.87	-	-	4558.72	4558.72
C <sub>4</sub> H <sub>10</sub>	-	195.88	-	-	-	-	-	-	-	-	-	5351.83	5351.83
C <sub>5</sub> H <sub>12</sub>	-	350.26	-	-	-	-	-	-	-	-	-	5314.44	5314.44
C <sub>6</sub> H <sub>14</sub>	-	456.72	-	-	-	-	-	-	-	-	-	4378.96	4378.96
C <sub>7</sub> H <sub>16</sub>	-	481.95	-	-	-	-	-	-	-	-	-	2746.68	2746.68
C <sub>8</sub> H <sub>18</sub>	-	562.83	-	-	-	-	-	-	-	-	-	1354.93	1354.93
C <sub>9</sub> H <sub>20</sub>	-	884.38	-	-	-	-	-	-	-	-	-	570.53	570.53
C <sub>10</sub> H <sub>22</sub>	-	2055.01	-	-	-	-	-	-	-	-	-	221.35	221.35
C <sub>11</sub> H <sub>24</sub>	-	3218.88	-	-	-	-	-	-	-	-	-	85.77	85.77
C <sub>12</sub> H <sub>26</sub>	-	4353.17	-	-	-	-	-	-	-	-	-	30.96	30.96
C <sub>13</sub> H <sub>28</sub>	-	6062.95	-	-	-	-	-	-	-	-	-	11.15	11.15
C <sub>14</sub> H <sub>30</sub>	-	11409.02	-	-	-	-	-	-	-	-	-	4.07	4.07
C <sub>15</sub> H <sub>32</sub>	-	40433.02	-	-	-	-	-	-	-	-	-	1.31	1.31
C <sub>16</sub> H <sub>34</sub>	-	18720.00	-	-	-	-	-	-	-	-	-	4.56E-01	4.56E-01
C <sub>17</sub> H <sub>36</sub>	-	14670.73	-	-	-	-	-	-	-	-	-	1.20E-01	1.20E-01
C <sub>18</sub> H <sub>38</sub>	-	55098.70	-	-	-	-	-	-	-	-	-	3.77E-02	3.77E-02
C <sub>19</sub> H <sub>40</sub>	-	213844.66	-	-	-	-	-	-	-	-	-	1.11E-02	1.11E-02
C <sub>20</sub> H <sub>42</sub>	-	8877.04	-	-	-	-	-	-	-	-	-	2.66E-03	2.66E-03
C <sub>21</sub> H <sub>44</sub>	-	8600.98	-	-	-	-	-	-	-	-	-	7.76E-04	7.76E-04
C <sub>22</sub> H <sub>46</sub>	-	8257.12	-	-	-	-	-	-	-	-	-	2.47E-04	2.47E-04
C <sub>23</sub> H <sub>48</sub>	-	7845.46	-	-	-	-	-	-	-	-	-	5.16E-05	5.16E-05
C <sub>24</sub> H <sub>50</sub>	-	7366.00	-	-	-	-	-	-	-	-	-	1.26E-05	1.26E-05
C <sub>25</sub> H <sub>52</sub>	-	7671.09	-	-	-	-	-	-	-	-	-	3.90E-06	3.90E-06
C <sub>26</sub> H <sub>54</sub>	-	7089.94	-	-	-	-	-	-	-	-	-	8.70E-07	8.70E-07
C <sub>27</sub> H <sub>56</sub>	-	6440.99	-	-	-	-	-	-	-	-	-	1.54E-07	1.54E-07
C <sub>28</sub> H <sub>58</sub>	-	6678.28	-	-	-	-	-	-	-	-	-	6.15E-08	6.15E-08
C <sub>29</sub> H <sub>60</sub>	-	5927.63	-	-	-	-	-	-	-	-	-	1.93E-08	1.93E-08
C <sub>30</sub> H <sub>62</sub>	-	108314.82	-	-	-	-	-	-	-	-	-	9.43E-08	9.43E-08

Table 20 Continued

Stream	S8	O2-FEED	S9	S10	S13	S17	S18	S19	PWATER2	CO2	SYNGAS	A-SYNGAS	TO-PSA
Temperature (F)	940	95	212	940	940	1950	122	120	120	120	120	120	120
Pressure (Psia)	435	17	435	435	435	435	435	332	332	332	332	332	332
Mass Flows (Lb/hr)	1763376.87	1107593.90	1107593.90	1107593.90	2870970.77	2870970.77	2870970.77	2373059.38	497911.39	310426.67	2062632.71	2043602.65	19030.06
CO	255683.28	-	-	-	255683.28	1722507.29	1722507.29	1722506.12	1.17	-	1722506.12	1706614.10	15892.02
CO <sub>2</sub>	56144.66	-	-	-	56144.66	310648.85	310648.85	310569.53	79.32	310426.67	142.86	141.54	1.32
H <sub>2</sub> O	422426.91	-	-	-	422426.91	517805.16	517805.16	19977.15	497828.01	-	19977.15	19792.84	184.31
H <sub>2</sub>	45620.16	-	-	-	45620.16	266464.91	266464.91	266464.31	0.61	-	266464.31	264005.88	2458.43
O <sub>2</sub>	-	1107593.90	1107593.90	1107593.90	1107593.90	3.36E-10	3.36E-10	-	-	-	-	-	-
N <sub>2</sub>	2517.06	-	-	-	2517.06	2517.06	2517.06	2517.06	1.65E-03	-	2517.06	2493.84	23.22
CH <sub>4</sub>	952870.44	-	-	-	952870.44	51027.50	51027.50	51025.21	2.29	-	51025.21	50554.45	470.76
C <sub>2</sub> H <sub>6</sub>	3483.03	-	-	-	3483.03	-	-	-	-	-	-	-	-
C <sub>3</sub> H <sub>8</sub>	4558.72	-	-	-	4558.72	-	-	-	-	-	-	-	-
C <sub>4</sub> H <sub>10</sub>	5351.83	-	-	-	5351.83	-	-	-	-	-	-	-	-
C <sub>5</sub> H <sub>12</sub>	5314.44	-	-	-	5314.44	-	-	-	-	-	-	-	-
C <sub>6</sub> H <sub>14</sub>	4378.96	-	-	-	4378.96	-	-	-	-	-	-	-	-
C <sub>7</sub> H <sub>16</sub>	2746.68	-	-	-	2746.68	-	-	-	-	-	-	-	-
C <sub>8</sub> H <sub>18</sub>	1354.93	-	-	-	1354.93	-	-	-	-	-	-	-	-
C <sub>9</sub> H <sub>20</sub>	570.53	-	-	-	570.53	-	-	-	-	-	-	-	-
C <sub>10</sub> H <sub>22</sub>	221.35	-	-	-	221.35	-	-	-	-	-	-	-	-
C <sub>11</sub> H <sub>24</sub>	85.77	-	-	-	85.77	-	-	-	-	-	-	-	-
C <sub>12</sub> H <sub>26</sub>	30.96	-	-	-	30.96	-	-	-	-	-	-	-	-
C <sub>13</sub> H <sub>28</sub>	11.15	-	-	-	11.15	-	-	-	-	-	-	-	-
C <sub>14</sub> H <sub>30</sub>	4.07	-	-	-	4.07	-	-	-	-	-	-	-	-
C <sub>15</sub> H <sub>32</sub>	1.31	-	-	-	1.31	-	-	-	-	-	-	-	-
C <sub>16</sub> H <sub>34</sub>	4.56E-01	-	-	-	4.56E-01	-	-	-	-	-	-	-	-
C <sub>17</sub> H <sub>36</sub>	1.20E-01	-	-	-	1.20E-01	-	-	-	-	-	-	-	-
C <sub>18</sub> H <sub>38</sub>	3.77E-02	-	-	-	3.77E-02	-	-	-	-	-	-	-	-
C <sub>19</sub> H <sub>40</sub>	1.11E-02	-	-	-	1.11E-02	-	-	-	-	-	-	-	-
C <sub>20</sub> H <sub>42</sub>	2.66E-03	-	-	-	2.66E-03	-	-	-	-	-	-	-	-
C <sub>21</sub> H <sub>44</sub>	7.76E-04	-	-	-	7.76E-04	-	-	-	-	-	-	-	-
C <sub>22</sub> H <sub>46</sub>	2.47E-04	-	-	-	2.47E-04	-	-	-	-	-	-	-	-
C <sub>23</sub> H <sub>48</sub>	5.16E-05	-	-	-	5.16E-05	-	-	-	-	-	-	-	-
C <sub>24</sub> H <sub>50</sub>	1.26E-05	-	-	-	1.26E-05	-	-	-	-	-	-	-	-
C <sub>25</sub> H <sub>52</sub>	3.90E-06	-	-	-	3.90E-06	-	-	-	-	-	-	-	-
C <sub>26</sub> H <sub>54</sub>	8.70E-07	-	-	-	8.70E-07	-	-	-	-	-	-	-	-
C <sub>27</sub> H <sub>56</sub>	1.54E-07	-	-	-	1.54E-07	-	-	-	-	-	-	-	-
C <sub>28</sub> H <sub>58</sub>	6.15E-08	-	-	-	6.15E-08	-	-	-	-	-	-	-	-
C <sub>29</sub> H <sub>60</sub>	1.93E-08	-	-	-	1.93E-08	-	-	-	-	-	-	-	-
C <sub>30</sub> H <sub>62</sub>	9.43E-08	-	-	-	9.43E-08	-	-	-	-	-	-	-	-

Table 20 Continued

Stream	S21	S22	S23	FT-VAPOR	S24	FT-TAIL	FT-REC	FUEL1	FT-COND	FT-WATER	S25	S26	FT-WAX
Temperature (F)	141	428	428	428	122	122	122	122	122	122	124	662	428
Pressure (Psia)	363	363	363	363	363	363	363	363	363	363	1015	1015	363
Mass Flows (Lb/hr)	2043602.65	2043602.65	2043603.57	1659148.82	1659148.82	716045.78	358022.89	358022.89	162984.07	780118.97	162984.07	162984.07	384454.75
CO	1706614.10	1706614.10	511984.23	511614.24	511614.24	511163.13	255581.56	255581.56	449.17	1.94	449.17	449.17	369.99
CO <sub>2</sub>	141.54	141.54	141.54	141.30	141.30	140.16	70.08	70.08	9.57E-01	1.92E-01	9.57E-01	9.57E-01	2.39E-01
H <sub>2</sub> O	19792.84	19792.84	787751.74	786258.38	786258.38	6142.10	3071.05	3071.05	28.38	780087.91	28.38	28.38	1493.37
H <sub>2</sub>	264005.88	264005.88	85212.99	85166.86	85166.86	85133.41	42566.71	42566.71	32.37	1.07	32.37	32.37	46.14
O <sub>2</sub>	-	-	-	-	-	-	-	-	-	-	-	-	-
N <sub>2</sub>	2493.84	2493.84	2493.84	2492.08	2492.08	2490.03	1245.02	1245.02	2.04	9.09E-03	2.04	2.04	1.76
CH <sub>4</sub>	50554.45	50554.45	54931.24	54870.23	54870.23	54748.23	27374.12	27374.12	108.76	1.32E+01	108.76	108.76	61.02
C <sub>2</sub> H <sub>6</sub>	-	-	7049.98	7034.77	7034.77	6966.06	3483.03	3483.03	67.43	1.28E+00	67.43	67.43	15.21
C <sub>3</sub> H <sub>8</sub>	-	-	9398.78	9365.54	9365.54	9117.44	4558.72	4558.72	245.23	2.87E+00	245.23	245.23	33.24
C <sub>4</sub> H <sub>10</sub>	-	-	11645.17	11577.73	11577.73	10703.66	5351.83	5351.83	869.12	4.94E+00	869.12	869.12	67.44
C <sub>5</sub> H <sub>12</sub>	-	-	13225.24	13103.16	13103.16	10628.88	5314.44	5314.44	2470.74	3.54E+00	2470.74	2470.74	122.08
C <sub>6</sub> H <sub>14</sub>	-	-	14694.31	14481.26	14481.26	8757.91	4378.96	4378.96	5721.80	1.54E+00	5721.80	5721.80	213.05
C <sub>7</sub> H <sub>16</sub>	-	-	15804.61	15449.96	15449.96	5493.36	2746.68	2746.68	9956.21	3.89E-01	9956.21	9956.21	354.66
C <sub>8</sub> H <sub>18</sub>	-	-	16556.16	15987.55	15987.55	2709.86	1354.93	1354.93	13277.65	4.60E-02	13277.65	13277.65	568.60
C <sub>9</sub> H <sub>20</sub>	-	-	16948.94	16068.13	16068.13	1141.07	570.53	570.53	14927.06	4.48E-03	14927.06	14927.06	880.80
C <sub>10</sub> H <sub>22</sub>	-	-	17589.48	16217.41	16217.41	442.71	221.35	221.35	15774.70	2.57E-04	15774.70	15774.70	1372.08
C <sub>11</sub> H <sub>24</sub>	-	-	17990.86	15927.91	15927.91	171.54	85.77	85.77	15756.38	8.33E-06	15756.38	15756.38	2062.94
C <sub>12</sub> H <sub>26</sub>	-	-	18153.05	15160.95	15160.95	61.92	30.96	30.96	15099.04	3.51E-07	15099.04	15099.04	2992.10
C <sub>13</sub> H <sub>28</sub>	-	-	18076.07	13908.19	13908.19	22.30	11.15	11.15	13885.89	2.59E-09	13885.89	13885.89	4167.88
C <sub>14</sub> H <sub>30</sub>	-	-	17759.91	12205.08	12205.08	8.13	4.07	4.07	12196.95	2.07E-11	12196.95	12196.95	5554.83
C <sub>15</sub> H <sub>32</sub>	-	-	17204.58	10195.09	10195.09	2.62	1.31	1.31	10192.47	3.31E-13	10192.47	10192.47	7009.49
C <sub>16</sub> H <sub>34</sub>	-	-	17375.37	8566.65	8566.65	9.13E-01	4.56E-01	4.56E-01	8565.73	4.64E-14	8565.73	8565.73	8808.72
C <sub>17</sub> H <sub>36</sub>	-	-	16401.48	6377.69	6377.69	2.40E-01	1.20E-01	1.20E-01	6377.45	1.17E-14	6377.45	6377.45	10023.79
C <sub>18</sub> H <sub>38</sub>	-	-	16273.30	4918.08	4918.08	7.54E-02	3.77E-02	3.77E-02	4918.00	3.45E-15	4918.00	4918.00	11355.22
C <sub>19</sub> H <sub>40</sub>	-	-	16025.53	3624.01	3624.01	2.22E-02	1.11E-02	1.11E-02	3623.99	1.42E-15	3623.99	3623.99	12401.52
C <sub>20</sub> H <sub>42</sub>	-	-	15658.17	2515.06	2515.06	5.32E-03	2.66E-03	2.66E-03	2515.05	9.86E-16	2515.05	2515.05	13143.11
C <sub>21</sub> H <sub>44</sub>	-	-	15171.22	1754.17	1754.17	1.55E-03	7.76E-04	7.76E-04	1754.17	6.87E-16	1754.17	1754.17	13417.05
C <sub>22</sub> H <sub>46</sub>	-	-	14564.69	1224.09	1224.09	4.94E-04	2.47E-04	2.47E-04	1224.09	4.80E-16	1224.09	1224.09	13340.60
C <sub>23</sub> H <sub>48</sub>	-	-	13838.57	770.96	770.96	1.03E-04	5.16E-05	5.16E-05	770.96	3.02E-16	770.96	770.96	13067.60
C <sub>24</sub> H <sub>50</sub>	-	-	12992.86	494.34	494.34	2.51E-05	1.26E-05	1.26E-05	494.34	1.94E-16	494.34	494.34	12498.51
C <sub>25</sub> H <sub>52</sub>	-	-	13531.00	361.59	361.59	7.79E-06	3.90E-06	3.90E-06	361.59	1.42E-16	361.59	361.59	13169.41
C <sub>26</sub> H <sub>54</sub>	-	-	12505.91	222.67	222.67	1.74E-06	8.70E-07	8.70E-07	222.67	8.73E-17	222.67	222.67	12283.24
C <sub>27</sub> H <sub>56</sub>	-	-	11361.23	128.97	128.97	3.07E-07	1.54E-07	1.54E-07	128.97	5.05E-17	128.97	128.97	11232.26
C <sub>28</sub> H <sub>58</sub>	-	-	11779.79	99.16	99.16	1.23E-07	6.15E-08	6.15E-08	99.16	3.89E-17	99.16	99.16	11680.63
C <sub>29</sub> H <sub>60</sub>	-	-	10455.73	64.33	64.33	3.86E-08	1.93E-08	1.93E-08	64.33	2.52E-17	64.33	64.33	10391.40
C <sub>30</sub> H <sub>62</sub>	-	-	191056.01	801.24	801.24	1.89E-07	9.43E-08	9.43E-08	801.24	3.14E-16	801.24	801.24	190254.77

Table 20 Continued

Stream	S27	S28	S29	S30	S31	S32	S33	S34	FUEL4	S35	S36	S37	S38
Temperature (F)	430	662	661	662	400	403	150	150	150	150	756	403	150
Pressure (Psia)	1015	1015	1015	1015	1015	55	55	55	55	55	1015	55	55
Mass Flows (Lb/hr)	384454.75	384454.75	1317519.15	1317519.17	1317519.17	23130.00	23130.00	7555.80	5289.06	2266.74	2279.06	1301890.21	15662.70
CO	369.99	369.99	1134.05	1134.05	1134.05	1045.00	1045.00	1043.20	730.24	312.96	314.58	89.51	1.81
CO <sub>2</sub>	2.39E-01	2.39E-01	1.58	1.58	1.58	1.30	1.30	1.29	9.00E-01	3.86E-01	3.88E-01	2.85E-01	1.53E-02
H <sub>2</sub> O	1493.37	1493.37	2019.86	2019.86	2019.86	1667.69	1667.69	1652.66	1156.86	495.80	498.40	354.02	15.10
H <sub>2</sub>	46.14	46.14	2420.57	719.09	719.09	677.52	677.52	676.98	473.89	203.09	204.34	41.83	0.54
O <sub>2</sub>	-	-	-	-	-	-	-	-	-	-	-	-	-
N <sub>2</sub>	1.76	1.76	5.25	5.25	5.25	4.85	4.85	4.84	3.39	1.45	1.46	4.04E-01	7.87E-03
CH <sub>4</sub>	61.02	61.02	230.70	230.70	230.70	203.23	203.23	202.48	141.73	60.74	61.08	27.62	7.60E-01
C <sub>2</sub> H <sub>6</sub>	15.21	15.21	107.60	107.60	107.60	84.04	84.04	82.62	57.83	24.79	24.91	23.68	1.43
C <sub>3</sub> H <sub>8</sub>	33.24	33.24	346.98	346.98	346.98	234.24	234.24	224.48	157.14	67.34	67.69	113.31	9.81
C <sub>4</sub> H <sub>10</sub>	67.44	67.44	1104.88	1104.88	1104.88	603.89	603.89	536.91	375.84	161.07	161.91	503.57	67.31
C <sub>5</sub> H <sub>12</sub>	122.08	122.08	2898.45	2898.45	2898.45	1212.59	1212.59	907.89	635.52	272.37	273.81	1694.69	306.25
C <sub>6</sub> H <sub>14</sub>	213.05	213.05	6357.25	6357.25	6357.25	1927.79	1927.79	1021.16	714.81	306.35	308.02	4453.24	911.42
C <sub>7</sub> H <sub>16</sub>	354.66	354.66	10802.62	10830.78	10830.78	2280.96	2280.96	689.07	482.35	206.72	207.89	8597.13	1600.63
C <sub>8</sub> H <sub>18</sub>	568.60	568.60	14470.56	15018.60	15018.60	2120.84	2120.84	305.60	213.92	91.68	92.21	12970.71	1825.49
C <sub>9</sub> H <sub>20</sub>	880.80	880.80	16821.11	21053.97	21053.97	1948.97	1948.97	121.39	84.97	36.42	36.63	19214.39	1838.05
C <sub>10</sub> H <sub>22</sub>	1372.08	1372.08	19517.68	39207.11	39207.11	2329.59	2329.59	58.76	41.13	17.63	17.73	37089.72	2283.92
C <sub>11</sub> H <sub>24</sub>	2062.94	2062.94	21532.46	47614.68	47614.68	1810.06	1810.06	18.95	13.27	5.69	5.72	46068.50	1801.45
C <sub>12</sub> H <sub>26</sub>	2992.10	2992.10	23104.20	49958.31	49958.31	1209.40	1209.40	5.09	3.56	1.53	1.54	49029.91	1211.27
C <sub>13</sub> H <sub>28</sub>	4167.88	4167.88	25024.75	53397.75	53397.75	822.57	822.57	1.43	1.00	4.30E-01	4.32E-01	52878.37	825.88
C <sub>14</sub> H <sub>30</sub>	5554.83	5554.83	30858.88	75463.72	75463.72	738.84	738.84	5.59E-01	3.92E-01	1.68E-01	1.69E-01	75156.04	742.55
C <sub>15</sub> H <sub>32</sub>	7009.49	7009.49	63575.85	202497.48	202497.48	1260.78	1260.78	3.89E-01	2.73E-01	1.17E-01	1.18E-01	202398.52	1267.69
C <sub>16</sub> H <sub>34</sub>	8808.72	8808.72	38604.11	68614.02	68614.02	274.79	274.79	3.69E-02	2.59E-02	1.11E-02	1.11E-02	68734.22	276.35
C <sub>17</sub> H <sub>36</sub>	10023.79	10023.79	32264.49	37216.58	37216.58	93.20	93.20	4.73E-03	3.31E-03	1.42E-03	1.43E-03	37338.80	93.74
C <sub>18</sub> H <sub>38</sub>	11355.22	11355.22	41798.52	42118.88	42118.88	68.93	68.93	1.50E-03	1.05E-03	4.51E-04	4.54E-04	42292.93	69.32
C <sub>19</sub> H <sub>40</sub>	12401.52	12401.52	465724.22	465724.22	465724.22	493.11	493.11	4.54E-03	3.18E-03	1.36E-03	1.37E-03	467955.72	496.00
C <sub>20</sub> H <sub>42</sub>	13143.11	13143.11	24089.46	8431.31	8431.31	5.58	5.58	1.90E-05	1.33E-05	5.71E-06	5.75E-06	8474.27	5.61
C <sub>21</sub> H <sub>44</sub>	13417.05	13417.05	23340.34	8169.12	8169.12	3.54	3.54	5.33E-06	3.73E-06	1.60E-06	1.61E-06	8212.61	3.57
C <sub>22</sub> H <sub>46</sub>	13340.60	13340.60	22407.21	7842.52	7842.52	2.30	2.30	1.65E-06	1.15E-06	4.95E-07	4.97E-07	7885.39	2.31
C <sub>23</sub> H <sub>48</sub>	13067.60	13067.60	21290.10	7451.54	7451.54	1.34	1.34	3.42E-07	2.39E-07	1.03E-07	1.03E-07	7493.11	1.35
C <sub>24</sub> H <sub>50</sub>	12498.51	12498.51	19989.01	6996.15	6996.15	8.05E-01	8.05E-01	8.31E-08	5.82E-08	2.49E-08	2.51E-08	7035.64	8.10E-01
C <sub>25</sub> H <sub>52</sub>	13169.41	13169.41	20816.93	7285.93	7285.93	5.59E-01	5.59E-01	2.58E-08	1.81E-08	7.74E-09	7.78E-09	7327.33	5.63E-01
C <sub>26</sub> H <sub>54</sub>	12283.24	12283.24	19239.86	6733.95	6733.95	3.26E-01	3.26E-01	5.81E-09	4.07E-09	1.74E-09	1.75E-09	6772.42	3.28E-01
C <sub>27</sub> H <sub>56</sub>	11232.26	11232.26	17478.82	6117.59	6117.59	1.78E-01	1.78E-01	1.05E-09	7.35E-10	3.15E-10	3.17E-10	6152.65	1.79E-01
C <sub>28</sub> H <sub>58</sub>	11680.63	11680.63	18122.75	6342.96	6342.96	1.32E-01	1.32E-01	4.20E-10	2.94E-10	1.26E-10	1.27E-10	6379.37	1.33E-01
C <sub>29</sub> H <sub>60</sub>	10391.40	10391.40	16085.73	5630.01	5630.01	8.25E-02	8.25E-02	1.33E-10	9.29E-11	3.98E-11	4.00E-11	5662.36	8.30E-02
C <sub>30</sub> H <sub>62</sub>	190254.77	190254.77	293932.32	102876.31	102876.31	9.82E-01	9.82E-01	6.57E-10	4.60E-10	1.97E-10	1.98E-10	103467.95	9.88E-01



Table 20 Continued

Stream	S39	S40	S41	S42	PRODUCT	S43	S44	HYDROGEN	S45	S46	S47	FUEL2	FUEL3
Temperature (F)	400	733	733	302	122	669	677	120	432	668	662	120	302
Pressure (Psia)	55	51	50	30	30	34	1015	332	1015	1015	1015	332	30
Mass Flows (Lb/hr)	1309963.35	1309963.35	1309963.35	542415.70	542415.70	765673.11	770136.53	2140.49	2152.99	774568.58	770080.33	16889.57	1878.27
CO	90.85	90.85	90.85	20.65	20.65	3.43E-01	3.44E-01	1.59	1.60	316.52	314.89	15890.43	69.85
CO <sub>2</sub>	2.99E-01	2.99E-01	2.99E-01	1.50E-01	1.50E-01	1.79E-03	1.80E-03	1.32E-04	1.33E-04	3.90E-01	3.88E-01	1.32E+00	1.47E-01
H <sub>2</sub> O	367.20	367.20	367.20	174.79	174.79	2.30	2.31	1.84E-02	1.85E-02	500.7325301	498.1139419	184.2928044	190.1061718
H <sub>2</sub>	42.11	42.11	42.11	6.59	6.59	1.40E-01	1.41E-01	2138.83	2151.32	2355.80	2342.07	319.60	35.38
O <sub>2</sub>	-	-	-	-	-	-	-	-	-	-	-	-	-
N <sub>2</sub>	4.09E-01	4.09E-01	4.09E-01	9.02E-02	9.02E-02	1.52E-03	1.53E-03	2.32E-03	2.34E-03	1.46	1.46	23.22	3.18E-01
CH <sub>4</sub>	28.23	28.23	28.23	9.63	9.63	1.39E-01	1.40E-01	4.71E-02	4.74E-02	61.27	60.93	470.72	18.46
C <sub>2</sub> H <sub>6</sub>	24.98	24.98	24.98	14.24	14.24	1.79E-01	1.80E-01	-	-	25.09	24.97	-	10.55
C <sub>3</sub> H <sub>8</sub>	122.50	122.50	122.50	88.29	88.29	1.17	1.18	-	-	68.87	68.52	-	33.03
C <sub>4</sub> H <sub>10</sub>	567.96	567.96	567.96	472.76	472.76	7.24	7.28	-	-	169.19	168.31	-	87.97
C <sub>5</sub> H <sub>12</sub>	1990.56	1990.56	1990.56	1786.14	1786.14	33.27	33.44	-	-	307.25	305.63	-	171.15
C <sub>6</sub> H <sub>14</sub>	5336.08	5336.08	5336.08	4970.58	4970.58	116.05	116.68	-	-	424.70	422.39	-	249.45
C <sub>7</sub> H <sub>16</sub>	10141.70	10141.70	10141.70	9600.49	9600.49	285.03	286.62	-	-	494.52	491.75	-	256.18
C <sub>8</sub> H <sub>18</sub>	14713.00	14713.00	14713.00	13980.93	13980.93	532.63	535.68	-	-	627.89	624.31	-	199.43
C <sub>9</sub> H <sub>20</sub>	20932.58	20932.58	20932.58	19803.16	19803.16	976.83	982.48	-	-	1019.11	1013.24	-	152.60
C <sub>10</sub> H <sub>22</sub>	39148.35	39148.35	39148.35	36643.44	36643.44	2353.28	2366.95	-	-	2384.69	2370.91	-	151.64
C <sub>11</sub> H <sub>24</sub>	47595.72	47595.72	47595.72	43788.94	43788.94	3707.46	3729.03	-	-	3734.75	3713.15	-	99.33
C <sub>12</sub> H <sub>26</sub>	49953.22	49953.22	49953.22	44886.08	44886.08	5011.53	5040.69	-	-	5042.23	5013.06	-	55.62
C <sub>13</sub> H <sub>28</sub>	53396.32	53396.32	53396.32	46394.01	46394.01	6970.55	7011.10	-	-	7011.54	6970.98	-	31.79
C <sub>14</sub> H <sub>30</sub>	75463.16	75463.16	75463.16	62332.32	62332.32	13106.93	13183.19	-	-	13183.36	13107.09	-	23.97
C <sub>15</sub> H <sub>32</sub>	202497.09	202497.09	202497.09	156090.29	156090.29	46373.77	46643.57	-	-	46643.69	46373.89	-	33.20
C <sub>16</sub> H <sub>34</sub>	68613.99	68613.99	68613.99	47378.59	47378.59	21229.64	21353.28	-	-	21353.30	21229.65	-	5.73
C <sub>17</sub> H <sub>36</sub>	37216.57	37216.57	37216.57	21351.56	21351.56	15863.25	15956.23	-	-	15956.23	15863.25	-	1.38
C <sub>18</sub> H <sub>38</sub>	42118.88	42118.88	42118.88	16593.18	16593.18	25525.30	25673.09	-	-	25673.09	25525.30	-	6.17E-01
C <sub>19</sub> H <sub>40</sub>	465724.21	465724.21	465724.21	16028.78	16028.78	449698.71	452333.92	-	-	452333.92	449698.71	-	3.38E-01
C <sub>20</sub> H <sub>42</sub>	8431.31	8431.31	8431.31	1.74E-02	1.74E-02	8431.29	8479.86	-	-	8479.86	8431.29	-	1.96E-07
C <sub>21</sub> H <sub>44</sub>	8169.12	8169.12	8169.12	8.06E-07	8.06E-07	8169.12	8216.18	-	-	8216.18	8169.12	-	5.26E-12
C <sub>22</sub> H <sub>46</sub>	7842.52	7842.52	7842.52	5.87E-11	5.87E-11	7842.52	7887.70	-	-	7887.70	7842.52	-	2.32E-16
C <sub>23</sub> H <sub>48</sub>	7451.54	7451.54	7451.54	1.08E-15	1.08E-15	7451.54	7494.46	-	-	7494.46	7451.54	-	2.21E-21
C <sub>24</sub> H <sub>50</sub>	6996.15	6996.15	6996.15	2.18E-16	2.18E-16	6996.15	7036.45	-	-	7036.45	6996.15	-	2.50E-22
C <sub>25</sub> H <sub>52</sub>	7285.93	7285.93	7285.93	-	-	7285.93	7327.90	-	-	7327.90	7285.93	-	-
C <sub>26</sub> H <sub>54</sub>	6733.95	6733.95	6733.95	-	-	6733.95	6772.74	-	-	6772.74	6733.95	-	-
C <sub>27</sub> H <sub>56</sub>	6117.59	6117.59	6117.59	1.94E-33	1.94E-33	6117.59	6152.83	-	-	6152.83	6117.59	-	3.57E-40
C <sub>28</sub> H <sub>58</sub>	6342.96	6342.96	6342.96	-	-	6342.96	6379.50	-	-	6379.50	6342.96	-	-
C <sub>29</sub> H <sub>60</sub>	5630.01	5630.01	5630.01	-	-	5630.01	5662.44	-	-	5662.44	5630.01	-	-
C <sub>30</sub> H <sub>62</sub>	102876.31	102876.31	102876.31	-	-	102876.31	103468.94	-	-	103468.94	102876.31	-	-

Table 20 Continued

Stream	FUEL5	FUELGAS	S48	AIR	S49	S50	FLARE	CONH2O	PWATER
Temperature (F)	213	121	2000	86	2000	2000	2000	125	230
Pressure (Psia)	20	20	20	15	15	15	15	332	20
Mass Flows (Lb/hr)	402.00	382481.80	384738.12	7143906.54	7143906.54	7528644.66	7526388.34	1325011.66	1324609.66
CO	3.11	272275.20	273840.36	-	-	273840.36	6.21E-01	3.11	5.11E-14
CO2	81.20188529	153.6444838	154.7670901	-	-	154.77	603384.98	81.20	7.24E-05
H2O	264.858058	4867.169647	4894.32571	-	-	4894.33	505631.59	1324874.52	1324609.66
H2	1.68	43397.25	43687.62	-	-	43687.62	4.55E-02	1.68	1.28E-12
O2	-	-	-	1663937.60	1663937.60	1663937.60	936130.20	-	-
N2	1.24E-02	1271.96	1279.46	5479968.94	5479968.94	5481248.40	5481240.90	1.24E-02	1.80E-16
CH4	35.41	28040.44	28215.15	-	-	28215.15	5.36E-26	35.41	9.91E-08
C2H6	2.38	3553.80	3574.26	-	-	3574.26	2.95E-53	2.38	2.49E-09
C3H8	2.88	4751.78	4779.12	-	-	4779.12	3.75E-80	2.88	6.73E-09
C4H10-1	4.94	5820.58	5854.11	-	-	5854.11	4.61E-90	4.94	1.64E-08
C5H12-1	3.54	6124.65	6160.20	-	-	6160.20	-	3.54	2.32E-09
C6H14-1	1.54	5344.76	5376.35	-	-	5376.35	-	1.54	7.93E-11
C7H16-1	3.89E-01	3485.60	3506.70	-	-	3506.70	-	3.89E-01	6.19E-13
C8H18-1	4.60E-02	1768.33	1779.21	-	-	1779.21	-	4.60E-02	4.39E-16
C9H20-1	4.48E-03	808.11	813.09	-	-	813.09	-	4.48E-03	2.09E-19
C10H22-1	2.57E-04	414.12	416.63	-	-	416.63	-	2.57E-04	1.38E-23
C11H24	8.33E-06	198.37	199.55	-	-	199.55	-	8.33E-06	8.73E-29
C12H26	3.51E-07	90.14	90.67	-	-	90.67	-	3.51E-07	1.97E-33
C13H28	-	43.94	44.19	-	-	44.19	-	2.59E-09	-
C14H30	-	28.43	28.59	-	-	28.59	-	2.07E-11	-
C15H32	-	34.78	34.98	-	-	34.98	-	3.31E-13	-
C16H34	-	6.21	6.24	-	-	6.24	-	4.64E-14	-
C17H36	-	1.51	1.52	-	-	1.52	-	1.17E-14	-
C18H38	-	6.56E-01	6.60E-01	-	-	6.60E-01	-	3.45E-15	-
C19H40	-	3.52E-01	3.54E-01	-	-	3.54E-01	-	1.42E-15	-
C20H42	-	2.67E-03	2.69E-03	-	-	2.69E-03	-	9.86E-16	-
C21H44	-	7.80E-04	7.85E-04	-	-	7.85E-04	-	6.87E-16	-
C22H46	-	2.48E-04	2.50E-04	-	-	2.50E-04	-	4.80E-16	-
C23H48	-	5.18E-05	5.22E-05	-	-	5.22E-05	-	3.02E-16	-
C24H50	-	1.26E-05	1.27E-05	-	-	1.27E-05	-	1.94E-16	-
C25H52	-	3.92E-06	3.94E-06	-	-	3.94E-06	-	1.42E-16	-
C26H54	-	8.74E-07	8.79E-07	-	-	8.79E-07	-	8.73E-17	-
C27H56	-	1.54E-07	1.55E-07	-	-	1.55E-07	-	5.05E-17	-
C28H58	-	6.18E-08	6.22E-08	-	-	6.22E-08	-	3.89E-17	-
C29H60	-	1.94E-08	1.95E-08	-	-	1.95E-08	-	2.52E-17	-
C30H62	-	9.47E-08	9.53E-08	-	-	9.53E-08	-	3.14E-16	-

**Table 21** CARGEN™-based GTL model mass balance

Stream	NATGAS	S1	S2	WASHH2O	SAT-NG	PWATER1	HPSTEAM1	S3	S4	S5	S6	S7	S8
Temperature (F)	79	111	300	230	218	217	437	700	645	638	452	509	788
Pressure (Psia)	310	370	370	435	370	370	370	370	370	370	290	363	363
Mass Flows (Lb/hr)	1584668.48	1584668.48	1584668.48	162345.49	1668819.63	78194.34	619025.80	1668819.63	2287845.43	2287845.43	4940278.09	4940278.09	4940278.09
CO	-	-	-	-	-	-	-	-	-	169.30	260916.13	260916.13	260916.13
CO <sub>2</sub>	24530.01	24530.01	24530.01	-	24527.19	2.82	-	24527.19	24527.19	93328.93	2275623.80	2275623.80	2275623.80
H <sub>2</sub> O	-	-	-	162345.49	84188.93	78156.56	619025.80	84188.93	703214.73	646778.28	650513.12	650513.12	650513.12
H <sub>2</sub>	-	-	-	-	-	-	-	-	-	5082.08	48047.24	48047.24	48047.24
O <sub>2</sub>	-	-	-	-	-	-	-	-	-	8.59E-30	8.59E-30	8.59E-30	8.59E-30
N <sub>2</sub>	2117.16	2117.16	2117.16	-	2117.16	2.69E-03	-	2117.16	2117.16	2117.16	4190.06	4190.06	4190.06
CH <sub>4</sub>	1445700.39	1445700.39	1445700.39	-	1445667.29	33.10	-	1445667.29	1445667.29	1540369.69	1670628.92	1670628.92	1670628.92
C <sub>2</sub> H <sub>6</sub>	111071.17	111071.17	111071.17	-	111069.34	1.83	-	111069.34	111069.34	-	3559.47	3559.47	3559.47
C <sub>3</sub> H <sub>8</sub>	1249.75	1249.75	1249.75	-	1249.72	2.35E-02	-	1249.72	1249.72	-	4673.20	4673.20	4673.20
C <sub>4</sub> H <sub>10</sub>	-	-	-	-	-	-	-	-	-	-	5537.88	5537.88	5537.88
C <sub>5</sub> H <sub>12</sub>	-	-	-	-	-	-	-	-	-	-	5625.75	5625.75	5625.75
C <sub>6</sub> H <sub>14</sub>	-	-	-	-	-	-	-	-	-	-	4848.08	4848.08	4848.08
C <sub>7</sub> H <sub>16</sub>	-	-	-	-	-	-	-	-	-	-	3236.05	3236.05	3236.05
C <sub>8</sub> H <sub>18</sub>	-	-	-	-	-	-	-	-	-	-	1671.81	1671.81	1671.81
C <sub>9</sub> H <sub>20</sub>	-	-	-	-	-	-	-	-	-	-	733.66	733.66	733.66
C <sub>10</sub> H <sub>22</sub>	-	-	-	-	-	-	-	-	-	-	291.55	291.55	291.55
C <sub>11</sub> H <sub>24</sub>	-	-	-	-	-	-	-	-	-	-	115.03	115.03	115.03
C <sub>12</sub> H <sub>26</sub>	-	-	-	-	-	-	-	-	-	-	42.24	42.24	42.24
C <sub>13</sub> H <sub>28</sub>	-	-	-	-	-	-	-	-	-	-	15.49	15.49	15.49
C <sub>14</sub> H <sub>30</sub>	-	-	-	-	-	-	-	-	-	-	5.76	5.76	5.76
C <sub>15</sub> H <sub>32</sub>	-	-	-	-	-	-	-	-	-	-	1.90	1.90	1.90
C <sub>16</sub> H <sub>34</sub>	-	-	-	-	-	-	-	-	-	-	6.75E-01	6.75E-01	6.75E-01
C <sub>17</sub> H <sub>36</sub>	-	-	-	-	-	-	-	-	-	-	1.82E-01	1.82E-01	1.82E-01
C <sub>18</sub> H <sub>38</sub>	-	-	-	-	-	-	-	-	-	-	5.82E-02	5.82E-02	5.82E-02
C <sub>19</sub> H <sub>40</sub>	-	-	-	-	-	-	-	-	-	-	1.75E-02	1.75E-02	1.75E-02
C <sub>20</sub> H <sub>42</sub>	-	-	-	-	-	-	-	-	-	-	4.27E-03	4.27E-03	4.27E-03
C <sub>21</sub> H <sub>44</sub>	-	-	-	-	-	-	-	-	-	-	1.26E-03	1.26E-03	1.26E-03
C <sub>22</sub> H <sub>46</sub>	-	-	-	-	-	-	-	-	-	-	4.08E-04	4.08E-04	4.08E-04
C <sub>23</sub> H <sub>48</sub>	-	-	-	-	-	-	-	-	-	-	8.63E-05	8.63E-05	8.63E-05
C <sub>24</sub> H <sub>50</sub>	-	-	-	-	-	-	-	-	-	-	2.13E-05	2.13E-05	2.13E-05
C <sub>25</sub> H <sub>52</sub>	-	-	-	-	-	-	-	-	-	-	6.66E-06	6.66E-06	6.66E-06
C <sub>26</sub> H <sub>54</sub>	-	-	-	-	-	-	-	-	-	-	1.50E-06	1.50E-06	1.50E-06
C <sub>27</sub> H <sub>56</sub>	-	-	-	-	-	-	-	-	-	-	2.69E-07	2.69E-07	2.69E-07
C <sub>28</sub> H <sub>58</sub>	-	-	-	-	-	-	-	-	-	-	1.08E-07	1.08E-07	1.08E-07
C <sub>29</sub> H <sub>60</sub>	-	-	-	-	-	-	-	-	-	-	3.43E-08	3.43E-08	3.43E-08
C <sub>30</sub> H <sub>62</sub>	-	-	-	-	-	-	-	-	-	-	1.69E-07	1.69E-07	1.69E-07
C	-	-	-	-	-	-	-	-	-	-	-	-	-

Table 21 Continued

Stream	S9	S10	CO2-FEED	S11	S12	S13	S14	MWCNT	S15	S16	S17	S18	S19
Temperature (F)	212	788	2000	79	788	788	1008	1008	966	1508	1508	122	122
Pressure (Psia)	363	363	15	15	363	363	363	363	290	290	290	290	290
Mass Flows (Lb/hr)	63997.60	63997.60	2492621.11	2492734.65	2492734.65	7497010.33	6351456.49	1145553.84	6351456.49	6351456.49	6351456.49	6351456.49	4505876.02
CO	-	-	-	-	-	260916.13	96559.55	-	96559.55	96559.55	1756964.02	1756964.02	1756960.89
CO <sub>2</sub>	-	-	2492621.11	2492734.65	2492734.65	4768358.45	2941049.35	-	2941049.35	2941049.35	2184247.75	2184247.75	2182853.91
H <sub>2</sub> O	-	-	-	-	-	650513.12	2324289.50	-	2324289.50	2324289.50	1875966.12	1875966.12	31813.49
H <sub>2</sub>	-	-	-	-	-	48047.24	51039.32	-	51039.32	51039.32	270870.22	270870.22	270868.61
O <sub>2</sub>	63997.60	63997.60	-	-	-	63997.60	9.91E-20	-	9.91E-20	9.91E-20	4.36E-13	4.36E-13	-
N <sub>2</sub>	-	-	-	-	-	4190.06	4190.06	-	4190.06	4190.06	4190.06	4190.06	4190.05
CH <sub>4</sub>	-	-	-	-	-	1670628.92	934328.72	-	934328.72	934328.72	259218.33	259218.33	259189.07
C <sub>2</sub> H <sub>6</sub>	-	-	-	-	-	3559.47	-	-	-	-	-	-	-
C <sub>3</sub> H <sub>8</sub>	-	-	-	-	-	4673.20	-	-	-	-	-	-	-
C <sub>4</sub> H <sub>10</sub>	-	-	-	-	-	5537.88	-	-	-	-	-	-	-
C <sub>5</sub> H <sub>12</sub>	-	-	-	-	-	5625.75	-	-	-	-	-	-	-
C <sub>6</sub> H <sub>14</sub>	-	-	-	-	-	4848.08	-	-	-	-	-	-	-
C <sub>7</sub> H <sub>16</sub>	-	-	-	-	-	3236.05	-	-	-	-	-	-	-
C <sub>8</sub> H <sub>18</sub>	-	-	-	-	-	1671.81	-	-	-	-	-	-	-
C <sub>9</sub> H <sub>20</sub>	-	-	-	-	-	733.66	-	-	-	-	-	-	-
C <sub>10</sub> H <sub>22</sub>	-	-	-	-	-	291.55	-	-	-	-	-	-	-
C <sub>11</sub> H <sub>24</sub>	-	-	-	-	-	115.03	-	-	-	-	-	-	-
C <sub>12</sub> H <sub>26</sub>	-	-	-	-	-	42.24	-	-	-	-	-	-	-
C <sub>13</sub> H <sub>28</sub>	-	-	-	-	-	15.49	-	-	-	-	-	-	-
C <sub>14</sub> H <sub>30</sub>	-	-	-	-	-	5.76	-	-	-	-	-	-	-
C <sub>15</sub> H <sub>32</sub>	-	-	-	-	-	1.90	-	-	-	-	-	-	-
C <sub>16</sub> H <sub>34</sub>	-	-	-	-	-	6.75E-01	-	-	-	-	-	-	-
C <sub>17</sub> H <sub>36</sub>	-	-	-	-	-	1.82E-01	-	-	-	-	-	-	-
C <sub>18</sub> H <sub>38</sub>	-	-	-	-	-	5.82E-02	-	-	-	-	-	-	-
C <sub>19</sub> H <sub>40</sub>	-	-	-	-	-	1.75E-02	-	-	-	-	-	-	-
C <sub>20</sub> H <sub>42</sub>	-	-	-	-	-	4.27E-03	-	-	-	-	-	-	-
C <sub>21</sub> H <sub>44</sub>	-	-	-	-	-	1.26E-03	-	-	-	-	-	-	-
C <sub>22</sub> H <sub>46</sub>	-	-	-	-	-	4.08E-04	-	-	-	-	-	-	-
C <sub>23</sub> H <sub>48</sub>	-	-	-	-	-	8.63E-05	-	-	-	-	-	-	-
C <sub>24</sub> H <sub>50</sub>	-	-	-	-	-	2.13E-05	-	-	-	-	-	-	-
C <sub>25</sub> H <sub>52</sub>	-	-	-	-	-	6.66E-06	-	-	-	-	-	-	-
C <sub>26</sub> H <sub>54</sub>	-	-	-	-	-	1.50E-06	-	-	-	-	-	-	-
C <sub>27</sub> H <sub>56</sub>	-	-	-	-	-	2.69E-07	-	-	-	-	-	-	-
C <sub>28</sub> H <sub>58</sub>	-	-	-	-	-	1.08E-07	-	-	-	-	-	-	-
C <sub>29</sub> H <sub>60</sub>	-	-	-	-	-	3.43E-08	-	-	-	-	-	-	-
C <sub>30</sub> H <sub>62</sub>	-	-	-	-	-	1.69E-07	-	-	-	-	-	-	-
C	-	-	-	-	-	-	-	1145553.84	-	-	-	-	-

Table 21 Continued

Stream	CO2	SYNGAS	A-SYNGAS	S20	TO-PSA	S21	S22	S23	FT-VAPOR	S24	FT-TAIL	FT-REC	FUEL1
Temperature (F)	122	122	122	130	122	184	428	428	428	122	122	122	122
Pressure (Psia)	290	290	290	290	290	363	363	363	363	363	363	363	363
Mass Flows (Lb/hr)	2181849.80	2324026.22	2302510.67	2302510.67	21515.55	2302510.67	2302510.67	2302511.61	1915983.14	1915983.14	941243.82	470631.05	470621.91
CO	-	1756960.89	1740695.16	1740695.16	16265.73	1740695.16	1740695.16	522208.55	521878.44	521878.44	521488.04	260746.83	260744.02
CO <sub>2</sub>	2181849.80	1004.11	994.82	994.82	9.30	994.82	994.82	994.82	993.35	993.35	986.57	493.27	493.28
H <sub>2</sub> O	-	31813.49	31518.96	31518.96	294.53	31518.96	31518.96	814814.00	813486.57	813486.57	7469.53	3734.84	3734.77
H <sub>2</sub>	-	270868.61	268360.95	268360.95	2507.67	268360.95	268360.95	85997.57	85956.84	85956.84	85927.99	42965.15	42963.99
O <sub>2</sub>	-	-	-	-	-	-	-	-	-	-	-	-	-
N <sub>2</sub>	-	4190.05	4151.26	4151.26	38.79	4151.26	4151.26	4151.26	4148.71	4148.71	4145.81	2072.91	2072.91
CH <sub>4</sub>	-	259189.07	256789.53	256789.53	2399.54	256789.53	256789.53	261253.72	260999.84	260999.84	260509.38	130259.23	130254.69
C <sub>2</sub> H <sub>6</sub>	-	-	-	-	-	-	-	7190.77	7177.20	7177.20	7118.87	3559.47	3559.44
C <sub>3</sub> H <sub>8</sub>	-	-	-	-	-	-	-	9586.47	9556.80	9556.80	9346.29	4673.20	4673.14
C <sub>4</sub> H <sub>10</sub>	-	-	-	-	-	-	-	11877.72	11817.50	11817.50	11075.62	5537.88	5537.81
C <sub>5</sub> H <sub>12</sub>	-	-	-	-	-	-	-	13489.34	13380.28	13380.28	11251.30	5625.75	5625.65
C <sub>6</sub> H <sub>14</sub>	-	-	-	-	-	-	-	14987.75	14797.25	14797.25	9695.90	4848.08	4847.95
C <sub>7</sub> H <sub>16</sub>	-	-	-	-	-	-	-	16120.23	15802.92	15802.92	6471.86	3236.05	3235.93
C <sub>8</sub> H <sub>18</sub>	-	-	-	-	-	-	-	16886.78	16376.27	16376.27	3343.55	1671.81	1671.78
C <sub>9</sub> H <sub>20</sub>	-	-	-	-	-	-	-	17287.41	16495.99	16495.99	1467.30	733.66	733.65
C <sub>10</sub> H <sub>22</sub>	-	-	-	-	-	-	-	17940.75	16703.73	16703.73	583.10	291.55	291.55
C <sub>11</sub> H <sub>24</sub>	-	-	-	-	-	-	-	18350.13	16481.45	16481.45	230.06	115.03	115.03
C <sub>12</sub> H <sub>26</sub>	-	-	-	-	-	-	-	18515.57	15787.63	15787.63	84.48	42.24	42.24
C <sub>13</sub> H <sub>28</sub>	-	-	-	-	-	-	-	18437.05	14604.89	14604.89	30.98	15.49	15.49
C <sub>14</sub> H <sub>30</sub>	-	-	-	-	-	-	-	18114.58	12952.54	12952.54	11.52	5.76	5.76
C <sub>15</sub> H <sub>32</sub>	-	-	-	-	-	-	-	17548.16	10953.12	10953.12	3.79	1.90	1.90
C <sub>16</sub> H <sub>34</sub>	-	-	-	-	-	-	-	17722.36	9324.59	9324.59	1.35	6.75E-01	6.75E-01
C <sub>17</sub> H <sub>36</sub>	-	-	-	-	-	-	-	16729.02	7038.58	7038.58	3.63E-01	1.82E-01	1.82E-01
C <sub>18</sub> H <sub>38</sub>	-	-	-	-	-	-	-	16598.27	5491.12	5491.12	1.16E-01	5.82E-02	5.82E-02
C <sub>19</sub> H <sub>40</sub>	-	-	-	-	-	-	-	16345.56	4088.10	4088.10	3.49E-02	1.75E-02	1.75E-02
C <sub>20</sub> H <sub>42</sub>	-	-	-	-	-	-	-	15970.86	2862.56	2862.56	8.54E-03	4.27E-03	4.27E-03
C <sub>21</sub> H <sub>44</sub>	-	-	-	-	-	-	-	15474.19	2008.81	2008.81	2.53E-03	1.26E-03	1.26E-03
C <sub>22</sub> H <sub>46</sub>	-	-	-	-	-	-	-	14855.55	1407.78	1407.78	8.15E-04	4.08E-04	4.08E-04
C <sub>23</sub> H <sub>48</sub>	-	-	-	-	-	-	-	14114.92	8.90E+02	890.11	1.73E-04	8.63E-05	8.63E-05
C <sub>24</sub> H <sub>50</sub>	-	-	-	-	-	-	-	13252.32	572.10	572.10	4.25E-05	2.13E-05	2.13E-05
C <sub>25</sub> H <sub>52</sub>	-	-	-	-	-	-	-	13801.22	419.06	419.06	1.33E-05	6.66E-06	6.66E-06
C <sub>26</sub> H <sub>54</sub>	-	-	-	-	-	-	-	12755.65	258.37	258.37	3.00E-06	1.50E-06	1.50E-06
C <sub>27</sub> H <sub>56</sub>	-	-	-	-	-	-	-	11588.11	149.78	149.78	5.37E-07	2.69E-07	2.69E-07
C <sub>28</sub> H <sub>58</sub>	-	-	-	-	-	-	-	12015.03	115.19	115.19	2.17E-07	1.08E-07	1.08E-07
C <sub>29</sub> H <sub>60</sub>	-	-	-	-	-	-	-	10664.53	74.73	74.73	6.85E-08	3.43E-08	3.43E-08
C <sub>30</sub> H <sub>62</sub>	-	-	-	-	-	-	-	194871.39	930.95	930.95	3.38E-07	1.69E-07	1.69E-07
C	-	-	-	-	-	-	-	-	-	-	-	-	-

Table 21 Continued

Stream	FT-WATER	S25	S26	FT-WAX	S27	S28	S29	S30	S31	S32	S33	S34	FUEL4
Temperature (F)	122	124	662	428	430	662	661	662	400	403	150	150	150
Pressure (Psia)	363	1015	1015	363	1015	1015	1015	1015	1015	55	55	55	55
Mass Flows (Lb/hr)	806057.72	168681.59	168681.59	386528.47	386528.47	386528.47	1338330.07	1338330.08	1338330.08	23180.72	23180.72	7600.06	5320.04
CO	1.68	388.71	388.71	330.11	330.11	330.11	995.94	995.94	995.94	918.83	918.83	917.31	642.12
CO <sub>2</sub>	1.14	5.64	5.64	1.47	1.47	1.47	9.42	9.42	9.42	7.76	7.76	7.67	5.37
H <sub>2</sub> O	805987.95	29.09	29.09	1327.42	1327.42	1327.42	1802.45	1802.45	1802.45	1492.23	1492.23	1479.57	1035.70
H <sub>2</sub>	9.29E-01	27.92	27.92	40.73	40.73	40.73	2453.45	717.98	717.98	677.06	677.06	676.62	473.64
O <sub>2</sub>	-	-	-	-	-	-	-	-	-	-	-	-	-
N <sub>2</sub>	1.29E-02	2.88	2.88	2.56	2.56	2.56	7.53	7.53	7.53	6.96	6.96	6.95	4.87
CH <sub>4</sub>	53.36	437.10	437.10	253.88	253.88	253.88	939.69	939.69	939.69	829.28	829.28	826.37	578.46
C <sub>2</sub> H <sub>6</sub>	1.10	57.23	57.23	13.56	13.56	13.56	92.30	92.30	92.30	72.33	72.33	71.17	49.82
C <sub>3</sub> H <sub>8</sub>	2.45	208.07	208.07	29.66	29.66	29.66	296.70	296.70	296.70	201.26	201.26	193.27	135.29
C <sub>4</sub> H <sub>10</sub>	4.23	737.66	737.66	60.22	60.22	60.22	943.18	943.18	943.18	518.95	518.95	463.90	324.73
C <sub>5</sub> H <sub>12</sub>	3.07	2125.92	2125.92	109.07	109.07	109.07	2503.76	2503.76	2503.76	1056.35	1056.35	800.68	560.48
C <sub>6</sub> H <sub>14</sub>	1.39	5099.96	5099.96	190.50	190.50	190.50	5676.63	5676.63	5676.63	1738.78	1738.78	942.82	659.98
C <sub>7</sub> H <sub>16</sub>	3.68E-01	9330.69	9330.69	317.31	317.31	317.31	10117.84	10146.56	10146.56	2161.21	2161.21	675.83	473.08
C <sub>8</sub> H <sub>18</sub>	4.57E-02	13032.67	13032.67	510.52	510.52	510.52	14161.18	14720.16	14720.16	2103.95	2103.95	316.15	221.31
C <sub>9</sub> H <sub>20</sub>	4.56E-03	15028.69	15028.69	791.41	791.41	791.41	16843.39	21160.80	21160.80	1984.09	1984.09	129.50	90.65
C <sub>10</sub> H <sub>22</sub>	2.66E-04	16120.63	16120.63	1237.02	1237.02	1237.02	19775.62	39858.35	39858.35	2399.63	2399.63	63.53	44.47
C <sub>11</sub> H <sub>24</sub>	8.69E-06	16251.39	16251.39	1868.69	1868.69	1868.69	21913.71	48516.94	48516.94	1869.10	1869.10	20.55	14.39
C <sub>12</sub> H <sub>26</sub>	3.69E-07	15703.15	15703.15	2727.94	2727.94	2727.94	23555.47	50946.01	50946.01	1249.94	1249.94	5.52	3.87
C <sub>13</sub> H <sub>28</sub>	2.74E-09	14573.90	14573.90	3832.16	3832.16	3832.16	25532.49	54472.26	54472.26	850.43	850.43	1.56	1.09
C <sub>14</sub> H <sub>30</sub>	2.22E-11	12941.01	12941.01	5162.04	5162.04	5162.04	31501.40	76997.27	76997.27	763.96	763.96	6.07E-01	4.25E-01
C <sub>15</sub> H <sub>32</sub>	3.59E-13	10949.33	10949.33	6595.04	6595.04	6595.04	64940.78	206637.47	206637.47	1303.71	1303.71	4.23E-01	2.96E-01
C <sub>16</sub> H <sub>34</sub>	5.08E-14	9323.24	9323.24	8397.77	8397.77	8397.77	39413.93	70023.32	70023.32	284.14	284.14	4.01E-02	2.81E-02
C <sub>17</sub> H <sub>36</sub>	1.30E-14	7038.22	7038.22	9690.43	9690.43	9690.43	32933.97	37984.98	37984.98	96.37	96.37	5.13E-03	3.59E-03
C <sub>18</sub> H <sub>38</sub>	3.87E-15	5491.00	5491.00	11107.15	11107.15	11107.15	42659.86	42986.62	42986.62	71.26	71.26	1.63E-03	1.14E-03
C <sub>19</sub> H <sub>40</sub>	1.62E-15	4088.06	4088.06	12257.46	12257.46	12257.46	472543.01	472543.01	472543.01	506.78	506.78	4.89E-03	3.42E-03
C <sub>20</sub> H <sub>42</sub>	1.13E-15	2862.55	2862.55	13108.30	13108.30	13108.30	24570.66	8599.73	8599.73	5.76	5.76	2.06E-05	1.44E-05
C <sub>21</sub> H <sub>44</sub>	7.94E-16	2008.80	2008.80	13465.39	13465.39	13465.39	23806.58	8332.30	8332.30	3.66	3.66	5.77E-06	4.04E-06
C <sub>22</sub> H <sub>46</sub>	5.56E-16	1407.78	1407.78	13447.76	13447.76	13447.76	22854.82	7999.19	7999.19	2.38	2.38	1.78E-06	1.25E-06
C <sub>23</sub> H <sub>48</sub>	3.52E-16	890.11	890.11	13224.81	13224.81	13224.81	21715.39	7600.39	7600.39	1.38	1.38	3.69E-07	2.59E-07
C <sub>24</sub> H <sub>50</sub>	2.26E-16	572.10	572.10	12680.22	12680.22	12680.22	20388.31	7135.91	7135.91	8.32E-01	8.32E-01	8.98E-08	6.29E-08
C <sub>25</sub> H <sub>52</sub>	1.66E-16	419.06	419.06	13382.16	13382.16	13382.16	21232.76	7431.47	7431.47	5.78E-01	5.78E-01	2.79E-08	1.95E-08
C <sub>26</sub> H <sub>54</sub>	1.02E-16	258.37	258.37	12497.29	12497.29	12497.29	19624.20	6868.47	6868.47	3.36E-01	3.36E-01	6.27E-09	4.39E-09
C <sub>27</sub> H <sub>56</sub>	5.92E-17	149.78	149.78	11438.34	11438.34	11438.34	17827.97	6239.79	6239.79	1.84E-01	1.84E-01	1.13E-09	7.94E-10
C <sub>28</sub> H <sub>58</sub>	4.55E-17	115.19	115.19	11899.84	11899.84	11899.84	18484.77	6469.67	6469.67	1.36E-01	1.36E-01	4.53E-10	3.17E-10
C <sub>29</sub> H <sub>60</sub>	2.95E-17	74.73	74.73	10589.79	10589.79	10589.79	16407.06	5742.47	5742.47	8.51E-02	8.51E-02	1.43E-10	1.00E-10
C <sub>30</sub> H <sub>62</sub>	3.68E-16	930.95	930.95	193940.44	193940.44	193940.44	299803.85	104931.35	104931.35	1.01	1.01	7.08E-10	4.95E-10
C	-	-	-	-	-	-	-	-	-	-	-	-	-

Table 21 Continued

Stream	S36	S37	S38	S39	S40	S41	S42	PRODUCT	S43	S44	HYDROGEN	S45	S46
Temperature (F)	765	403	150	401	733	733	302	122	670	678	122	669	662
Pressure (Psia)	1015	55	55	55	51	50	30	30	34	1015	290	1015	1015
Mass Flows (Lb/hr)	2280.02	1315149.36	15580.82	1330730.18	1330730.18	1330730.18	550275.62	550275.62	778656.41	778656.41	2183.57	783120.00	783120.00
CO	275.19	77.11	1.50	78.61	78.61	78.61	17.91	17.91	2.98E-01	2.98E-01	1.63	277.12	277.12
CO <sub>2</sub>	2.30	1.66	8.61E-02	1.75	1.75	1.75	8.79E-01	8.79E-01	1.05E-02	1.05E-02	9.30E-04	2.31	2.31
H <sub>2</sub> O	443.87	310.21	12.65	322.86	322.86	322.86	153.89	153.89	2.03	2.03	2.95E-02	445.93	445.93
H <sub>2</sub>	202.99	40.92	5.08E-01	41.43	41.43	41.43	6.50	6.50	1.39E-01	1.39E-01	2181.67	2384.80	2384.80
O <sub>2</sub>	-	-	-	-	-	-	-	-	-	-	-	-	-
N <sub>2</sub>	2.09	5.67E-01	1.07E-02	5.78E-01	5.78E-01	5.78E-01	1.28E-01	1.28E-01	2.16E-03	2.16E-03	3.88E-03	2.09	2.09
CH <sub>4</sub>	247.91	110.41	2.93	113.34	113.34	113.34	38.74	38.74	5.61E-01	5.61E-01	2.40E-01	248.71	248.71
C <sub>2</sub> H <sub>6</sub>	21.35	19.97	1.16	21.13	21.13	21.13	12.07	12.07	1.52E-01	1.52E-01	-	21.50	21.50
C <sub>3</sub> H <sub>8</sub>	57.98	95.44	8.00	103.43	103.43	103.43	74.64	74.64	9.93E-01	9.93E-01	-	58.97	58.97
C <sub>4</sub> H <sub>10</sub>	139.17	424.23	55.05	479.28	479.28	479.28	399.21	399.21	6.13	6.13	-	145.30	145.30
C <sub>5</sub> H <sub>12</sub>	240.21	1447.40	255.68	1703.08	1703.08	1703.08	1528.76	1528.76	28.57	28.57	-	268.78	268.78
C <sub>6</sub> H <sub>14</sub>	282.85	3937.85	795.99	4733.84	4733.84	4733.84	4.41E+03	4410.37	103.33	103.33	-	386.17	386.17
C <sub>7</sub> H <sub>16</sub>	202.75	7985.35	1485.41	9470.77	9470.77	9470.77	8965.80	8965.80	267.09	267.09	-	469.84	469.84
C <sub>8</sub> H <sub>18</sub>	94.85	12616.21	1787.82	14404.03	14404.03	14404.03	13686.87	13686.87	523.15	523.15	-	618.00	618.00
C <sub>9</sub> H <sub>20</sub>	38.85	19176.72	1854.59	21031.31	21031.31	21031.31	19894.58	19894.58	984.43	984.43	-	1023.28	1023.28
C <sub>10</sub> H <sub>22</sub>	19.06	37458.72	2336.11	39794.83	39794.83	39794.83	37242.89	37242.89	2398.91	2398.91	-	2417.97	2417.97
C <sub>11</sub> H <sub>24</sub>	6.17	46647.84	1848.55	48496.38	48496.38	48496.38	44608.51	44608.51	3787.46	3787.46	-	3793.63	3793.63
C <sub>12</sub> H <sub>26</sub>	1.66	49696.07	1244.42	50940.49	50940.49	50940.49	45761.56	45761.56	5122.73	5122.73	-	5124.38	5124.38
C <sub>13</sub> H <sub>28</sub>	4.67E-01	53621.84	848.87	54470.71	54470.71	54470.71	47312.68	47312.68	7125.96	7125.96	-	7126.43	7126.43
C <sub>14</sub> H <sub>30</sub>	1.82E-01	76233.31	763.35	76996.66	76996.66	76996.66	63574.32	63574.32	13398.17	13398.17	-	13398.35	13398.35
C <sub>15</sub> H <sub>32</sub>	1.27E-01	205333.76	1303.28	206637.05	206637.05	206637.05	159207.51	159207.51	47396.28	47396.28	-	47396.41	47396.41
C <sub>16</sub> H <sub>34</sub>	1.20E-02	69739.18	284.10	70023.28	70023.28	70023.28	48324.78	48324.78	21692.92	21692.92	-	21692.93	21692.93
C <sub>17</sub> H <sub>36</sub>	1.54E-03	37888.61	96.37	37984.98	37984.98	37984.98	21778.72	21778.72	16205.32	16205.32	-	16205.32	16205.32
C <sub>18</sub> H <sub>38</sub>	4.89E-04	42915.36	71.26	42986.62	42986.62	42986.62	16924.64	16924.64	26061.70	26061.70	-	26061.70	26061.70
C <sub>19</sub> H <sub>40</sub>	1.47E-03	472036.23	506.78	472543.00	472543.00	472543.00	16349.65	16349.65	456197.49	456197.49	-	456197.49	456197.49
C <sub>20</sub> H <sub>42</sub>	6.19E-06	8593.97	5.76	8599.73	8599.73	8599.73	1.80E-02	1.80E-02	8599.80	8599.80	-	8599.80	8599.80
C <sub>21</sub> H <sub>44</sub>	1.73E-06	8328.64	3.66	8332.30	8332.30	8332.30	8.42E-07	8.42E-07	8332.39	8332.39	-	8332.39	8332.39
C <sub>22</sub> H <sub>46</sub>	5.35E-07	7996.81	2.38	7999.19	7999.19	7999.19	6.17E-11	6.17E-11	7999.27	7999.27	-	7999.27	8.00E+03
C <sub>23</sub> H <sub>48</sub>	1.11E-07	7599.01	1.38	7600.39	7600.39	7600.39	1.75E-15	1.75E-15	7600.47	7600.47	-	7600.47	7600.47
C <sub>24</sub> H <sub>50</sub>	2.69E-08	7135.08	8.32E-01	7135.91	7135.91	7135.91	4.58E-18	4.58E-18	7135.98	7135.98	-	7135.98	7135.98
C <sub>25</sub> H <sub>52</sub>	8.36E-09	7430.89	5.78E-01	7431.47	7431.47	7431.47	-	-	7431.55	7431.55	-	7431.55	7431.55
C <sub>26</sub> H <sub>54</sub>	1.88E-09	6868.13	3.36E-01	6868.47	6868.47	6868.47	1.11E-27	1.11E-27	6868.54	6868.54	-	6868.54	6868.54
C <sub>27</sub> H <sub>56</sub>	3.40E-10	6239.61	1.84E-01	6239.79	6239.79	6239.79	2.16E-33	2.16E-33	6239.86	6239.86	-	6239.86	6239.86
C <sub>28</sub> H <sub>58</sub>	1.36E-10	6469.53	1.36E-01	6469.67	6469.67	6469.67	1.83E-15	1.83E-15	6469.74	6469.74	-	6469.74	6469.74
C <sub>29</sub> H <sub>60</sub>	4.29E-11	5742.39	8.51E-02	5742.47	5742.47	5742.47	4.43E-35	4.43E-35	5742.53	5742.53	-	5742.53	5742.53
C <sub>30</sub> H <sub>62</sub>	2.12E-10	1.05E+05	1.01	104931.35	104931.35	104931.35	1.86E-15	1.86E-15	104932.46	104932.46	-	104932.46	104932.46
C	-	-	-	-	-	-	-	-	-	-	-	-	-

Table 21 Continued

Stream	FUEL2	FUEL3	FUEL5	FUELGAS	S48	AIR	S49	S50	FLARE	CONH2O
Temperature (F)	122	302	186	119	2000	86	2000	2000	2000	125
Pressure (Psia)	290	30	20	20	20	15	15	15	15	290
Mass Flows (Lb/hr)	19331.98	1806.24	2063.31	499143.48	499143.48	6825969.14	6825969.14	7325112.62	7325112.62	2729832.53
CO	16264.11	60.40	4.81	277715.46	277715.46	-	-	277715.46	1.43	4.81
CO <sub>2</sub>	9.30	8.61E-01	1397.79	1906.60	1906.60	-	-	1906.60	908732.73	1397.79
H <sub>2</sub> O	294.50	166.95	527.92	5759.83	5759.83	-	-	5759.83	749665.68	2728297.14
H <sub>2</sub>	326.00	34.79	2.54	43800.95	43800.95	-	-	43800.95	1.03E-01	2.54
O <sub>2</sub>	-	-	-	-	-	1556773.62	1556773.62	1556773.62	395400.13	-
N <sub>2</sub>	38.79	4.48E-01	2.28E-02	2117.03	2117.03	5269195.52	5269195.52	5271312.55	5271312.55	2.28E-02
CH <sub>4</sub>	2399.30	74.05	115.72	133422.22	133422.22	-	-	133422.22	9.94E-25	115.72
C <sub>2</sub> H <sub>6</sub>	-	8.91	2.93	3621.10	3621.10	-	-	3621.10	4.49E-51	2.93
C <sub>3</sub> H <sub>8</sub>	-	27.80	2.47	4838.71	4838.71	-	-	4838.71	4.68E-77	2.47
C <sub>4</sub> H <sub>10</sub>	-	73.94	4.23	5940.70	5940.70	-	-	5940.70	4.46E-103	4.23
C <sub>5</sub> H <sub>12</sub>	-	145.75	3.07	6334.94	6334.94	-	-	6334.94	-	3.07
C <sub>6</sub> H <sub>14</sub>	-	220.14	1.39	5729.46	5729.46	-	-	5729.46	-	1.39
C <sub>7</sub> H <sub>16</sub>	-	237.88	3.68E-01	3947.26	3947.26	-	-	3947.26	-	3.68E-01
C <sub>8</sub> H <sub>18</sub>	-	194.02	4.57E-02	2087.15	2087.15	-	-	2087.15	-	4.57E-02
C <sub>9</sub> H <sub>20</sub>	-	152.33	4.56E-03	976.63	976.63	-	-	976.63	-	4.56E-03
C <sub>10</sub> H <sub>22</sub>	-	153.08	2.66E-04	489.10	489.10	-	-	489.10	-	2.66E-04
C <sub>11</sub> H <sub>24</sub>	-	100.47	8.69E-06	229.89	229.89	-	-	229.89	-	8.69E-06
C <sub>12</sub> H <sub>26</sub>	-	56.28	3.69E-07	102.39	102.39	-	-	102.39	-	3.69E-07
C <sub>13</sub> H <sub>28</sub>	-	32.16	-	48.74	48.74	-	-	48.74	-	2.74E-09
C <sub>14</sub> H <sub>30</sub>	-	24.24	-	30.43	30.43	-	-	30.43	-	2.22E-11
C <sub>15</sub> H <sub>32</sub>	-	33.58	-	35.77	35.77	-	-	35.77	-	3.59E-13
C <sub>16</sub> H <sub>34</sub>	-	5.79	-	6.49	6.49	-	-	6.49	-	5.08E-14
C <sub>17</sub> H <sub>36</sub>	-	1.40	-	1.58	1.58	-	-	1.58	-	1.30E-14
C <sub>18</sub> H <sub>38</sub>	-	6.24E-01	-	6.83E-01	6.83E-01	-	-	6.83E-01	-	3.87E-15
C <sub>19</sub> H <sub>40</sub>	-	3.42E-01	-	3.62E-01	3.62E-01	-	-	3.62E-01	-	1.62E-15
C <sub>20</sub> H <sub>42</sub>	-	2.01E-07	-	4.29E-03	4.29E-03	-	-	4.29E-03	-	1.13E-15
C <sub>21</sub> H <sub>44</sub>	-	5.44E-12	-	1.27E-03	1.27E-03	-	-	1.27E-03	-	7.94E-16
C <sub>22</sub> H <sub>46</sub>	-	2.41E-16	-	4.09E-04	4.09E-04	-	-	4.09E-04	-	5.56E-16
C <sub>23</sub> H <sub>48</sub>	-	3.57E-21	-	8.66E-05	8.66E-05	-	-	8.66E-05	-	3.52E-16
C <sub>24</sub> H <sub>50</sub>	-	5.18E-24	-	2.13E-05	2.13E-05	-	-	2.13E-05	-	2.26E-16
C <sub>25</sub> H <sub>52</sub>	-	-	-	6.68E-06	6.68E-06	-	-	6.68E-06	-	1.66E-16
C <sub>26</sub> H <sub>54</sub>	-	4.03E-34	-	1.51E-06	1.51E-06	-	-	1.51E-06	-	1.02E-16
C <sub>27</sub> H <sub>56</sub>	-	3.94E-40	-	2.69E-07	2.69E-07	-	-	2.69E-07	-	5.92E-17
C <sub>28</sub> H <sub>58</sub>	-	2.19E-22	-	1.09E-07	1.09E-07	-	-	1.09E-07	-	4.55E-17
C <sub>29</sub> H <sub>60</sub>	-	3.35E-42	-	3.44E-08	3.44E-08	-	-	3.44E-08	-	2.95E-17
C <sub>30</sub> H <sub>62</sub>	-	8.00E-23	-	1.69E-07	1.69E-07	-	-	1.69E-07	-	3.68E-16
C	-	-	-	-	-	-	-	-	-	-